SYNTHESIS AND CHARACTERIZATION OF POLYMERS CONTAINING OLIGOTHIOPHENES

Dissertation zur Erlangung des Grades
"Doktor der Naturwissenschaften"
am Fachbereich Chemie und Pharmazie der
Johannes-Gutenberg-Universität in Mainz

Nicola Ranieri
born in Lucca, Italy

Mainz 2001

Table of contents

So far as mathematic laws refer to reality, they are not certain.
So far trey are certain, they do not refer to reality
Albert Einstein

To my grandmother Ilia

1. INTRODUCTION

1.1. Properties of conjugated polythiophenes

Since the discovery of the semiconducting properties correlated to their π-electron conjugation in the early 80's, polythiophenes have been widely studied, due the possibility to combine the typical features of organic polymers, i.e. low specific weight and resistance to corrosion, and those typical of an inorganic semiconductor, i.e. electrical conductivity.

The electronic properties of polythiophene arise from the high delocalization of the π-electrons, possible through the conjugation of several thiophene units linked at the α (i.e. 2,5) positions (fig. 1).

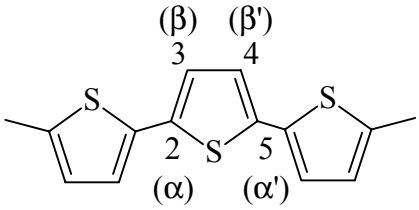

Figure 1: conjugated thiophene rings through the 2,5 positions

Due to such conjugation the polymer shows an energy gap (2.2 eV[1]) typical for an organic semiconductor, which dominates all processes that involve electronic transitions, such as for example the radiative processes of photo- and electro-luminescence or the absorptive process of electrochromism. Moreover, electrical conductivity is also shown. Oxidation (required for the conductivity) occurs at mild conditions due to the delocalization of the charges along the main chain[1]. Because of the latter property, polythiophenes belong to the class of so-called *electrical conducting polymers* (ECPs), as polyacetylenes, polypyrroles, and polyanilines also do.

The huge range of possible applications for conjugated polythiophenes, together with a relatively high chemical stability with respect to other conjugated polymers, explain why the investigation and development of a great number of thiophene polymers have gained so much attention[2].

Polythiophenes can be synthesized both by chemical or electrochemical synthesis.

The chemical routes offer several possibilities to obtain the monomeric units bound by α-α' bonds, while the α-β' and the β-β' bonds have to be considered as defects, because they interrupt the π–conjugation along the main chain (fig. 2).

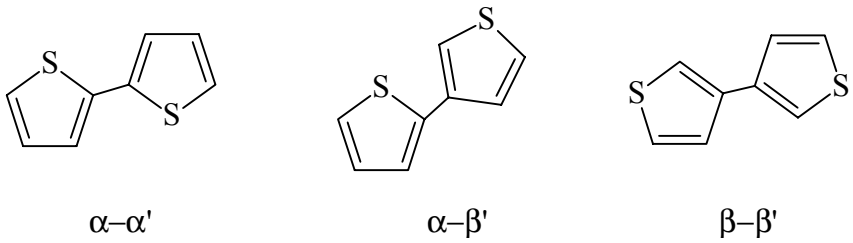

Figure 2: types of linkages in thiophene-thiophene bonds

The easiest chemical way to polythiophene (PT) is by oxidative polymerization of thiophene with the help of an oxidizing agent, such as Fe(III) salts[3], or AsF_5[4], nitronium[5] and Cu (II)[6] salts. The reaction proceeds according to the mechanism proposed in scheme 1 (*Diaz*[7]).

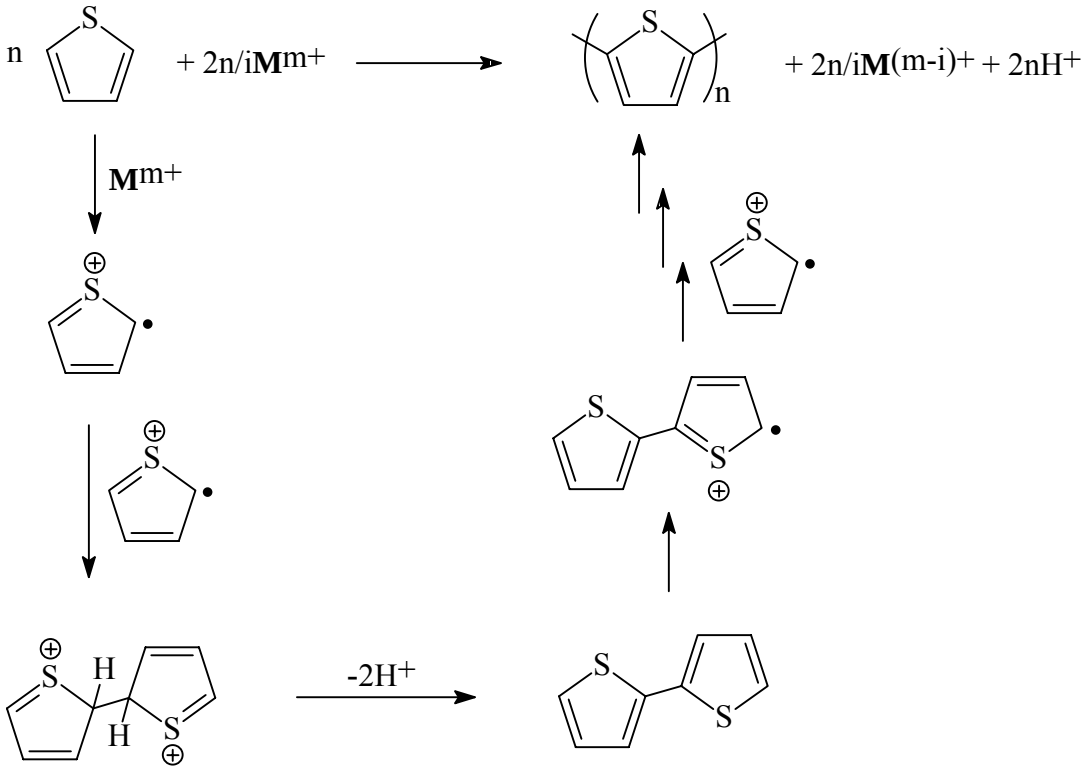

Scheme 1: oxidative polymerization of thiophene according to Diaz

The oxidant oxidizes the monomer to a radical cation, which couples to form the dication. Upon loss of two protons, a neutral dimer is generated, which undergoes then the same oxidation-coupling reaction steps and finally leads to the polymer.

The same mechanism is proposed when the oxidation is carried out in an electrochemical cell, where the anode plays the role of the oxidant and performs the oxidations. The polymer is obtained as a film at the anode, and it is worth mentioning that the electrochemical polymerization is the only means to achieve *in situ* film formation of the otherwise insoluble PTs. The electrochemical potential for the polymerization depends mainly on the structure of the monomer and it is generally in the range 1.4-2.3 V/SCE, depending on substitution at the thiophene ring.

This kind of polymerization is not very regioselective, as a certain percentage of α-β' mislinkages occurs, so the sequence length of conjugated thiophene units is on average not more than 10-12[8].

Other ways of chemical polymerization permit the regioselective formation of the α-α' bond: the thiophene has first to be functionalized in the α- and α'- positions, which take part in the propagation of the polymerization. The most widely used routes are the cross coupling[9] (sch. 2, sometimes referred to also as Grignard coupling[10]).

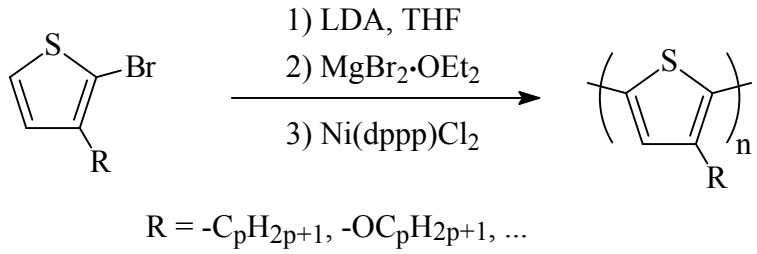

R = $-C_pH_{2p+1}$, $-OC_pH_{2p+1}$, ...

Scheme 2: cross coupling in polythiophene synthesis

Further examples in literature describe also the catalyzed reaction of 2,5-thienyl dimercury dichloride with metallic copper[11] (sch. 3A) or the Pd- or Ni-catalyzed coupling between 2-bromo-5-bromozinco-3-alkylthiophenes[12] (sch. 3B).

A

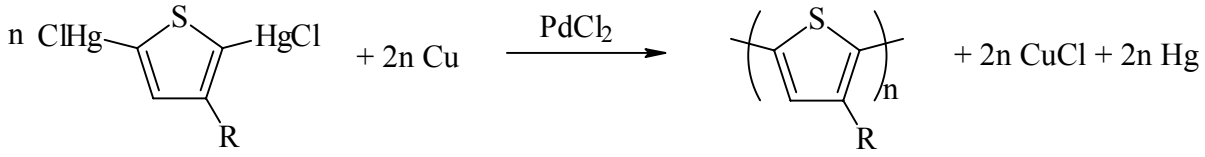

B

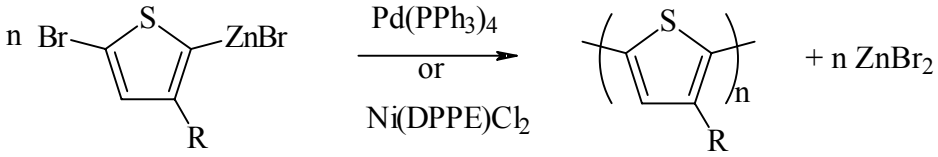

Scheme 3: catalyzed coupling of dimercury dichloride thiophenes (up) and bromozinco thiophenes

The above described catalyzed polymerizations represent a valid method to obtain regioregularly linked 3-alkylthiophene units in the polymer, that is, the monomers are linked in a *head-tail* fashion (fig. 3), in which the twisting angle between two adjacent rings can be minimized.

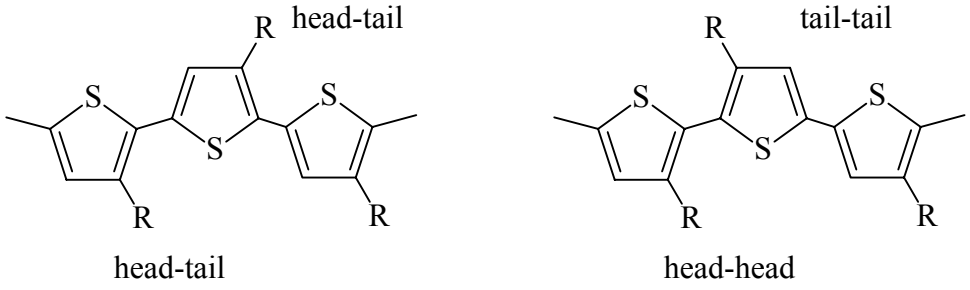

Figure 3: possible isomeric sequences in poly(3-alkylthiophene)s

The first property of PT to be investigated was its electrical conductivity. This phenomenon is observed if additional charges are located on the polymer chain, that happens through oxidizing agents ($FeCl_3$, I_2, …) or applying a defined electrochemical potential, whose magnitude depends on the nature and degree of substitution present on the polymer. For example, the oxidation potential for poly(3-alkyl)thiophenes varies between 0.66 and 0.92 V/SCE depending on the length of the side chain[13]. The charges are balanced by counterions, coming from the oxidizing agent or from the electrolyte, which are incorporated in the solid polymer and influence therefore the properties of the material. This oxidation process, common for all ECPs, is called *doping* of the polymer and occurs already in the oxidative

polymerization, where the PT is obtained directly in the oxidized state because of its lower oxidative potential with respect to the monomer; its oxidation is due to the excess of oxidant (chemical polymerization) or to the high applied potential (electrochemical polymerization). In polythiophenes the doping is of *p* type, that means that positive charges are formed on the polymer. Their presence allows electrons to move along the polymer chain and from chain to chain (interchain *hopping*), leading to a conductivity in the range of 1-100 S/cm. The doping is reversible, as the neutral state is reconstituted by reducing agents or by inverting the potential, that is electrochemical reduction.

The oxidation potential, both of monomer and polymer, depends mainly on the electronic properties of the substituents: the more electronwithdrawing the effect, the less stable the charged species and thus the higher the oxidation potential.

Polythiophene is insoluble and not moldable. Processability is achieved if the monomer contains at least one substituent that enhances the entropic contribution in the solvatation process and in the phase transition: poly(3-alkyl)[14] or (3-alkoxy)thiophenes[15] were the first examples of polythiophenes well soluble in organic solvents and moldable.

The possibility to functionalize all monomer ring positions is of great value in order to tune the properties of the polymer already before its synthesis. Various kinds of functional groups can be introduced on the thiophene ring (sch. 4[16,17]), giving access to polymers with different features.

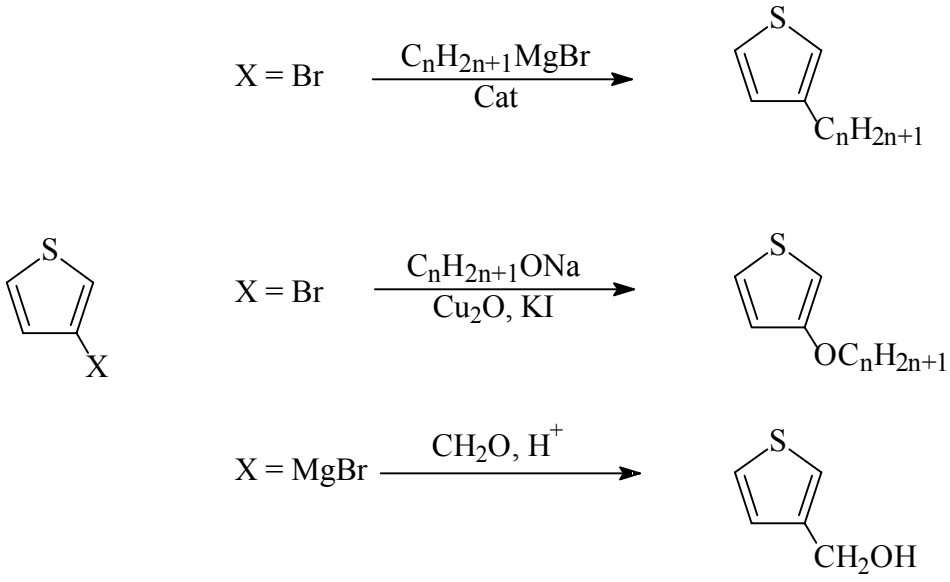

Scheme 4: functionalization of thiophene in the 3-position

Adding for example substituents with electron accepting or electron donating effect[18] will result in different energies of the molecular orbitals of the polymer, that means different electronic properties, such as UV-Vis absorption, light emission or oxidation potential.

As the delocalization of the π-electrons along the conjugated chain affects the energy gap of the molecular orbitals, one can design polymers consisting of oligothiophene sequences of different length in order to obtain different electronic properties[19], as schematized below (table 1). The values are shifted bathochromically compared to those of oligothiophenes of same length[20], due to the presence of the silyl group .

Table 1: different UV-Vis absorption peak position of different conjugated oligothiophenes

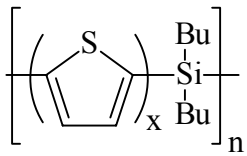

Sequence length (x)	λ_{max} (nm)	Oligothiophene	λ_{max} (nm)
2	330	Bithiophene	302
3	376	Terthiophene	355
4	412	Quaterthiophene	390
6	422	Sexithiophene	432

Beside that, any substituent that causes a twist of the thiophene rings along the main axis is responsible for a decreased conjugation and hence a larger energy gap.

Since these features are inscribed through the synthesis of the monomer, it is possible to prepare various polythiophenes with specific characteristics. Recent examples show how polythiophene was functionalized in order to meet a specific requirement: by using a PT bearing carboxylic side groups it was possible to bind the polymer to carbohydrates and to build a colorimetric sensor for viruses[21]. The same kind of polymer was self assembled on a chemically modified ITO substrate (fig. 4) that was then developed to a LED device[22].

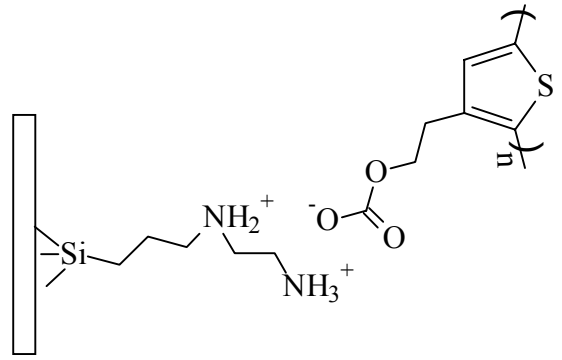

Figure 4: self assembly of polythiophene on modified ITO substrate

Poly(3,4-diethylenoxy)thiophene has found an interesting application in combination with fullerene in the design of a solar cell with good conversion efficiency[23]. Blends with polyvinylacetate and polycarbonate act as antistatic film[24] and poly(3-methylthiophene) seems suitable for electronic memory devices[25].

More unusual PT structures were described recently. It is the covalent combination of an electroinactive polymer with conjugated thiophene chains, leading to processable materials containing oligothiophene units. The classic way to synthesize such polymers is first to prepare a processable polymer that carries suitable functionalities in order to graft thiophene monomer under oxidative conditions. Thiophene could be grafted for example onto vinyl[26] or acrylic[27] polymers (sch. 5), because the electroinactive polymer carried oxidable side groups with a lower oxidation potential than thiophene monomer. During oxidation of a solution of the functionalized polymer and thiophene, the side chains of the former are oxidized first and can initiate the oxidative polymerization of thiophene, whose chains grow starting from the polymer side groups. The oxidizable thiophene groups in the precursor polymer needed to graft thiophene can be varied and contain functional groups that stabilize the monomer's oxidized state (i.e. alkyl, alkyloxy, thioalkyl …), and show therefore a lower oxidation potential than thiophene itself.

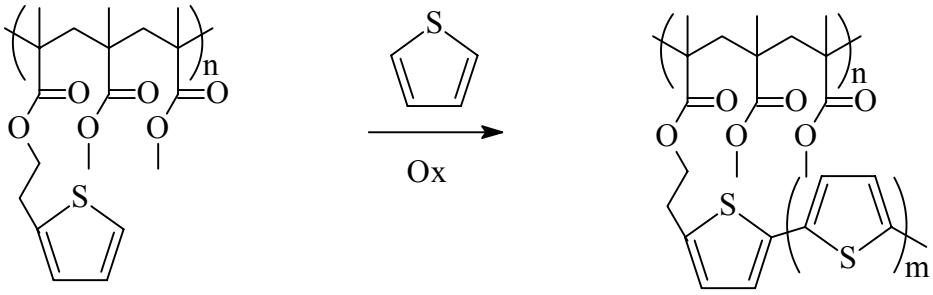

Scheme 5: grafting of thiophene onto not conjugated polymers

Oligothiophenes have also been widely used as initiators for oxidative polymer graft reactions, because they have a lower oxidizing potential than substituted thiophenes. For example the oxidation potential of bithiophene is 1.32 V/SCE[28] compared to 1.84 V/SCE[13] of 3-pentylthiophene. The redox potential of oligothiophenes decreases with increasing the number of α-linked thiophene units, as shown in figure 5 (from ref. 29) where the oxidation peak potential is plotted against the inverse conjugation length.

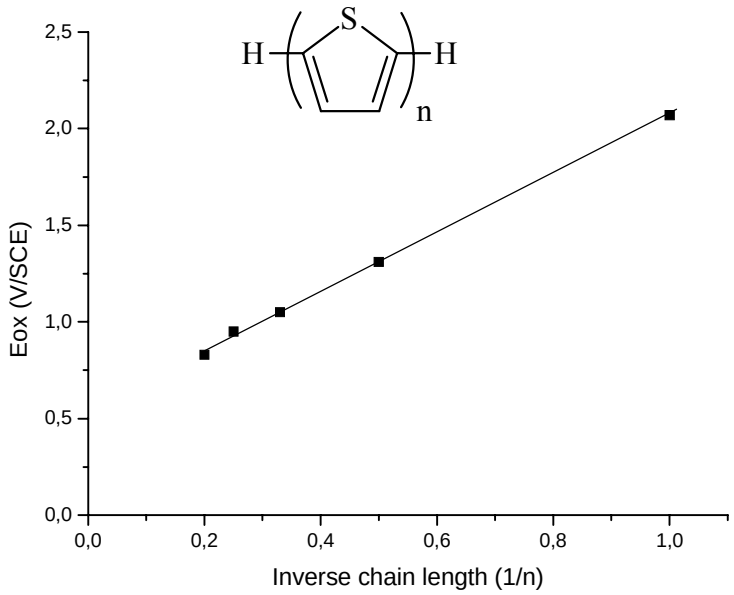

Figure 5: oxidation peak potential vs. inverse chain length (1/n) of oligothiophenes

If in an oxidating medium both thiophene and a thiophene oligomer are present, the oxidizing agent oxidizes first the oligothiophenes, that can thus initiate a graft reaction. This characteristic feature has been used to graft thiophene on processable polymers bearing oligothiophene side chains, as for example on methacrylic copolymers bearing terthiophene side chains[30] (sch. 6), as alternative way to that described in scheme 5.

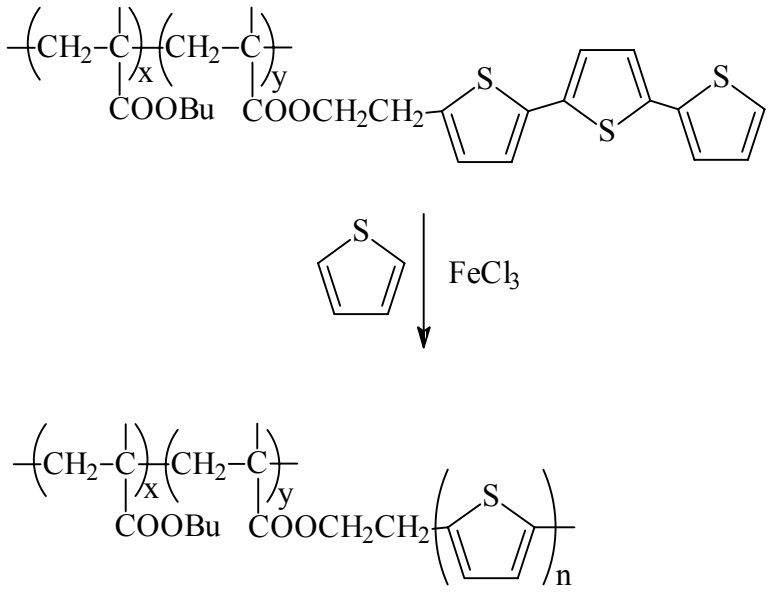

Scheme 6: grafting of thiophene on oligothiophene-functionalized polymers

1.2. The oligomeric strategy: defined structures with electrochemical properties

Oligothiophenes have been investigated not only as initiators for oxidative graft, but also as model compounds of the parent polythiophenes. As mentioned, polythiophene lacks through investigation due to the lack of solubility, so that it is necessary to furnish it with, e.g., alkyl substituents. This strategy has also disadvantages, because the substituents might change the intrinsic electronic properties of the polymer. The research focused therefore also on oligomers composed of few thiophene units (2-7)[31]. They exhibit similar electronic properties as polythiophene homopolymer, being at same time still soluble and moldable.

Polythiophenes obtained through oxidative polymerization show a detectable percentage of α-β' mislinkages that interrupt the conjugation of the rings. Plotting the UV-Vis transition energies against the inverse chain length (1/n) of oligothiophenes of defined structure, a good correlation is obtained (fig. 6, from ref. 32) from which the energy of the hypothetic polymer ($n \rightarrow \infty$, $1/n = 0$) can be extrapolated.

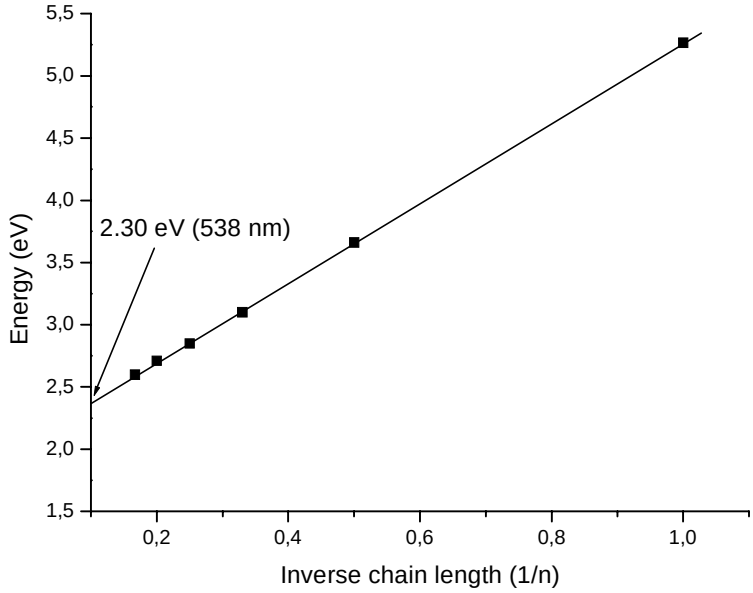

Figure 6: correlation of the absorption energies and inverse chain length (1/n) of oligothiophenes

Such extrapolated energy (2.30 eV) corresponds to a maximum absorption wavelength λ_{max} = 538 nm, which is higher than that found experimentally for polythiophene. The above correlation allows therefore the estimation of the apparent conjugation length of polythiophene, which is 10-11 α-linked units. That means that the electronic properties of the polymer should be modeled by oligomers containing the same amount of thiophene units[8], allowing one to better understand the structure-properties relationship of such well defined conjugated systems. Moreover, the possibility to purify the oligomers to a level not reachable for polymers, helps to clarify the mechanisms of electronic processes, e.g. charge transport, otherwise much influenced by impurities (e.g. solvent, electrolyte) present in polymer samples[33].

Beside that, the study of new synthetic strategies leading to fully characterizable α-α' linked oligothiophenes in quantitative yields represents a challenge to develop new polymerization routes.

-Synthesis

The synthetic routes that lead to polythiophenes can be used also for the synthesis of oligothiophenes. Indeed, under oxidative conditions a polymerization occurs if both α

positions of the oligomer, e.g. the dimer in scheme 7, are not protected. If one α-position of the dimer is blocked, the oxidation gives the tetramer exclusively.

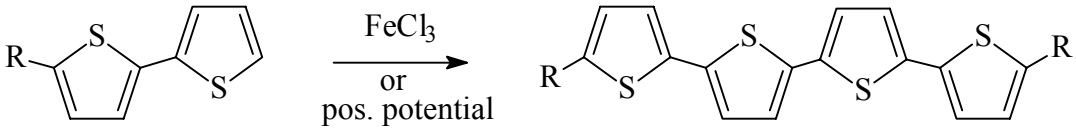

Scheme 7: oxidative synthesis of oligothiophenes

Most oligothiophenes are synthesized through reactions that lead to well defined α-α' linkages, such as the Pd-catalyzed cross coupling[34] (sch. 8A), the Ni-catalyzed *Kumada* coupling[35] (sch. 8B) or oxidative coupling reactions[36] (sch. 8C).

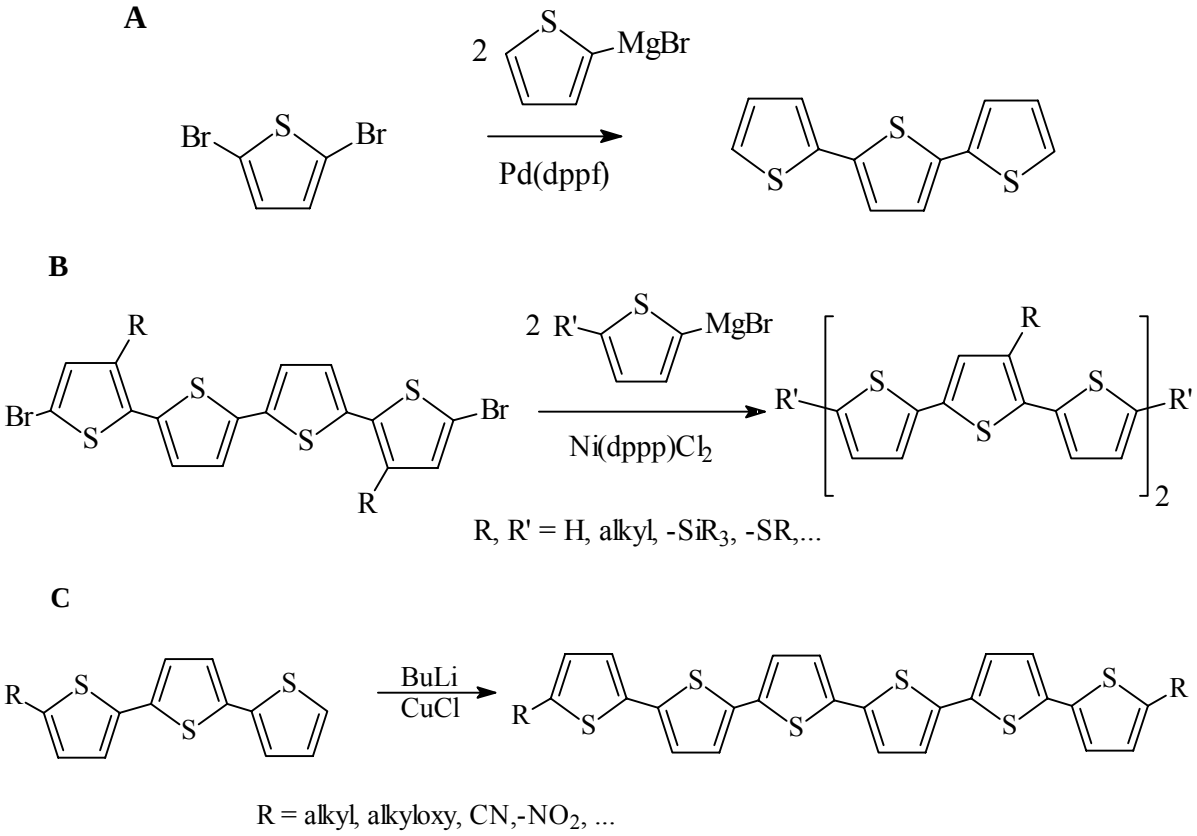

Scheme 8: Grignard and oxidative coupling reactions

Also the *Suzuki* coupling leads to α-oligothiophenes and offers the advantage that the organoboronic acid monomer can be isolated, in comparison to the Grignard and oxidative

couplings where the coupling reagent is obtained *in situ*. This increases therefore the yield of the catalyzed coupling[37] (sch. 9).

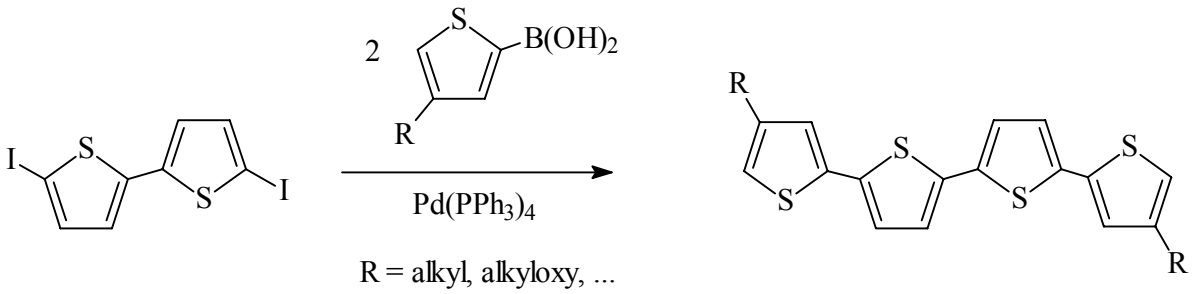

Scheme 9: Suzuki coupling between di-iodo-bithiophene and thienyl boronic acid

Another synthetic route concerns the formation of thiophene rings starting from diketones[8] or diethynyl[38] functionalities, leading to structures with an additional thiophene unit (sch. 10).

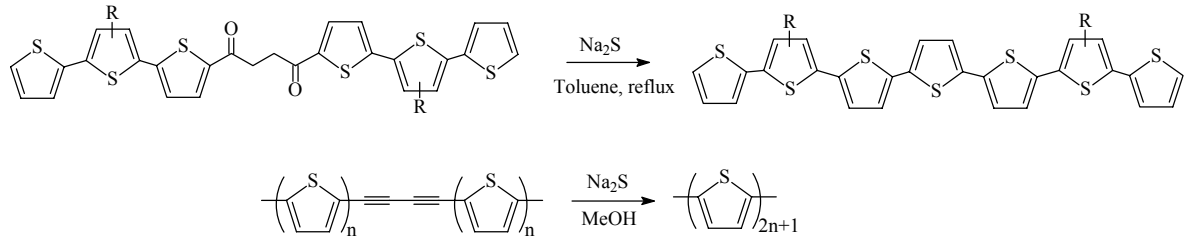

Scheme 10: ring-formation reactions as alternative routes to oligothiophenes

Lack of solubility occurs in all model compounds composed of more than 7 linearly linked thiophene units, so that side groups R are needed to provide for solubility and processability of the materials.

The preparation of electroinactive polymers bearing oligothiophenes is also of interest because in this way one introduces moieties that provide electrochemical properties to a electroinactive, processable polymer. Examples in literature deal with the preparation of polymers containing oligothiophenes as side chains[39,40] as well as in the backbone[41,42] (fig. 7)

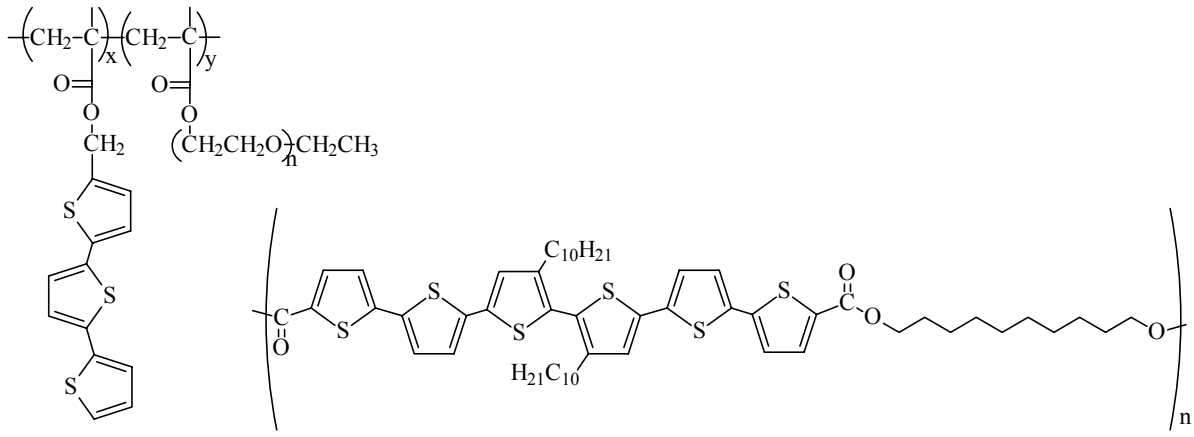

Figure 7: copolymers containing oligothiophene as side chains (left) or in the main chain (right)

A big advantage over low molecular weight materials is the possibility to prepare polymeric films of oligothiophenes, though incorporated in an electroinactive matrix, a feature of great importance in the design of electronic devices.

Such type of polymers are obtained performing a block copolymerization[43], a condensation polymerization[44,45] (sch. 11A), or an addition polymerization[46,47] (sch. 11B)

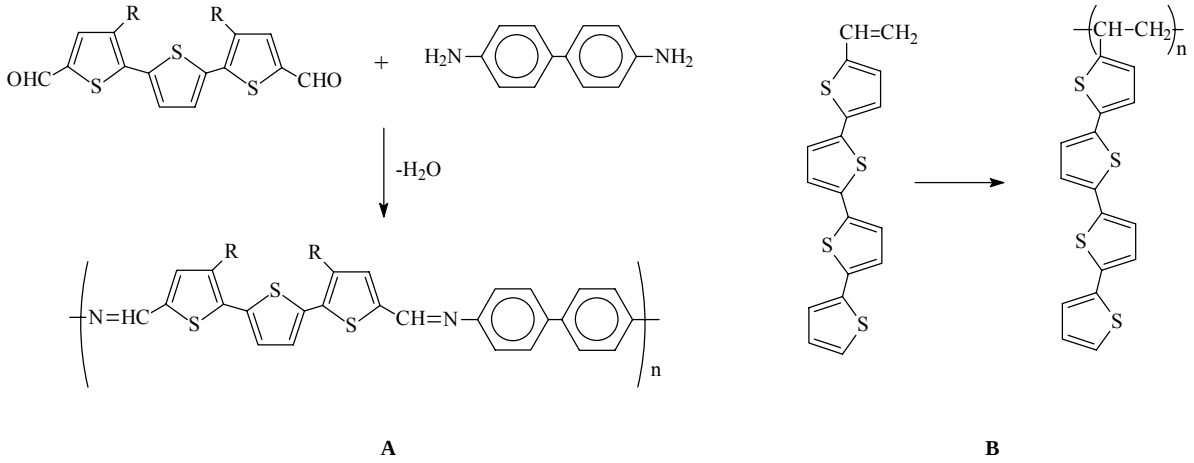

A **B**

Scheme 11: polycondensation (A) and chain polymerization (B) toward oligothiophene containing polymers

-Properties

When both α-positions of the oligothiophene are protected, the oxidative coupling cannot occur upon oxidation and instead a stable radical ion is obtained, which upon a further reduction step can go back to the neutral state. Such reversible oxidation-reduction cycles

(*doping* and *de-doping*) change the electronic structure of the molecule and therefore all the properties depending on them. This gives rise to different phenomena: for example, upon oxidation oligothiophenes show an electrical conductivity, whose magnitude is proportional to the degree of doping. Additionally, the doped oligothiophene shows a different UV-Vis absorption with respect to the neutral one: new absorption bands will be noticed (electrochromism), as other transitions are now possible due to new energy levels[46]. So the same doped molecule can be used in the preparation of a conducting material or can be applied as electrochemical device, depending on the macroscopic property (i.e. application) to which the oligothiophene is addressed.

The properties shown by oligothiophenes, such as fluorescence[48], thermochromism[49], electroluminescence[50], electrochromism[51] and electrical conductivity[52], suggest the application of such systems not only as model compounds but also as new electronic materials.

-Applications

The development of new technologies based on micro- and nanostructures offers many possibilities for the application of oligothiophenes, due to the versatility of the synthesis as instrument for tuning the properties of the resulting material. A high degree of order at a molecular level is required in order to obtain the maximum yield in the desired function of the device. Already in 1974 Schöler *et al.*[53] demonstrated the possibility of constructing photoelectric devices based on a planned molecular architecture, studying LB alternate monolayers of quinquethiophene and cadmium arachidate on Al-substrates.

A self assembling behavior, i.e. the achievement of ordered molecular structures on defined pre-existing matrices, causes an anisotropy of the conjugated chains that enhances the light emitting properties, important feature for electroluminescent and LED devices[22].

Chemical reactive side groups allow the ordering process on particular surfaces, like in the case of thiol-functionalized terthiophenes which were assembled on gold substrates[54]. The authors claim that such stable and highly oriented monolayers can represent the basic material for the development of *molecular electronic* devices to perform biochemical and chemical sensing.

A double alkylic substitution on the hexamer causes self assembling of α,α'-dihexylsexithiophene on a silicon substrate[55] (fig. 7, left), which was tested as a field effect

transistor. Otherwise, the moiety can be part of a polymer that shows good self assembling behavior, like in the case of the polyazomethine[45] of figure 8 (right) assembled on polar substrates: the latter case represents an additional method to obtain anisotropically disposed oligothiophene chains.

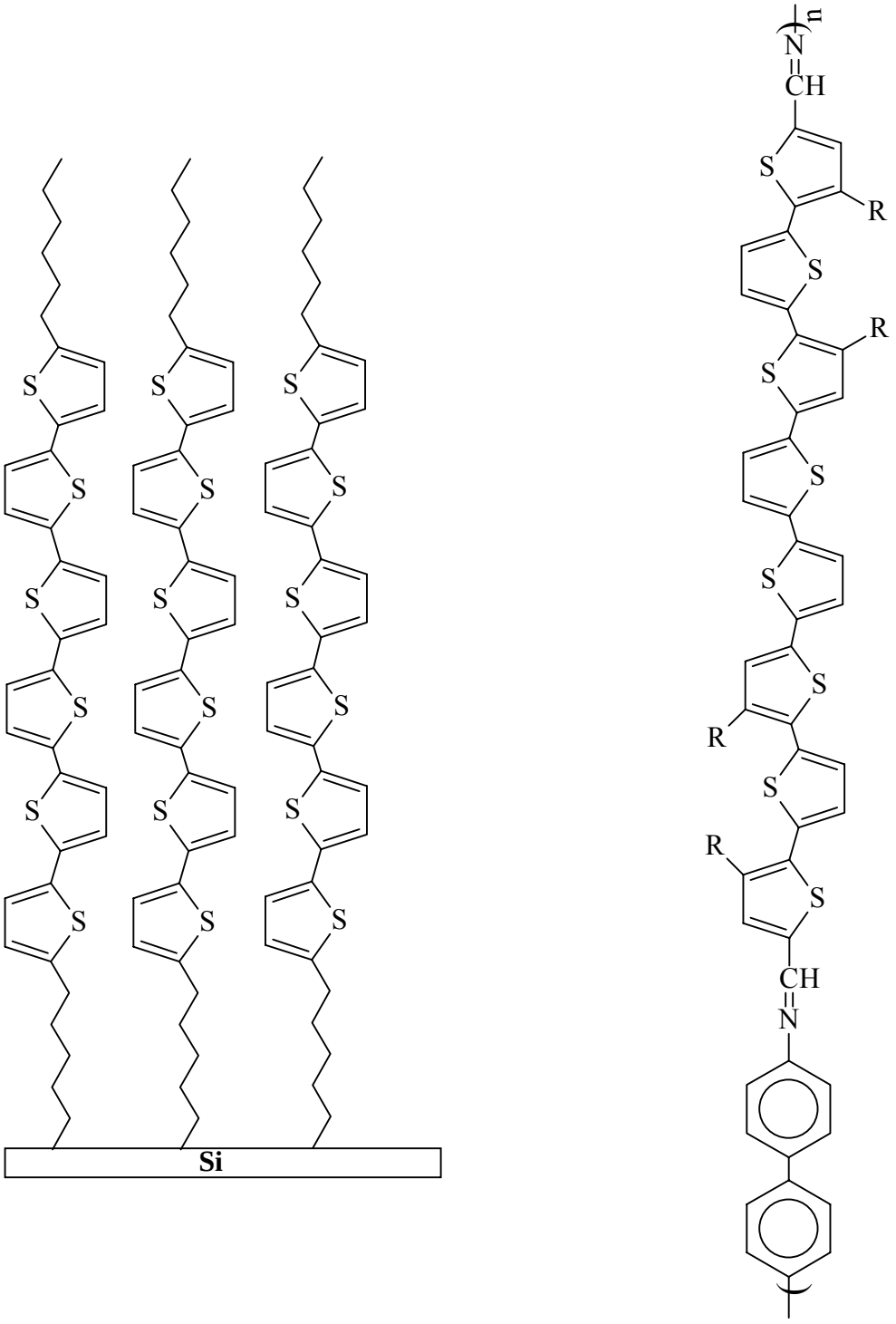

Figure 8: oligothiophenes showing self assembling behavior

2. AIM OF THE THESIS

Due to the increasing demand for electronic devices using conjugated poly- or oligothiophenes as electroactive materials[56], it is of interest to investigate polymeric materials containing chemically linked conjugated oligomers of thiophene. Such materials, having conjugated oligothiophenes with defined structure, permit a clear investigation of their structure-properties relationships.

The aim of the present work is the preparation and characterization of polymers bearing oligothiophene side chains and the investigation of their electrochemical properties. This goal can be reached in two ways: one is the functionalization of a polymer that carries functional groups suitable for the attachment of oligothiophenes. The other way is the synthesis of a monomer bearing oligothiophene side groups and its polymerization.

In both cases the aim of the work is the synthesis of a soluble polymer, so that a full investigation of its electrochemical properties can be carried out.

Our aim was the preparation of a cylinder-like polymer, whose long axis is represented by the macromolecular skeleton and the radius by the oligothiophene side chains, in order to obtain a material with anisotropic shape showing conductivity along the main direction (fig. 9).

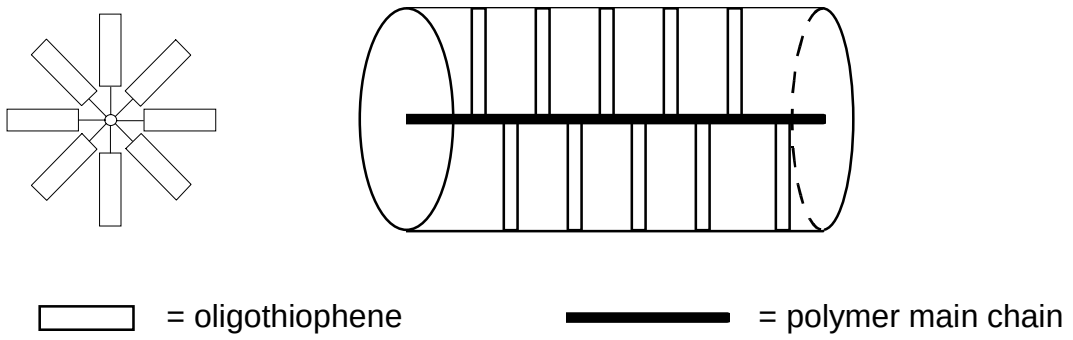

Figure 9: schematic representation of an anisotropic shaped polymer with oligothiophene side chains

This polymer can be viewed as a "nanowire", and the electrical conductivity of single macromolecules can be determined, as shown schematically in figure 10.

Contrary to single molecule conductivity reported in literature, it is not the conduction along one π-system but along several π-systems present on the same molecule which is of interest.

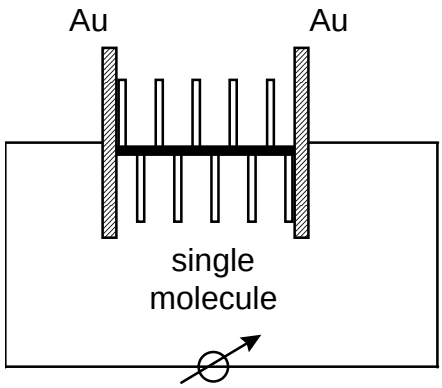

Figure 10: schematized device for the measurement of the electrical conductivity at a molecular level

This strategy consists in the preparation of an oligothiophene bearing a polymerizable functional group that leads to a polymer with flexible main chain, such as for example acrylic esters.

Properly substituted oligothiophenes represent suitable molecules that can be used in developing electronic devices where the electroactive moieties can be eventually ordered at a molecular level. This feature is essential to achieve high efficiencies related to charge carrier transport (e.g. electrical conductivity and light emission from LEDs). The Langmuir-Blodgett (LB) technique is useful to obtain a planned architecture on solid substrates of both low and high molecular weight materials and represents therefore an important tool where anisotropy at a molecular level is required. The interest of this study is also the electronic behavior, in particular conductivity, of conjugated oligothiophenes ordered at a supramolecular level. Therefore, a processable polymer, also suitable for the LB technique, was chosen as matrix for the graft of oligothiophenes.

3. RESULTS AND DISCUSSION

3.1. Synthetic strategies

The goal of the work was the preparation of a polymeric material with chemically linked oligothiophene moieties, which can show the properties typical of conjugated thiophenes, such as electrochromism, solvato- and thermochromism, as well as electrical conductivity.
The choice of the polymeric matrix depends on the strategy that is followed to obtain the desired macromolecule. It has in any case to be processable and to carry well defined units of conjugated thiophene moieties.
The synthetic strategies possible to obtain this kind of macromolecules are the following:

- the functionalization of a pre-existing polymer with an oligothiophene moiety (thiophene graft reaction)
- the synthesis of a monomer bearing oligothiophene side chains and its polymerization

The thiophene graft reaction is described in literature to obtain polythiophene side chains on a target polymer. In this case oligothiophenes themselves can be used to attach other thiophene monomers[30,57] (see scheme 6, page 9).
In general, the polymer onto which the oligothiophene will be linked should be well processable and have functional groups, through which the functionalization reaction can be carried out. One has the advantage represented by the choice among a wide variety of commercially available polymers, but on the other hand it has to be taken in account that functionalization reactions on polymers never lead to a 100 % yield, that means that it is impossible to substitute every monomer with the desired moiety.
The second strategy, i.e. the preparation of a monomer carrying oligothiophene side chain and its further polymerization, needs additional synthetic work compared to the first strategy, but in this way it is possible to obtain a polymer whose main chain will bear an oligothiophene moiety at every monomer unit.
We investigated polymers bearing oligothiophene side groups prepared by both synthetic strategies.
The structure of the oligothiophenes, in terms of conjugation length and type of substitution, was chosen as a compromise between length and synthetic efforts. In fact, the magnitude of

the electrical conductivity is directly correlated to the conjugation length of the oligomer and the stepwise oligomer formation, followed by purification, is time consuming.

3.1.1. Functionalization of a polymer with oligothiophene moieties

In order to follow this synthetic strategy, the polymer must have a functionality suitable for the attachment of the thiophene oligomer, that can be performed either through a coupling between two thiophene containing moieties or through a reaction between two different functionalities present both on the polymer and the oligothiophene.

The first possibility provides for a final polymer in which the length of the thiophene oligomer is at least one unit longer than the oligothiophene to be grafted and can be performed following an oxidative coupling or a Grignard coupling.

The second possibility takes into account the synthesis of a substituted oligothiophene carrying a functional group that can be reacted with the functional groups on the available polymer (sch. 12); this strategy offers the advantage that the synthetic work prior to the grafting concerns only the oligothiophene moiety.

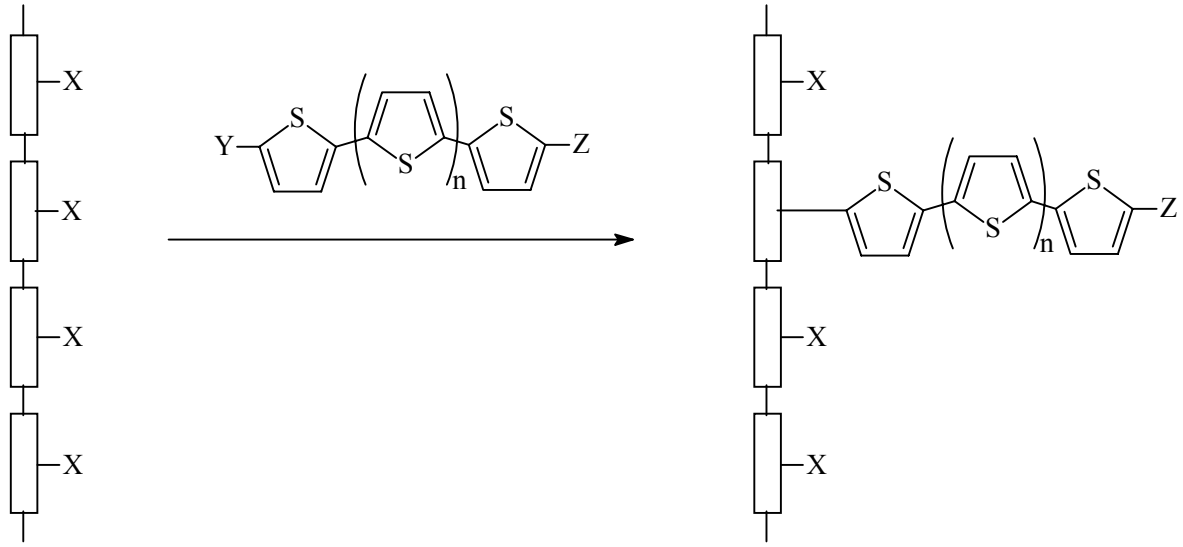

Scheme 12: functionalization of a polymer with an oligothiophene moiety

We chose to use the second strategy and our work was divided in the following three steps:

- Choice of the processable polymer with reactive functional groups

- Synthesis of a functionalized oligothiophene
- Linking reaction between polymer and oligothiophene

The polymer chosen was a cellulose derivative that shows good processability, gained through alkyl substituents, together with the possibility of being ordered at the air-water interface by means of the Langmuir-Blodgett (LB) technique[58].

The same cellulose derivative was functionalized with two kinds of oligothiophenes, aiming the investigation at the different features arising from the difference in the oligomeric structures. The chosen conjugated thiophene systems were α-substituted 2,2':5',2''-terthiophene (hereafter referred to as *terthiophene*) and α, α'-disubstituted-β', β''''-dialkyl-2,2':5',2'':5'',2''':5''',2'''':5'''',2''''':-sexithiophene (hereafter referred to as *sexithiophene*).

Although the sequence length is only three monomer units, terthiophene and its derivatives show some of the features observed in polythiophenes, like thermochromic[59], solvatochromic[60] and electrochromic behavior[47]. As already mentioned, the length of the molecule is enough to gain stability of the oxidized state of terthiophene with respect to the monomer. Hence terthiophene will undergo redox cycles in a totally reversible way if its α-positions are prevented to react[61]. Otherwise, if only one α-position bears a substituent, sexithiophene is obtained by terthiophene oxidation, or unsubstituted terthiophene can polymerize and a homopolymer is obtained.

Sexithiophene shows a lower oxidation potential than terthiophene, the former of 0.84 V/SCE[62] and the latter of 1.01 V/SCE[63], due to the increased length of six units. Electrochemical properties typical of conjugated thiophenes are also shown by sexithiophene[42,64], where a high stability of the radical-cation species that are formed upon oxidation is achieved due to the six conjugated rings. Therefore polymerization or dimerization of sexithiophene upon oxidation appear to be less probable than in the case of terthiophene[40]. The conjugation of the π-electrons along six thiophene rings is also responsible for a high charge mobility in the oxidized state, that is manifested in electrical conductivity [65] of about 10^{-6} S/cm.

3.1.2. Synthesis of monomers bearing oligothiophene side chains and their polymerization

We chose the synthesis of monomers carrying the oligothiophene moiety as side chain of the polymerizable functionality (sch.13). Accordingly, the oligothiophene system must be functionalized with a group suitable for a polymerization reaction in which the oligothiophene moiety itself does not take part. Addition or condensation polymerizations that concern functional groups present at the oligothiophene monomer lead to a homopolymer bearing conjugated thiophenes groups

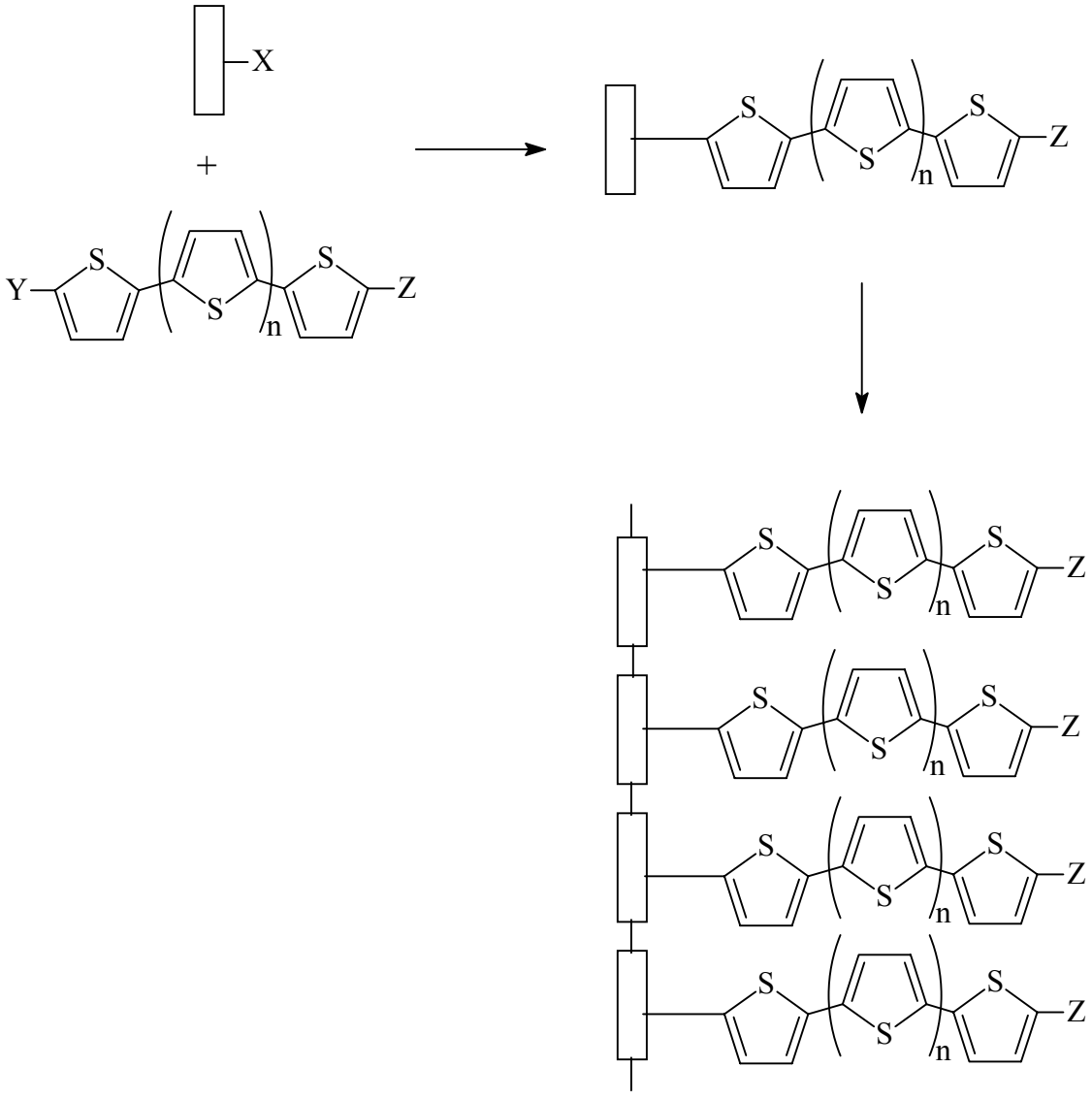

Scheme 13: polymerization of a monomer bearing an oligothiophene side chain

The chosen strategy followed these four steps:

- Choice of the polymerizable functional group
- Synthesis of substituted oligothiophene
- Linking reaction between polymerizable functional group and substituted oligothiophene
- Polymerization of the monomer bearing oligothiophene side chains

An acrylic system was chosen as polymerizable group in order to perform a free-radical polymerization. With this kind of polymerization an atactic polymer is obtained, whose main chain has a sufficient degree of freedom that provides for processability of the polymer, as found for poly(terthienylethyl)methacrylate in a previous work[30].
Also a catalyzed condensation polymerization between diethynyl- and diiodo-benzenes was performed, aiming at the preparation of a polymer with oligothiophene side chain with a different structure with respect to the acrylic one.
We synthesized for this purposes an oligothiophene monomer of six conjugated thiophene rings (i.e. sexithiophene) which was then differently functionalized according to the chosen polymerization route.

3.2. Synthesis of oligothiophenes

3.2.1. Synthesis of terthiophenes

Aiming at the synthesis of a substituted terthiophene suitable for the further derivatization of a cellulose derivative, terthiophene was first prepared following a Grignard coupling reaction described in scheme 14:

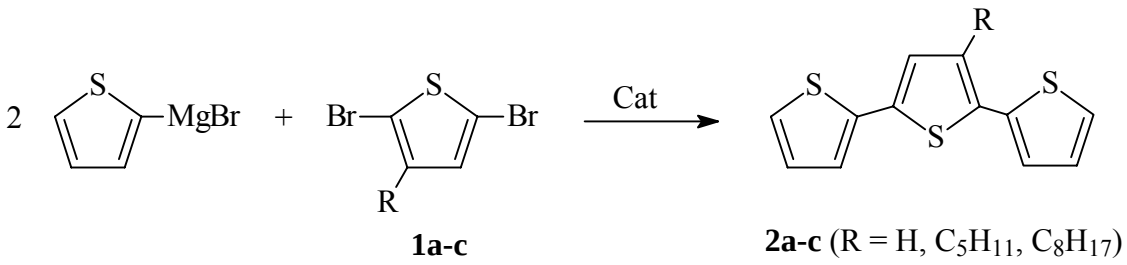

Scheme 14: synthesis of terthiophenes

Two widely used catalysts were used for this reaction, Palladium (II) 1,1'-bis(diphenylphosphinoferrocene) chloride and Nickel (II) 1,3-bis(diphenylphoshino)propane chloride, and it was found that conversion was higher using the former.

The same reaction conditions were followed for the synthesis of 3'-alkylsubstituted terthiophenes **2b-c**, where in this case the 2,5-dibromothiophene carries an alkyl substituent at the 3-position (sch. 14). The alkyl substituted terthiophene was then used as building block for the preparation of sexithiophene.

Several terthiophene derivatives have been prepared in recent works, bearing different substituents at their α positions, such as for instance methyl[31,32] or methoxyl[60]. The authors found a synthetic route[30] to provide terthiophene with the suitable functionality in order to obtain a cellulose derivative, which can be used to construct LB films. In order to couple the terthiophene moiety on the cellulose derivative, a Williamson ether synthesis was chosen, reacting the free -OH groups of cellulose with a primary chloride functionality, which has therefore to be introduced on the terthiophene molecule. This kind of substituted terthiophene was obtained in two steps, as described in scheme 15:

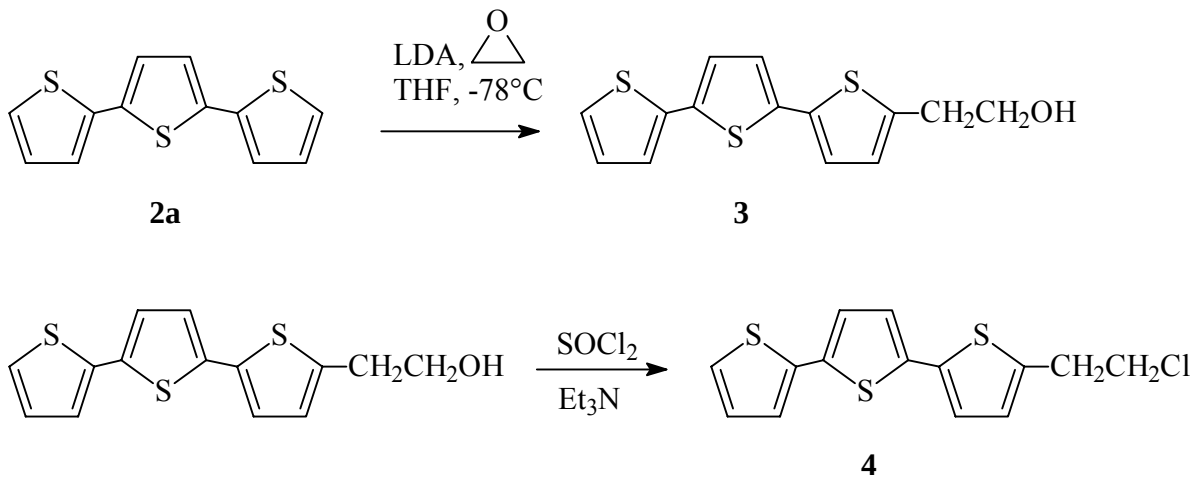

Scheme 15: functionalization of terthiophene

3.2.2. Synthesis of monomers containing α, α'-disubstituted sexithiophenes

As is well known from the literature[64], higher oligomers of thiophene as sexithiophene need an additional functional group to increase the solubility in common organic solvents, the unsubstituted sexithiophene being poorly soluble in most solvents.

Alkyl groups appear to be suitable to provide solubility for oligomers as well as for polythiophene[66], so we chose to synthesize a sexithiophene bearing two alkyl side chains. The length of the alkyl group should be chosen as the *optimum* value according to the solubility requirement and the need to avoid side chain crystallization, whose probability increases also with the chain length. In fact, crystallization of the alkyl side groups should be avoided because this may cause a decrease in the solubility of the resulting polymer carrying the alkyl-substituted sexithiophene, which itself is a stiff group that is expected to decrease the mobility of the polymer and hence its processability.

According to a literature procedure[64], we chose to synthesize sexithiophenes with a pentyl and with a octyl side chain (sch. 16), having so the possibility to study the influence of the two different chain lengths on the properties of the oligothiophene.

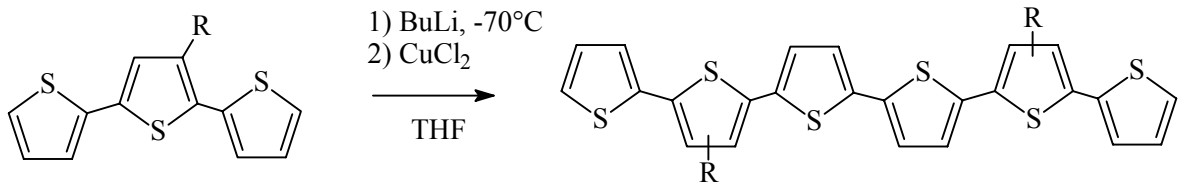

2b-c **5a-b** (R = C_5H_{11}, C_8H_{17})

Scheme 16: synthesis of alkylsexithiophenes

This reaction proceeds via deprotonation of the α-position of the terthiophene by *n*-butyllithium (BuLi). The further addition of copper (II) chloride is necessary for the oxidative coupling of two anions (sch. 17).

As both hydrogens on the α-positions show the same acidic character, non-symmetric terthiophenes (as **2b-c**) give after deprotonation a mixture of isomeric anions. Therefore, upon coupling with $CuCl_2$ three isomers of sexithiophene are generated, bearing the alkyl groups either in the 3', 4"" or 3', 3"" or 4',3"" positions of the oligomer, in a ratio of 1:2:1, respectively. The mixture of the three isomers is generally referred to as β', β""-dialkyl-sexithiophene.

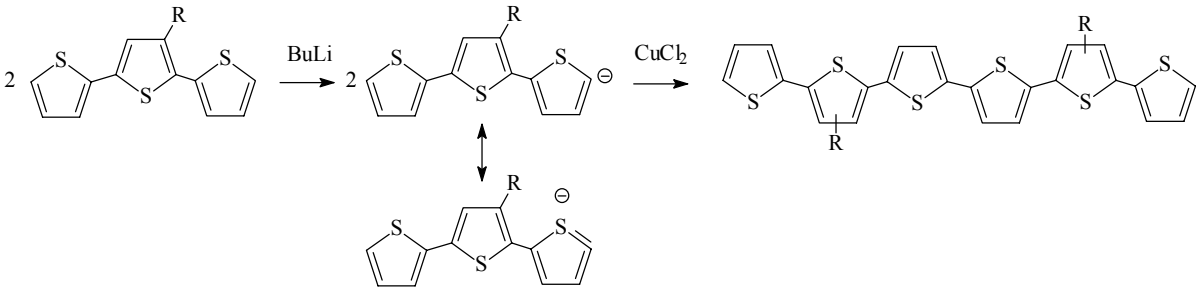

Scheme 17: mechanism of the copper-catalyzed oxidative coupling of terthiophene

The same reactivity of the α hydrogens of terthiophene makes it also statistical possible for BuLi to deprotonate both sides of a same terthiophene, that leads to polymerization of the molecule (sch. 18).

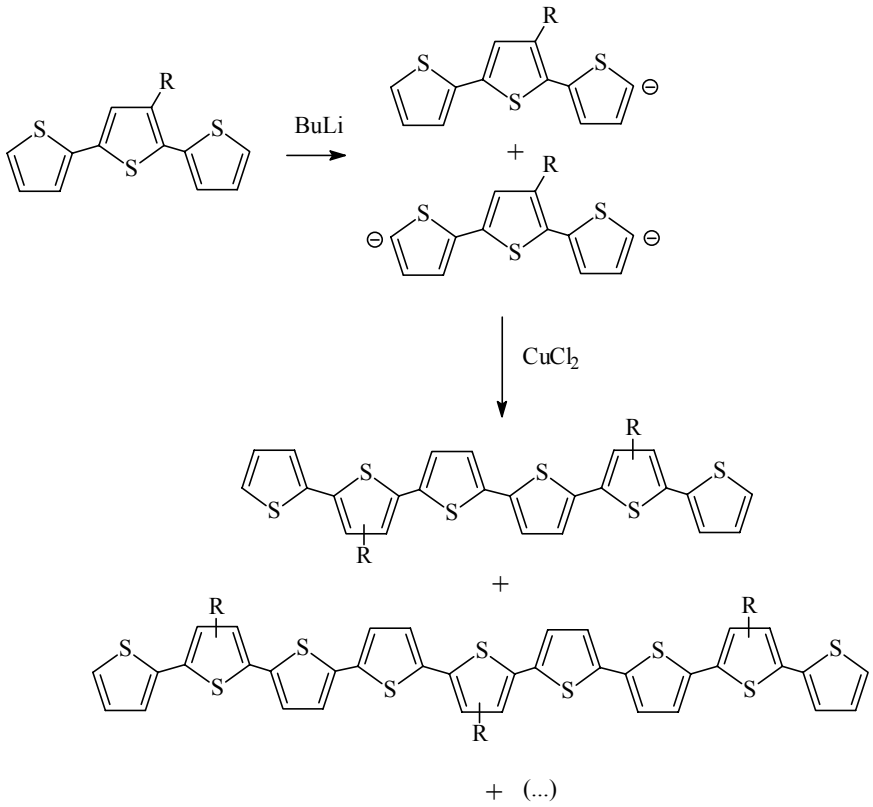

Scheme 18: side reaction during the terthiophene oxidative coupling

To minimize the double deprotonation of the terthiophene, an excess of terthiophene with respect to BuLi, respectively 2.5:1, was used. The amount of $CuCl_2$ appeared to play no role in the formation of higher oligomers, as one could suppose from the oxidative behavior of Cu (II) salts[6]. Indeed performing the synthesis using only $CuCl_2$ without BuLi led to unreacted terthiophene, that means that the formation of the anion is a necessary step for the coupling.

The functionalization of sexithiophene, with regard to the synthesis of a polymerizable monomer, was chosen with respect to the further investigations of the electrochemical properties of the resulting polymer. As already described, the electrochemical properties of sexithiophene arise from the oxidation of the molecule. Therefore, under oxidative conditions undesired coupling reactions through eventually free α-positions must be avoided, in order to prevent crosslinking of the sexithiophene-grafted polymer. Thus, the α-position of the sexithiophene which is not grafted to the polymeric backbone must be blocked with an electrochemically inactive group.

For this purpose, sexithiophene was di-functionalized by addition of ethylene oxide to the dianion. The product affords a new functional group (-OH) in the 2-hydroxyethyl pendant, that is suitable for further reactions. The hydroxy-ethylation was performed following the

same reaction conditions used for the synthesis of the 2-hydroxyethyl-terthiophene **3**[30], as the reactivity of the α-hydrogens of sexithiophene was expected to be comparable to those of terthiophene (sch. 19).

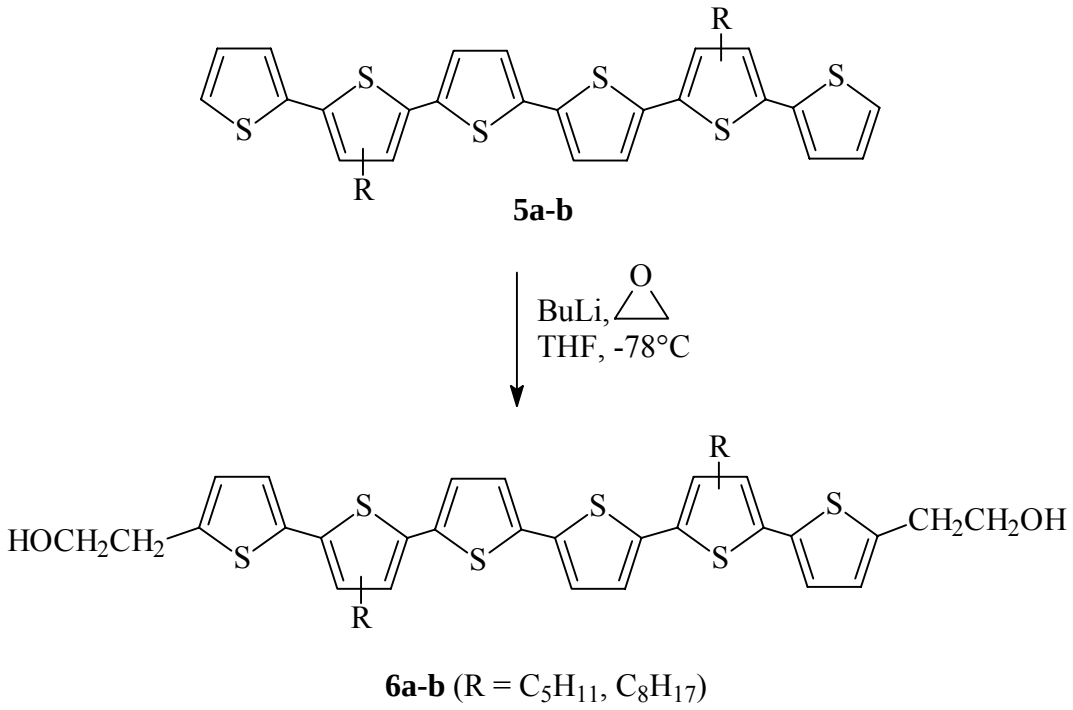

Scheme 19: synthesis of dihydroxyethyl-functionalized sexithiophene

After deprotonation of sexithiophene **5a-b** by BuLi, liquid ethylene oxide was added in a slight excess (ca 2.5 : 1). No poly(oxyethylene) substitution was observed because of the low reactivity of the formed Li-ethoxylate toward ethylene oxide. The product was obtained in a 35 % yield after repeated chromatography on silica-gel.

The new sexithiophene derivative **6a** was the building block for the synthesis of polymers containing sexithiophene side chains, prepared following both the polymer functionalization (graft) and the polymerization strategy. In any case, the sexithiophene molecule does not have the possibility to react upon oxidation through the substituted α-positions.

3.2.2.1.Synthesis of activated sexithiophene for cellulose functionalization

As in the case of derivatization of butylcellulose with terthiophene, a Williamson ether synthesis was chosen to obtain butylcellulose bearing sexithiophene side chains. In that case

the –OH groups of the cellulose act as nucleophiles and a proper activated terthiophene derivative as electrophile.

β',β''''-dipentyl-5,5''''''-bis(2-hydroxyethyl)-2,2':5',2'':5'',2''':5''',2'''':5'''',2''''':5''''',2''''''-sexithiophene (**6a**), hereafter referred to as $PenST(OH)_2$ (fig. 11), needs to be activated on a single –OH position in order to undergo the Williamson ether synthesis. Activation on both –OH groups was absolutely to be avoided because it would cause crosslinking between two cellulose macromolecules in the ether synthesis, resulting in an unprocessable material.

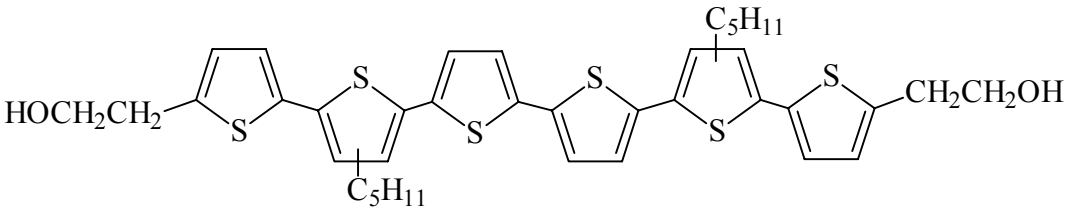

$PenST(OH)_2$ (6a)

Figure 11: β',β''''-dipentyl-5,5''''''-di(2-hydroxyethyl)-2,2':5',2'':5'',2''':5''',2'''':5'''',2''''':5''''',2''''''-sexithiophene

Since the activation of the bis(hydroxyethyl)sexithiophene is a statistical process, the activating group must be also easily cleavaged on need. This feature allows one to reconvert the statistically di-activated $PenST(OH)_2$ in the corresponding unsubstituted molecule.

On this basis, the p-toluenesulfonic monoester of $PenST(OH)_2$ was chosen as activated moiety for the functionalization of cellulose, because the p-toluenesulfonate is a good leaving group both in the Williamson ether synthesis and in the saponification reaction.

This new sexithiophene derivative **7**, i.e. 2-[β',β''''-dipentyl-5''''''-(2-hydroxyethyl)-2,2':5',2'':5'',2''':5''',2'''':5'''',2''''':5''''',2''''''-sexithiophen-5-yl]-ethyl p-toluensulfonate (hereafter referred to as PenSTOHTs) was synthesized reacting an equimolecular amount of $PenST(OH)_2$ (**6a**) and p-toluensulfonyl chloride, as described in scheme 20.

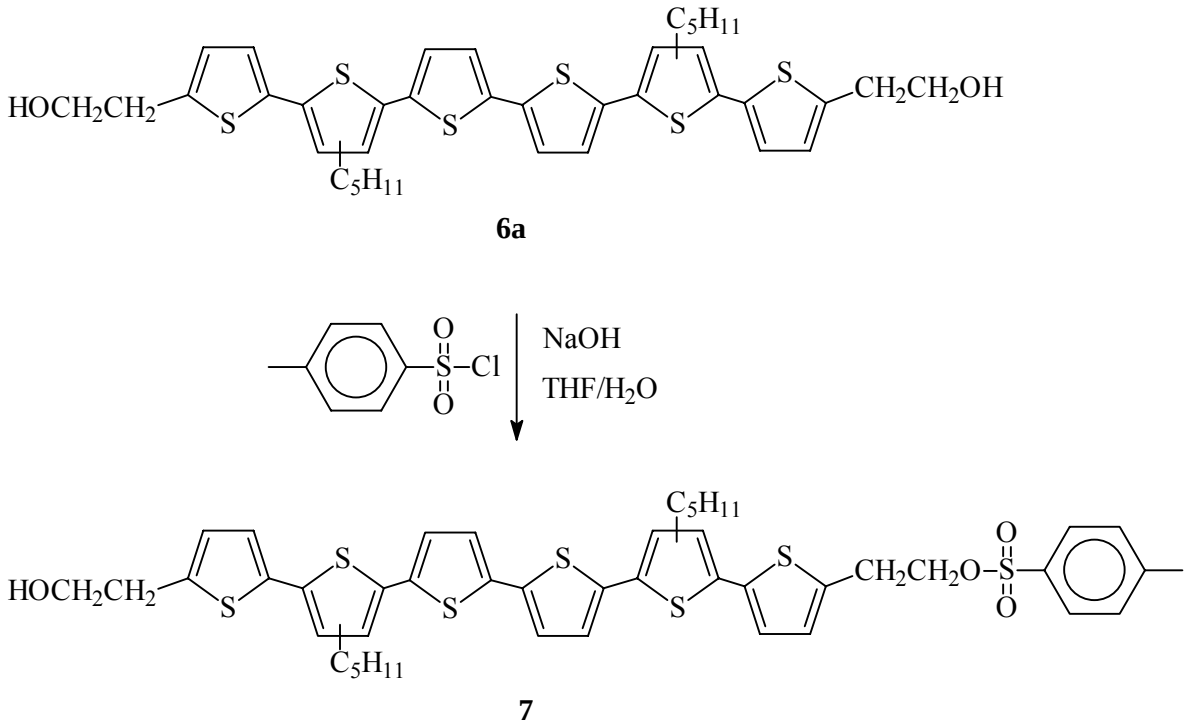

Scheme 20: activation of $PenST(OH)_2$

The product was obtained only in a low yield (25 %) and no formation of the di-substituted side-product was observed.

3.2.2.2.Synthesis of acrylates containing sexithiophene

$PenST(OH)_2$ was the conjugated block chosen for the synthesis of the acrylic monomer bearing sexithiophene. During the connection of such oligothiophene to the acrylic moiety a double functionalization had absolutely to be avoided, because the di-acrylic functionalized monomers would act as crosslinkers in the radical polymerization, giving rise to an insoluble polymer. Monofunctionalization of such a symmetrical structure needs the use of a large excess of the molecule with respect to the reagent, in order to react only one of the –OH groups present. Due to the limited availability of the sexithiophene derivative, this was not possible and synthetic steps outlined here involving monosubstitution on $PenST(OH)_2$ gave only an average yield of 20-30 %.

The acrylate functionality was introduced on PenST(OH)$_2$ (**6a**) performing an esterification of the alcoholic group with acryloyl chloride (sch. 21), in the presence of triethylamine (Et_3N) as base:

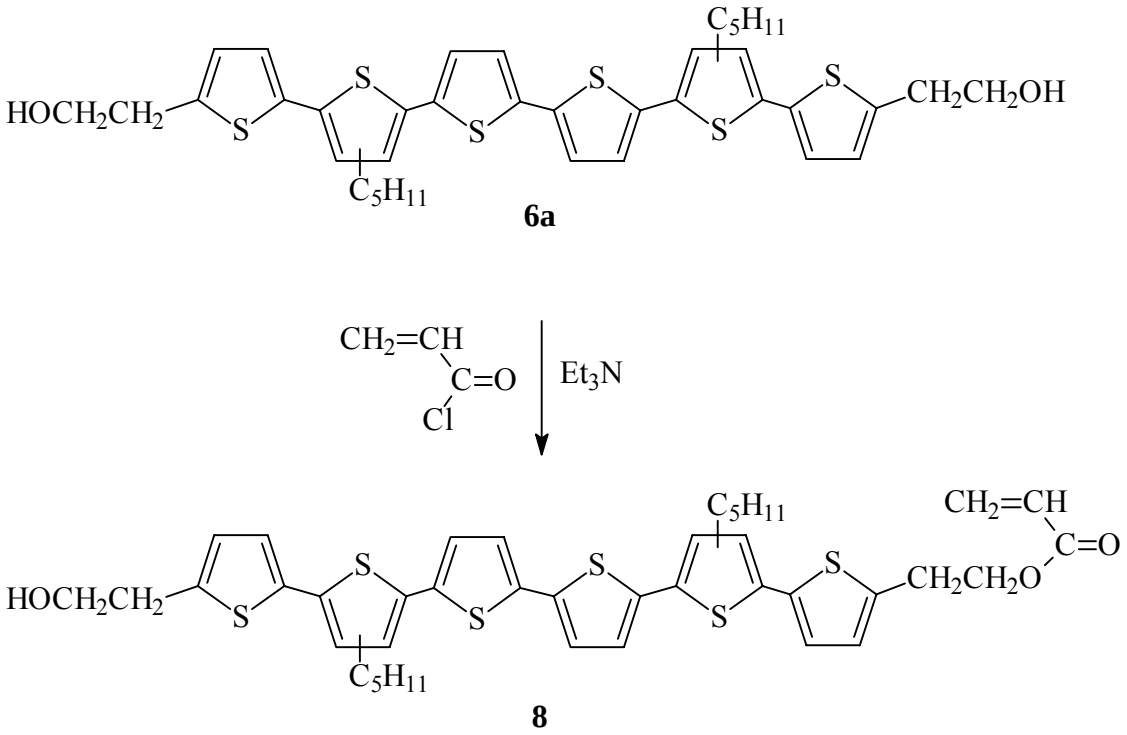

Scheme 21: introduction of the acryloyl moiety on PenST(OH)$_2$

PenST(OH)$_2$ and acryloyl chloride were used in a ratio of 2:1 ca., respectively, and the yield of the pure acrylate **8** was 35 %; chromatographic purification was necessary to isolate the monoacrylate from the statistically formed di-acrylate and the unreacted sexithiophene. The collected di-acrylate was then saponified by aqueous NaOH in THF in order to recover the PenST(OH)$_2$ moiety.

The acrylic double bond is two methylene units apart from the conjugated thiophene rings, so that any electronic effect of sexithiophene on its reactivity toward radical polymerization is considered to be negligible.

3.2.2.3.Synthesis of diethynyl-aryls bearing sexithiophene

Beside the radical polymerization, which leads to a more or less flexible polymer, the monomers described now should lead, after polymerization, to a rather rigid polymer.

For this purpose, we chose to perform a Pd-catalyzed polymerization of di-iodo benzenes with di-ethynyl benzenes, as such monomers can be substituted with the desired sexithiophene moiety on the benzene ring.

As for the synthesis of the acrylic monomer, also this strategy started from $PenST(OH)_2$ to link the conjugated thiophene moiety to the benzenic monomer. Again, the alcoholic functionality on the sexithiophene derivative can be esterified with the polymerizable monomer.

The final polymer must carry, according to our aims, a sexithiophene group on every monomer unit, so that on both the di-iodo and the di-ethynyl monomers the conjugated moiety must be present.

Following these criteria, we chose to start the synthesis from the commercially available 2-amino-5-iodobenzoic acid **9**, that was first converted to the corresponding diazonium salt, and then to the 2,5-diiodobenzoic acid **10** (sch. 22).

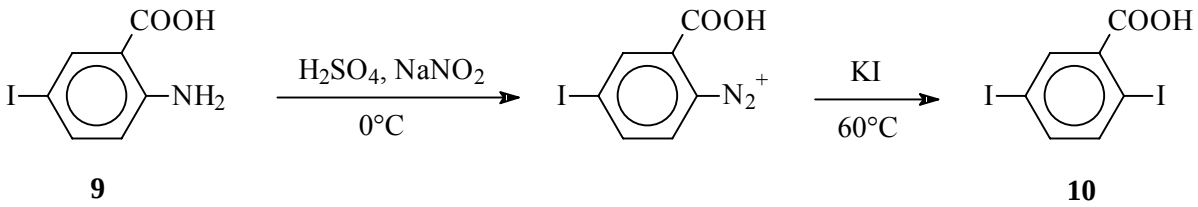

9 **10**

Scheme 22: reaction routes for the synthesis of 2,5-diiodobenzoic acid **15**

The obtained 2,5-diiodobenzoic acid **10** has now two different functionalities that can be used to introduce two different moieties: the sexithiophene containing di-alcohol at the carboxylic carbon and two ethynyl groups at the iodo-substituted ones. We chose to perform the derivation with sexithiophene as first reaction, following two different strategies.

The benzoic acid was converted to the corresponding acid chloride **11** by reaction with thionyl chloride (sch. 23).

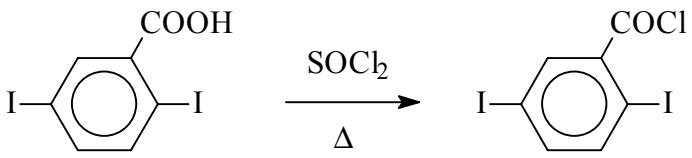

10 **11**

Scheme 23: formation of the diiodo-benzoic acid chloride

The product **11** appeared to be not very stable in air, it partly hydrolyzed back to the acid and traces of the corresponding anhydride were also found.

To assure a monosubstitution on the $PenST(OH)_2$ molecule during the esterification reaction, we decided to protect one of the two alcoholic groups with an alkylsilyl derivative (sch. 24). The obtained silanol ether **12** is stable under the reaction conditions that are planned for the further esterification.

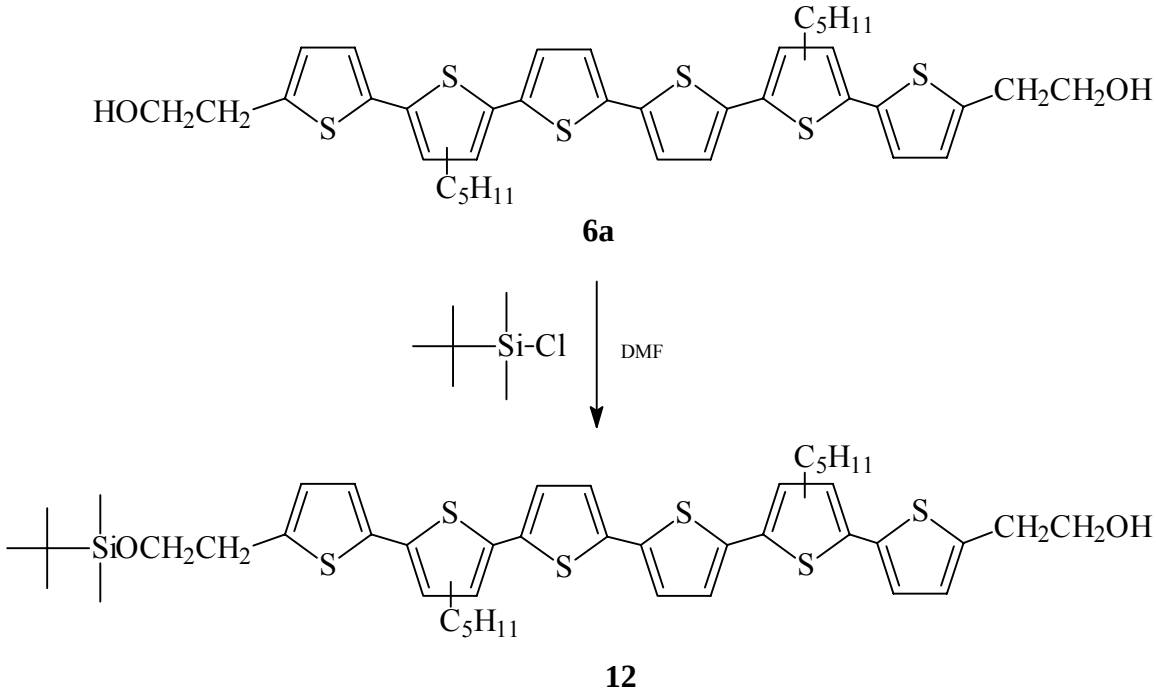

Scheme 24: protection of $PenST(OH)_2$

We obtained a statistical protection of the di-alcohol by the silyl groups even using an amount of the latter below the stochiometric molar ratio (0.9:1). Column chromatography was necessary to isolate the β',β''''-dipentyl-5-(2-hydroxyethyl)-5''''''-[2(tert-butyldimethylsiloxy) ethyl]-2,2':5',2'':5'',2''':5''',2'''':5'''',2''''':sexithiophene **12** (PenSTOHSi) in 45 % yield. The di-substituted silanol ether **13** was reconverted to $PenST(OH)_2$ by deprotection with tetrabutylammonium fluoride in THF.

PenSTOHSi (**12**) has only one –OH group that can react in the esterification reaction, so that an excess of the acid chloride **11** can be used with respect to the alcohol. The reaction is described in scheme 23.

Beside the expected product **14**, obtained in 20 % yield, we found also the deprotected ester **15**, i.e. with a free –OH group, and traces of the diester **16** resulting from the double esterification on the deprotected di-hydroxyl moiety **6a**. The deprotecting side-reaction is supposed to have taken place in the esterification reaction mixture. According to this hypothesis, the free anion Cl^- that leaves the carboxylic group acts as nucleophile attacking the silanol ether and forms the free –OH on the pre-formed ester. Such ester has therefore an additional –OH group that can be esterified (sch. 25).

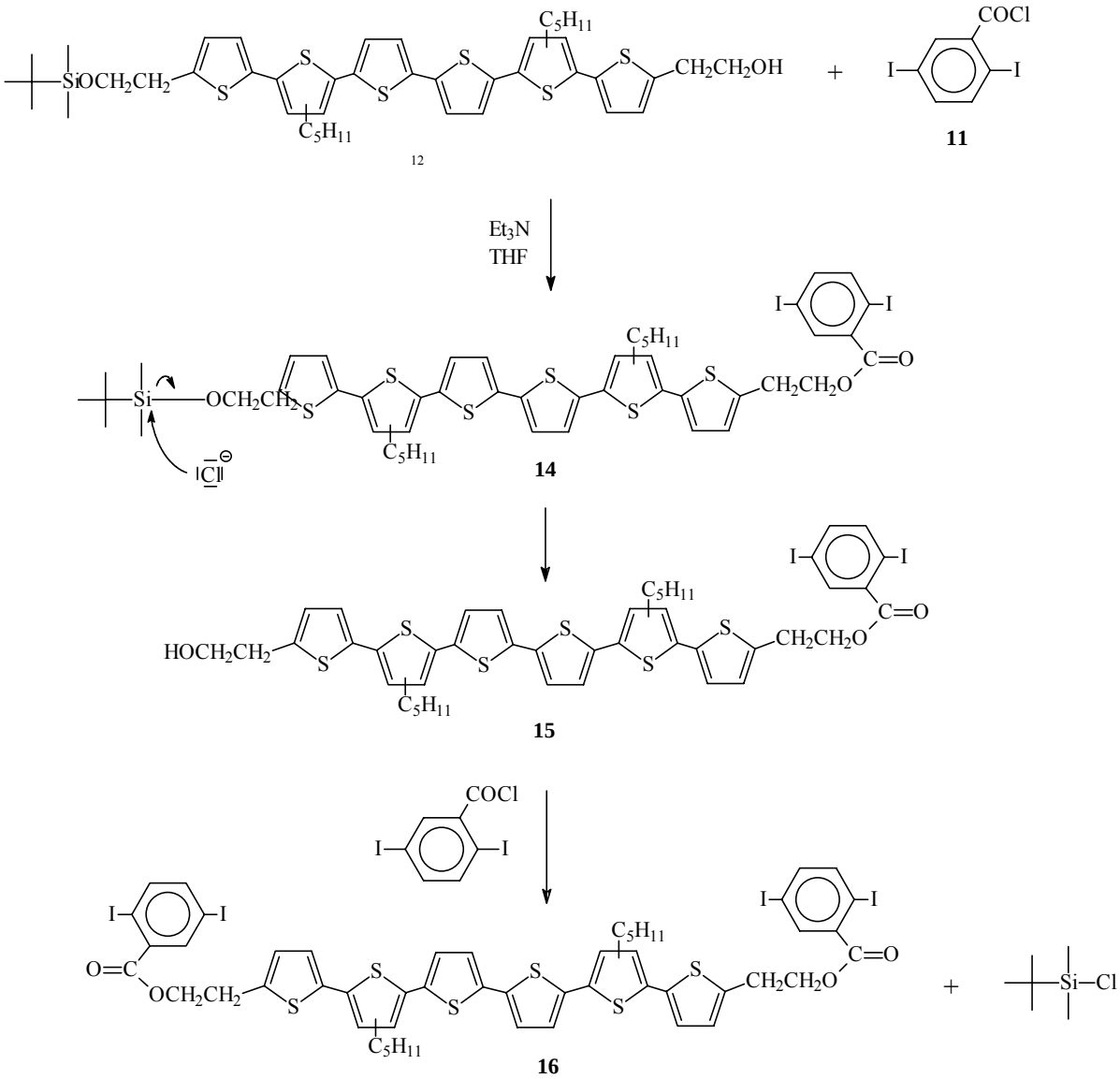

Scheme 25: reaction mechanism and side-products of the acylation reaction on PenSTOHSi

Although the di-iodobenzoic acid monoester with the deprotected hydroxyl group **15** is a suitable monomer for the further polymerization, and hence it was worth isolating it, a

different esterification route was investigated, in order to obtain the benzoic acid bearing the protected sexithiophene moiety in higher yield and purity.

Carboxylic acids can be activated by carbodiimide, thus, following the reaction conditions found in literature[67], we performed the esterification reaction using 2,5-diiodobenzoic acid **10** and $PenST(OH)_2$ (**6a**) in the presence of diisopropylcarbodiimide (DiPCI) and 4-(dimethylamino)pyridinium p-toluensulfonate (DPTS). The latter reagent is in the reaction mixture in equilibrium with 4-(dimethylamino)pyridine and p-toluensulfonic acid in a 1:1 ratio, which was found to be the best catalyst ratio for the conversion. Pyridine acts as a further activating and leaving group, promoting the attack of the hydroxylic substrate on the carbonyl carbon. As reported in scheme 26, also the acid anhydride is formed, but it can react further with the alcoholic moiety to give the ester.

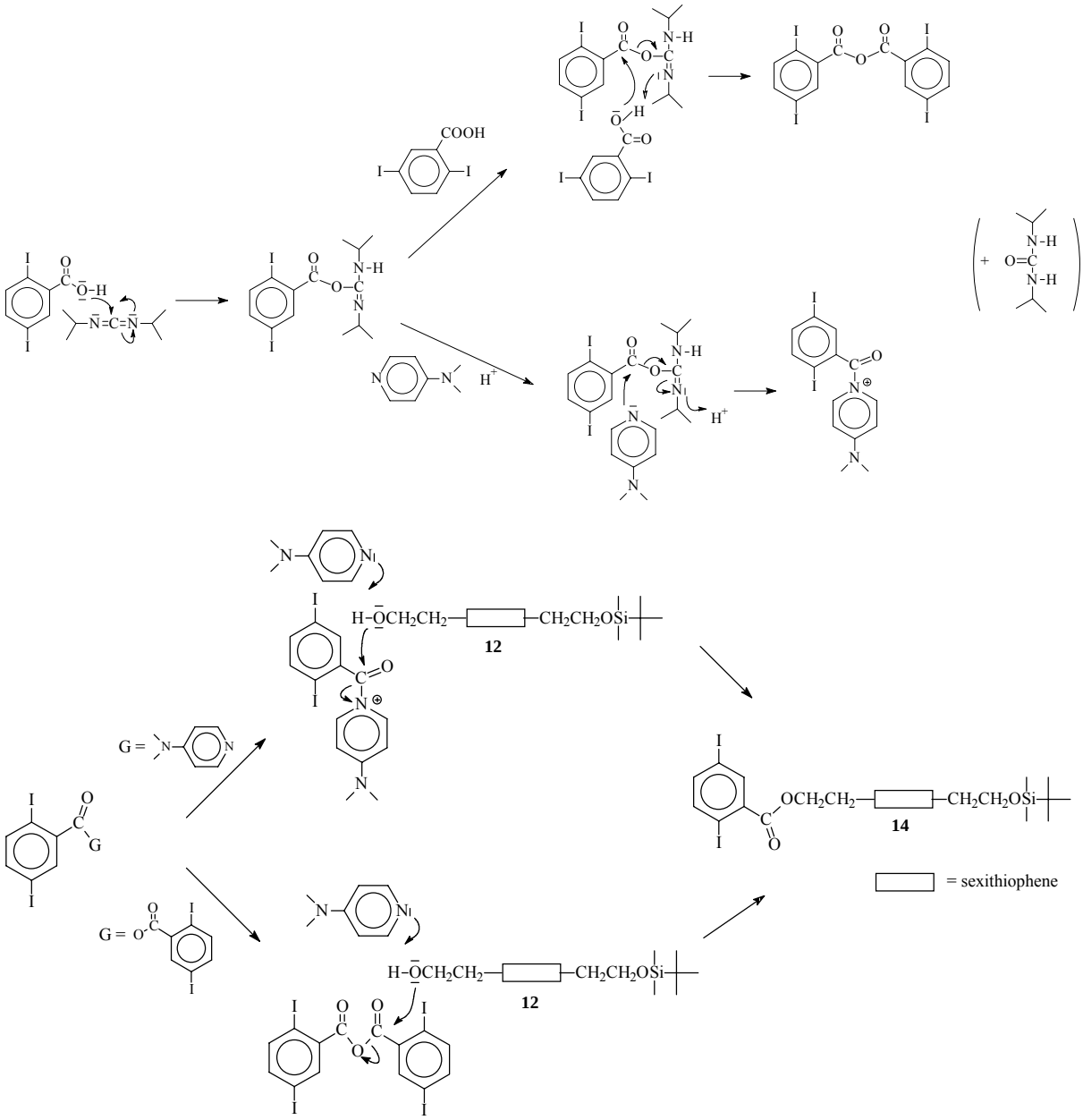

Scheme 26: reaction mechanism of the DiPCI-catalyzed esterification

This reaction route gave the desired product, i.e. 2-{β',β''''-dipentyl-5''''''-[2-(tert-butyldimethylsiloxy)-ethyl]-2,2':5',2'':5'',2''':5''',2'''':5'''',2''''':sexithiophen-5-yl}-ethyl 2,5-diodobenzoate (**14**, hereafter referred to as $BzI_2PenSTSi$) in 70 % yield.

The second monomer must carry two acetylenes, in order to perform a *Hagihara-Sonogashira* coupling reaction with the di-iodo compound **14** or **15**.

Since the acetylene-functionalized benzene monomer should also carry the sexithiophene moiety, we used $BzI_2PenSTSi$ as building block for the synthesis of the second monomer. In fact, only two reaction steps are needed to convert the di-iodo benzene derivative **14** to the

corresponding di-ethynyl compound **17**. The first is the *Hagihara-Sonogashira* coupling of **14** with trimethylsilylacetylene (sch. 27).

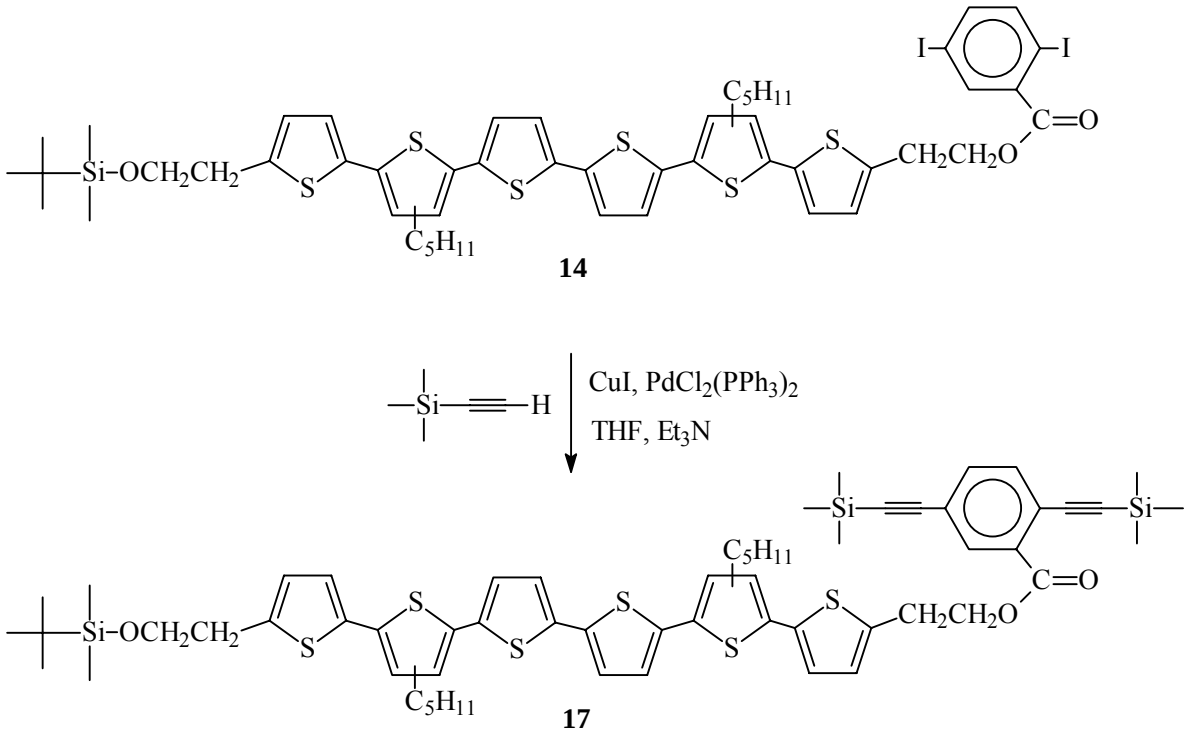

Scheme 27: di-acetylation reaction on $BzI_2PenSTSi$

The product 2-{β',β''''-dipentyl-5''''''-[2-(tert-butyldimethylsiloxy)-ethyl]-2,2':5',2'':5'',2''':5''',2'''':5'''',2''''':sexithiophen-5-yl}-ethyl 2,5-bis(trimethylsilylethynyl) benzoate (**17**, hereafter referred to as $BzAc_2PenSTSi$) was obtained in 40 % yield.

The second step, the deprotection, is carried out with tetrabutylammonium fluoride. In this reaction also the silyl group at the alcohol functionality is removed, as shown in scheme 28:

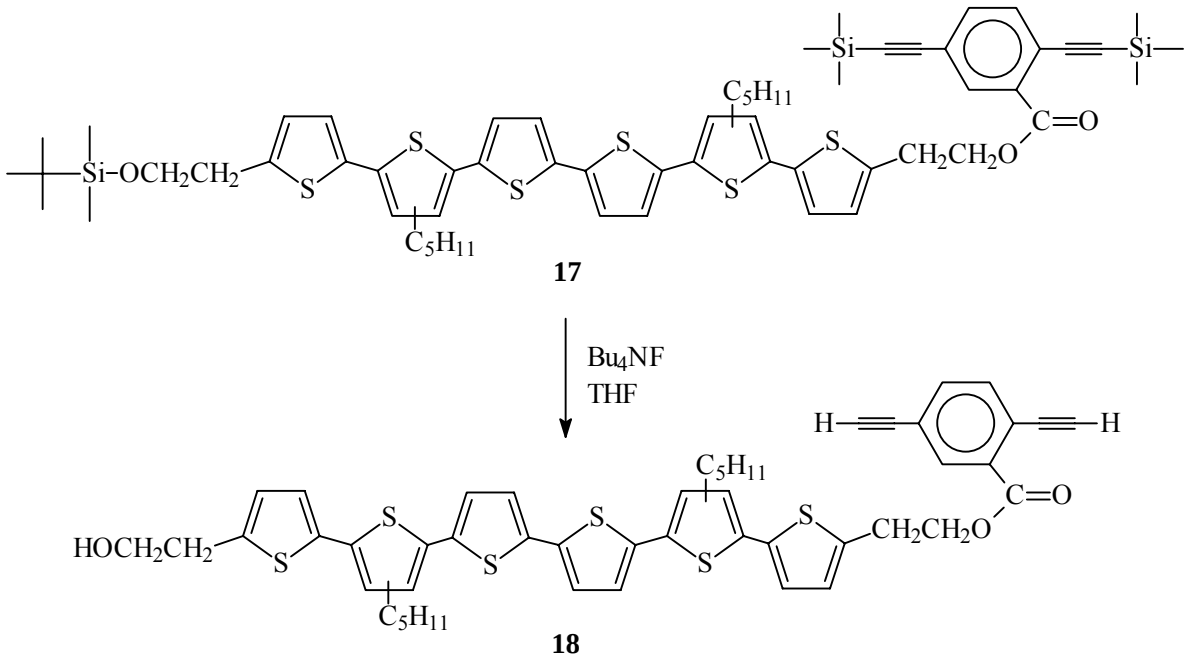

Scheme 28: deprotection reaction to obtain the polymerizable $BzAc_2PenSTOH$

Therefore, in order to have the same sexithiophene moiety as side chains in both monomers, the reaction was performed on $BzI_2PenSTSi$ (**14**) to deprotect the –OH. The two monomers **15** and **18** for the polymerization using the *Hagihara-Sonogashira* coupling are shown in figure 12.

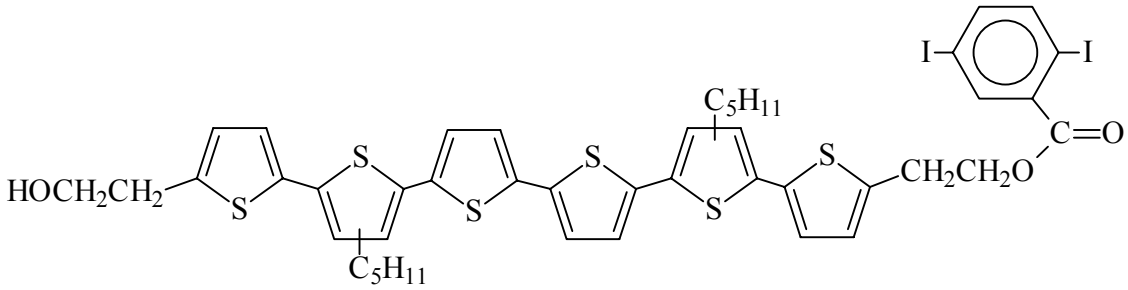

MONOMER 1: $BzI_2PenSTOH$ (**15**)

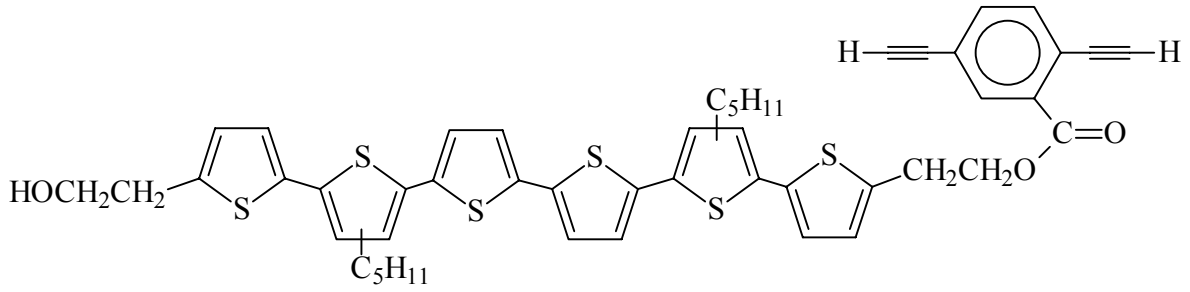

MONOMER 2: $BzAc_2PenSTOH$ (**18**)

Figure 12: monomers bearing α–protected sexithiophene side chains

3.2.3. Attempts to synthesize heptathiophene and substituted octylsexithiophenes

The synthesized pentyl- and octylsubstituted sexithiophenes represent a compromise between synthetic efforts and electrical conductivity, the former aspect being inversely and the latter directly proportional to the conjugation length. The correlation between conductivity and conjugation length can be shown by plotting the conductivity as a function of the inverse chain length of oligothiophenes, as shown in figure 13 (from ref. 68).

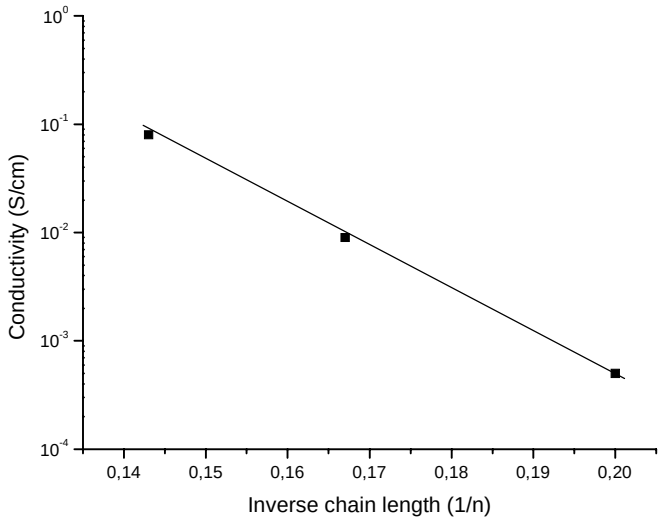

Figure 13: conductivities in dependence on the inverse chain length (1/n) of different oligothiophenes

Therefore, in order to improve the electrical conductivity of the material, we chose to synthesize a longer oligothiophene, consisting of seven thiophene rings (heptathiophene). The synthetic strategy started from the dioctyl-disubstituted sexithiophene **5b**, which was submitted to bromination with N-bromosuccinimide (NBS), as shown in scheme 29.

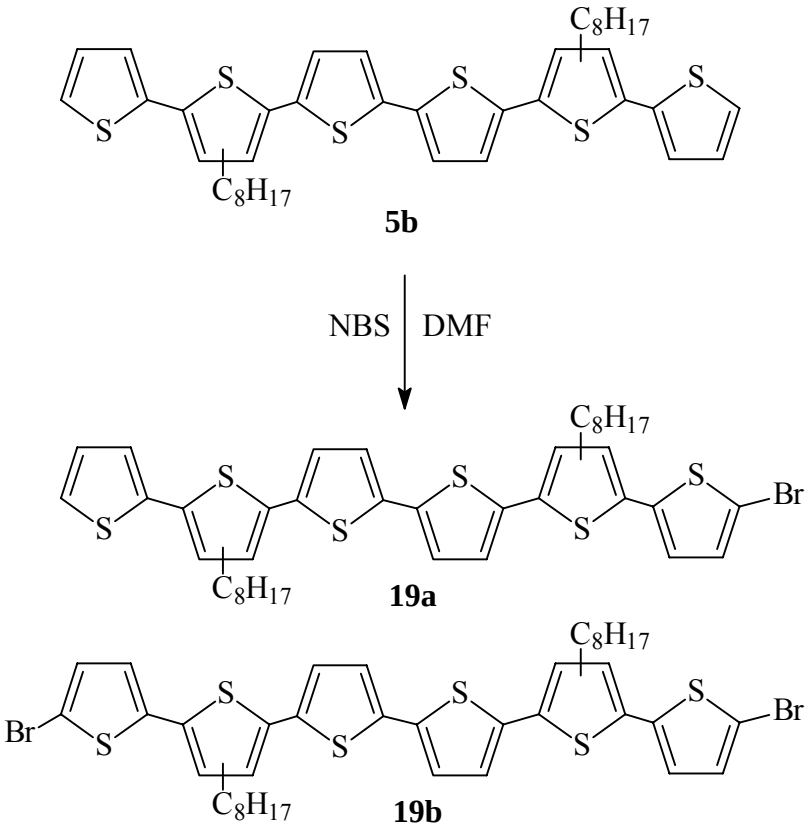

Scheme 29: bromination with NBS of octylsexithiophene

After the reaction a mixture of mono- and dibromosexithiophene **19a-b** was collected. Indeed, the bromination of oligothiophenes longer than terthiophene is described in literature as unselective[69], due to the same reactivity of the monobrominated and the unsubstituted oligothiophene toward the brominating agent. After purification of the reaction mixtures by means of column chromatography, the collected monobromo-sexithiophene **19a** was still contaminated with the dibrominated product **19b**.

We chose therefore to perform a cross coupling reaction between the mixture of the mono- and brominated sexithiophenes **19a-b** and 5-methyl-2-thienyl magnesium bromide, as described in scheme 30. We expected in this case an easier purification of the main products, i.e. heptathiophene **20** and octathiophene **21**.

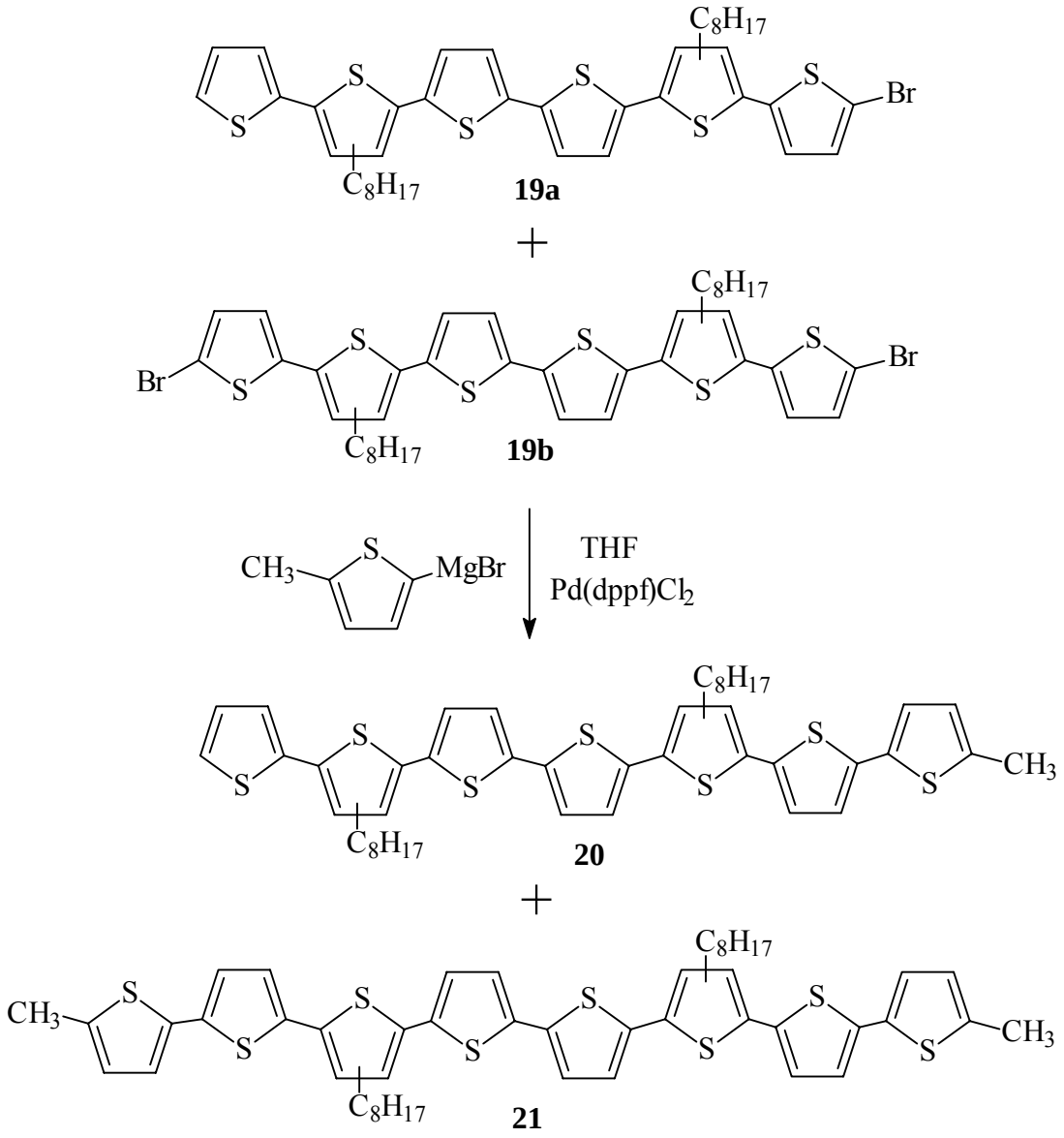

Scheme 30: cross coupling between brominated sexithiophenes and 5-methyl-2-thienyl magnesium bromide

The reaction did not afford any of the expected products, even not after repeated attempts. This might be due to impurities still present in a small in the starting material which was only available after a multistep reaction on a 100 mg scale.

In order to protect the reactive α-positions of sexithiophene we followed another synthetic strategy. According to that, the synthesis of an α-methyl-α'-hydroxyethyl-sexithiophene (**23**) was carried out, starting from the octylsexithiophene **5b**. The reaction strategy is described in scheme 31.

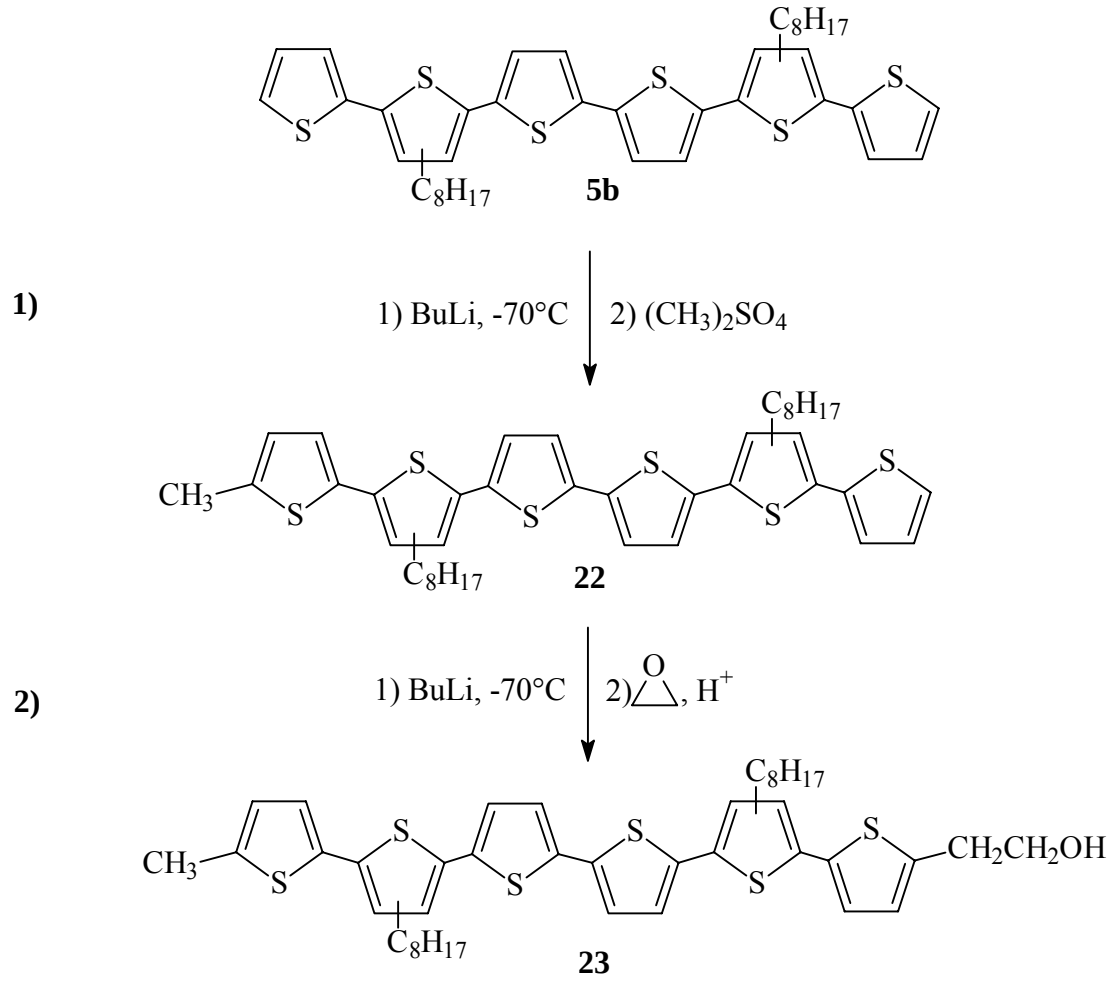

Scheme 31: synthetic strategy toward the synthesis of polar sexithiophenes

The first reaction (sch. 31, nr.1) afforded a mixture of unsubstituted, mono- and dimethyl substituted sexithiophene, due to the same reactivity of the monoalkyl- and unsubstituted sexithiophene toward strong basis. By means of column chromatography it was not possible to separate the monomethylsexithiophene **22** from **5b**, due to the similar polarity of the two oligothiophenes. In the following reaction (sch. 32), a polar group is introduced in the moiety by means of ethylene oxide that affords the hydroxyethyl substituent. Therefore the product mixture was expected to be separable into the single components, due to the different polarities between the alkyl and the hydroxyalkyl side chains of the sexithiophenes.

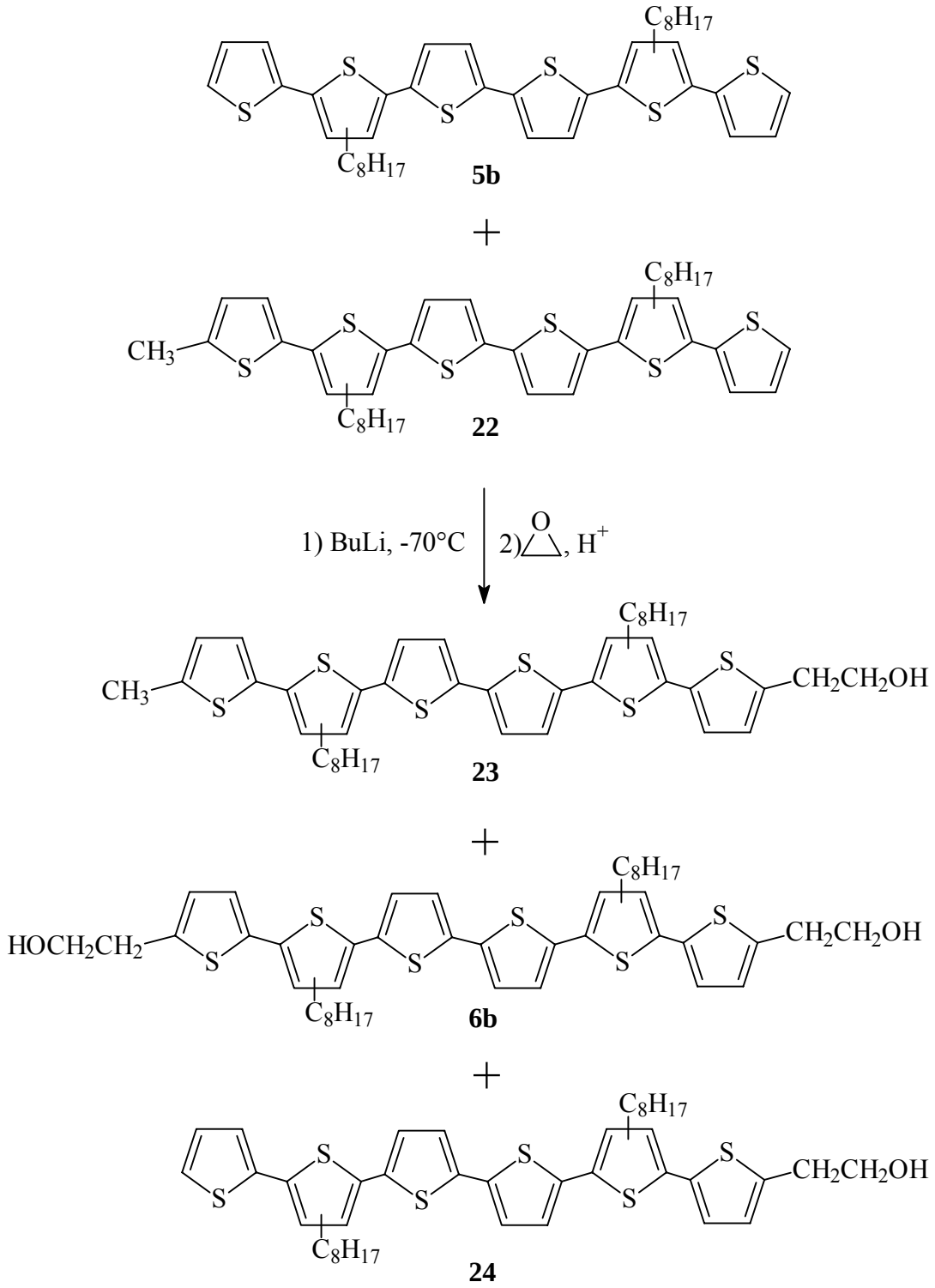

Scheme 32: hydroxyethylation of the mixture α-methylsexithiophene / sexithiophene

Also this reaction did not afford the desired product **23** in a acceptable purity after column chromatography, which afforded instead the pure product **6b** and a mixture of **23** and **24**.

3.3. Investigation of the sexithiophene chromophore and its electrochemical properties

The bis-hydroxylated PenST$(OH)_2$ is a suitable thiophene oligomer for the investigation of the properties arising upon oxidation of the conjugated moiety, as no side reactions (like dimerisation or polymerization) can take place, because the reactive α-positions are in this case protected. Therefore, oxidation-reduction cycles and the change of the UV-Vis absorption upon oxidation and reduction can be investigated on this monomer without generation of side products.

Our investigation aimed also at the study of the absorbance in the UV-Vis range of the sexithiophene chromophore, when dissolved in different solvents and at different temperatures.

3.3.1. Solvato- and thermochromism

Sexithiophenes present a broad and strong absorption band in the UV-Vis region, due to the π-π* transition. The strong absorbance is polarized along the molecular long axis[70]. The UV-Vis spectrum of sexithiophenes depends on many factors (see *Introduction*), among which the most important are the type of substituent present on the thiophene rings and the physical state in which the absorption is detected (solution, isotropic or self-assembled films, etc.) are the most important ones. As already mentioned, the substituents' electronic effect can strongly influence the magnitude of the excitation energy.

The effective conjugation length of sexithiophenes, and hence the peak absorbion wavelength, is correlated to the physical state (e.g. solution or bulk) in which the molecule undergoes interaction with the photon. Moreover, the transition energy depends on the degree of planarity of the system, so that there is a direct correlation between the absorption and the temperature (thermochromism). Because the UV-Vis absorption spectrum of sexithiophenes covers a large part of the visible range, a color change of the material can be observed passing from a fully conjugated system to a less conjugated one. This feature can be further used in the design of a sensor that detects physical or chemical changings in the environment. For example, it is described that an oligo(oxyethylene) substituted polythiophene changes its planarity, hence its UV-Vis absorption, depending on the presence of cations in solution[71].

We investigated the absorption spectra of the PenST(OH)$_2$ chromophore, in different solutions and at different temperatures. Three solutions of PenST(OH)$_2$ in hexane, toluene and ethanol (EtOH) with the same concentration were prepared and their absorption spectra measured at different temperatures (fig. 14).

The wavelength of the absorption peak (λ_{max}) and the corresponding extinction coefficient (ε_{max}) of the sexithiophene solutions at the given temperature are reported in table 2.

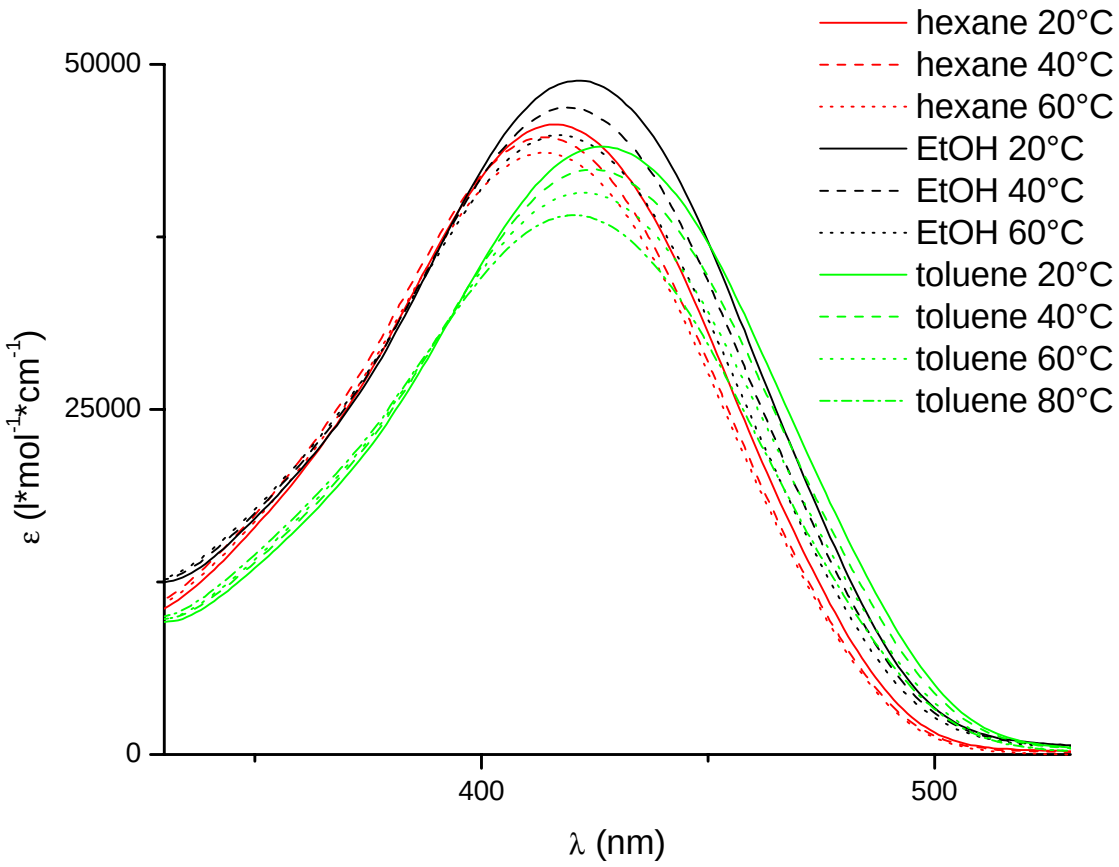

Figure 14: UV-Vis spectra of PenST(OH)2 in different solvents at different temperatures

Table 2: peak absorption wavelengths and corresponding molar extinction coefficients for spectra of fig. 14

Solvent at T (°C)	λ_{max} (nm)	ε_{max} ($l*mol^{-1}*cm^{-1}$)
Hexane 20	416	45600
Hexane 40	414	44700
Hexane 60	414	43600
EtOH 20	422	48800
EtOH 40	418	46700
EtOH 60	417	44800
Toluene 20	427	44000
Toluene 40	424	42400
Toluene 60	423	40700
Toluene 80	420	39100

In all the three solvents, the absorbance shows a blue shift of the maximum with increasing temperature. This behavior, called thermochromism, is due to a diminished effective conjugation length of the chromophore. In fact, by increasing temperature the contribution of more nonplanar conformations to the structure of the conjugated backbone increases, reflected also in a decrease of the oscillator strength (ε_{max}) are populated.

A rather negligible red shift (≈ 5 nm) of the absorption maximum was instead observed by changing solvent (solvatochromism) from hexane to ethanol and from ethanol to toluene.

3.3.2. Electrochromism

The π-electron rich sexithiophene molecule can be oxidized (*doping* process, see *Introduction*) by means of a chemical oxidant or by applying a positive potential to a solution or to a film deposited onto a suitable electrode of an electrochemical cell. In the latter case it is possible to record the response of the moiety to the applied potential by investigating the current flow from the sample during the scan of a potential range. The result of this experiment is a cyclic voltammogram (CV) where the current intensity is plotted vs. the applied potential. A current flow means an electrochemical process involving oxidation (or

reduction of the investigated molecule. We recorded a cyclic voltammogram of $PenST(OH)_2$ in CH_2Cl_2 solution (fig. 15).

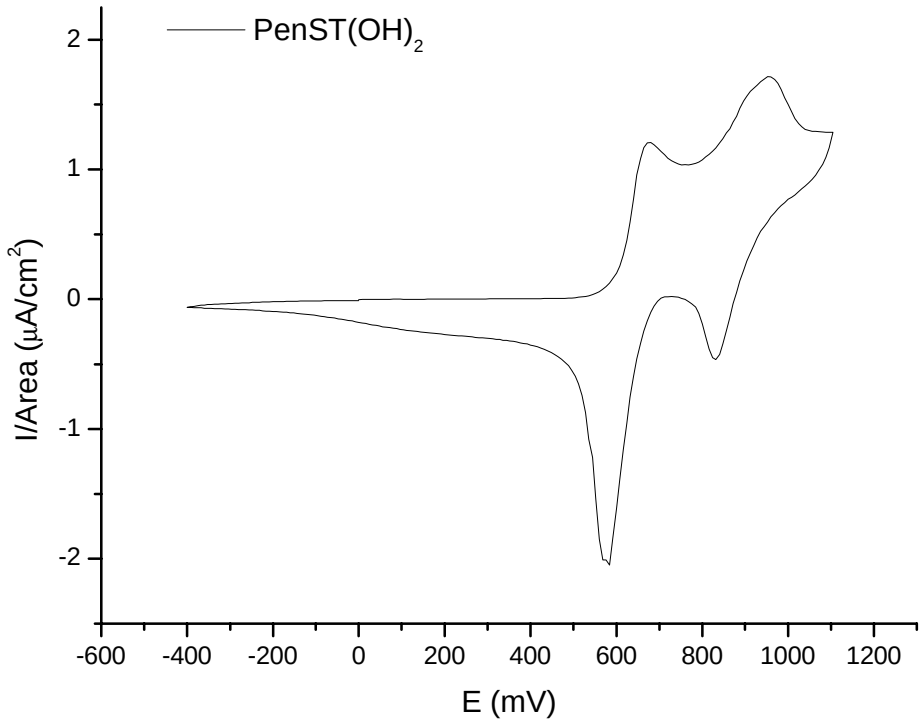

Figure 15: CV of $PenST(OH)_2$ in CH_2Cl_2 solution

By applying a positive potential, two oxidation peaks appear at about 680 mV (0.390 V/SCE if referred to the *Saturated Calomel Electrode* - SCE), and 950 mV (0.660 V/SCE), as expected for an oligothiophene of six conjugated units[72]. The first peak corresponds to the one electron oxidation of the sexithiophene moiety, that generates a positively charged radical species (cation-radical)[73] , typical of all conjugated thiophenes. Scanning the potential further to more positive values, a second oxidation peak appears, which is due to a further oxidation of the molecule and which generates a dication species[1]. By scanning the potential backwards toward negative values, two negative peaks are detected, that correspond to the reduction of the dication (at 830 mV) and of the radical-cation (580 mV) species respectively. In optimal experimental conditions, the oxidation-reduction cycles are reproducible for a large number of runs. This is in general the case if the chromophore has both α-positions protected, like in this case. The position of the peaks in the CV of an oligothiophene of defined length, i.e. sexithiophene in this case, depends on the nature of the substituents on the molecule[74]. Groups

with an electron donating effect stabilize the cation-radical and dication species and hence show less positive potentials compared to the same moiety with electron-attracting substituents.

The CV of the $PenST(OH)_2$ molecule is of high importance in order to investigate the behavior of the chromophore after oxidation or reduction. Aiming at this goal, we set an experimental cell to record the UV-Vis absorbance of $PenST(OH)_2$ and to study its change switching from the neutral state to the charged di-radical and *vice versa*. A film of the chromophore was deposited as casted on an ITO substrate, that was then placed in a nitromethane solution of tetrabutylammonium hexafluorophosphate (0.1 M) as inert electrolyte in a Teflon cell, together with a reference ($Ag/AgCl_{(s)}$) and a counter electrode (platinum), as described in figure 16. The chosen solvent is a bad solvent for the chromophore, in order to prevent its dissolution during the measurements.

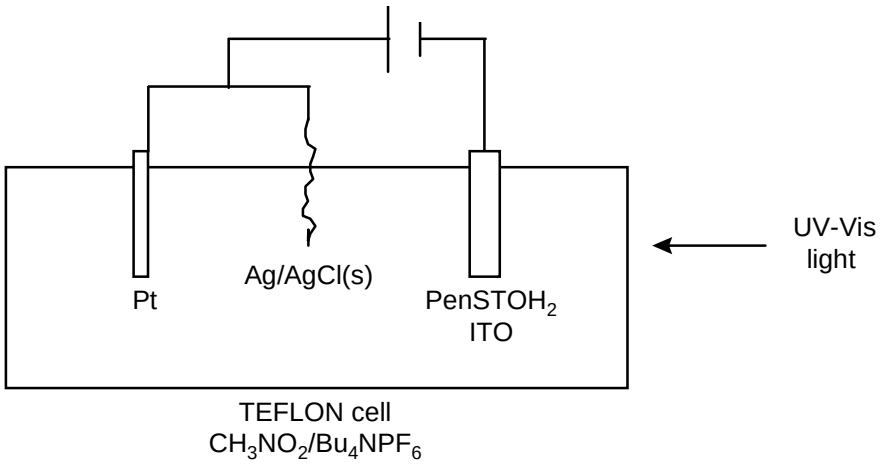

Figure 16: cell setup for electrochromism measurements

With this experimental setup, it was possible to impose a desired potential value to the solution and to record the UV-Vis spectrum corresponding to the molecular species present in equilibrium at such potential. We switched the potential from 0.0 V to 1.0 V, and applied the potential for 30 s, in order to investigate the corresponding neutral $PenST(OH)_2$ moiety and the oxidized species, respectively. In fact, as shown in the CV (fig.15), the value 1.0 V is above the second oxidative peak and at 0.0 V the reduction process is completed.

The UV-Vis spectra recorded at the above mentioned potentials are reported in fig. 17, where "RED#" means "reduction step number #", at 0.0 V, and "OX#" means "oxidation step number #", at 1.0 V.

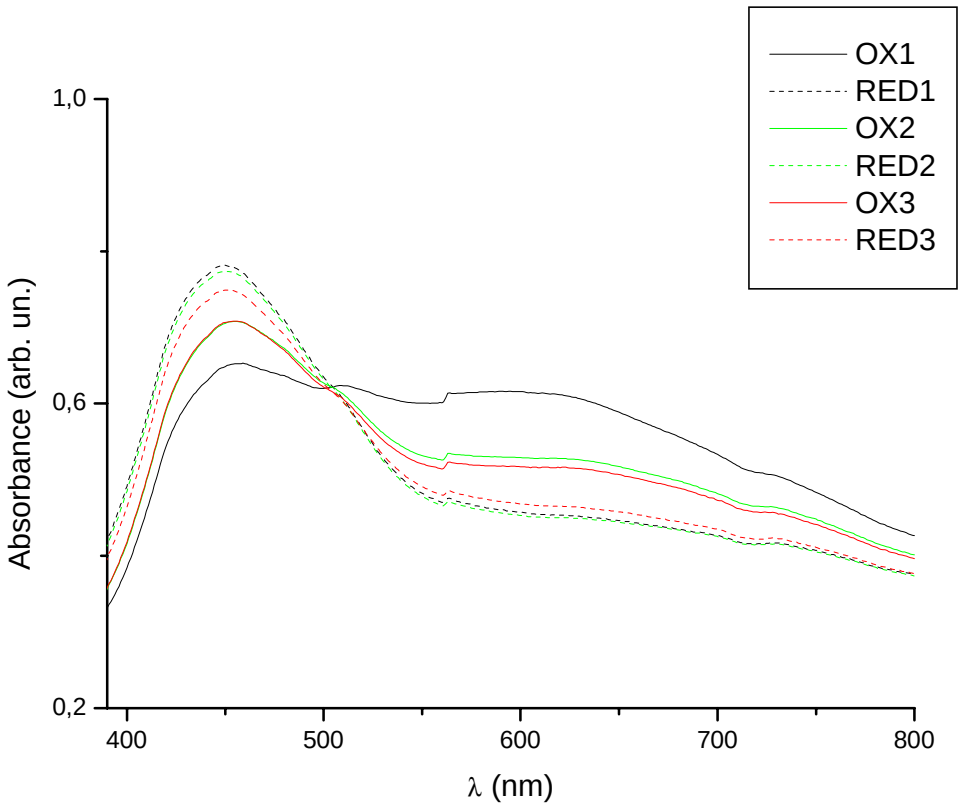

Figure 17: UV-Vis spectra of PenST(OH)$_2$-covered ITO substrate upon potential changes

The neutral PenST(OH)$_2$ has an absorption peak at about 450 nm: its red shift with respect to the absorbance in solution is due to the aggregation state of the stiff conjugated backbone, that allows π-π overlapping (π stacks) with a lower energy gap[75].

The broad band that appears upon oxidation in the range 570 – 700 nm is due to the absorbance of the formed di-radical di-cation moiety, where new energy levels are present between which new energy transitions are possible. As the oxidation potential was applied, the oxidized molecule appeared to be soluble in the solvent, and the solution became slightly yellow: the loss of material from the substrate was responsible for a diminishing absorbance of both neutral and oxidized chromophore during the redox cycles. Anyway, by switching the potential back to 0.0 V, the band at 570-700 nm disappeared and the band at 450 nm

increased its intensity, proving the back formation of the neutral molecule and hence the reversibility of the process.

The recorded spectra were in good agreement with a work found in literature dealing with the electrochemical properties of a monosubstituted sexithiophene moiety[40]. There, the authors found an additional band due to the duodecathiophene chromophore, formed *in situ* by coupling of two sexithiophenes through the not protected α-positions.

In our case, as it can be seen from the UV-Vis spectra (fig. 17), no longer oligothiophenes moieties are generated during the redox cycles, demonstrating that protection of the α-positions avoids effectively side reactions. Such feature allows one to design stable electrochemical sensors in which the protected sexithiophene responds with a color change (falling the absorption maximum in the visible range) to the presence of an oxidizing agent or to applied potentials, without undergoing side reactions that modify the active chromophore.

3.4. Synthesis, characterization and Langmuir-Blodgett (LB) films of oligothiophene functionalized cellulose derivatives

Cellulose is a polycarbohydrate that finds a wide range of applications in everyday life, both as homopolymer (e.g.: paper, cotton and viscose fibers) and in form of derivatives (e.g.: cellulose acetate in cigarette filters or in chewing gums).

The cellulose macromolecule is made out of stiff chains of repeating D-glucopyranose units linked through β-1,4 glycosidic bonds. The linearity of the main chain together with the presence of three hydroxyl groups on every monomeric unit makes the cellulose a very resistant fiber, which is not soluble in water or organic solvents. In fact the interchain hydrogen bonds, that can be formed very frequently through the high number of free hydroxyl groups, behave like physical crosslinks between several polymer chains. To overcome the problem of insolubility of cellulose and to perform substitution reactions on it, one must use a suitable and soluble cellulose derivative prior to the conversion to the desired substituted cellulose.

A successful strategy starts from the commercially available and soluble cellulose acetate, which undergoes a saponification reaction so that a proper functional group can access to the –OH residues in the same saponification medium, and provide thus for solubility of the resulting grafted cellulose copolymer[76].

Alkyl derivatives of cellulose show good solubilities in organic solvents and still contain a certain percentage of free –OH groups depending on the degree of substitution, which cannot be 100 %. The accessibility to the free –OH groups in cellulose derivatives with a lower degree of substitution is one way to obtain a further functionalized cellulose.

One of the aims of our work was to study processable polymers bearing oligothiophene side chains, obtained from a precursor polymer that additionally shows the feature to form films having a supramolecular order. Our choice of an alkylcellulose derivative as precursor polymer is due to its good solubility behavior together with the possibility to form stable films at the air-water interface by means of the Langmuir-Blodgett (LB) technique.

The preparation of ultrathin films of cellulosic materials has been frequently described in literature using alkyl-[58,77] and alkylsilyl-substituted[78] cellulose derivatives. Such films have a well defined supramolecular architecture, which can be viewed as an assembly of hairy rigid rods[79,80], as the rigid cellulose backbone is dispersed in the flexible side chains matrix at a molecular level. Even films of unsubstituted cellulose were obtained after the regeneration of LB films of the precursor polymer, trimetylsilyl-cellulose[81].

So far, copolymers with a non-conjugated main chain and oligothiophene side chains, or block copolymers containing the oligomer in the backbone, were studied only in solution or as a free standing, amorphous film. In our case we could use the feature of modified cellulose to form ordered films and study how two different oligothiophenes, i.e. terthiophene and sexithiophene, are organized in such matrices.

3.4.1. Synthesis of butylcellulose bearing terthiophene side chains

Butylcellulose derivatives were prepared starting from cellulose acetate and performing an ether synthesis reaction between *n*-butyl bromide and the *in-situ* regenerated cellulose, according to the literature[82] (sch. 33).

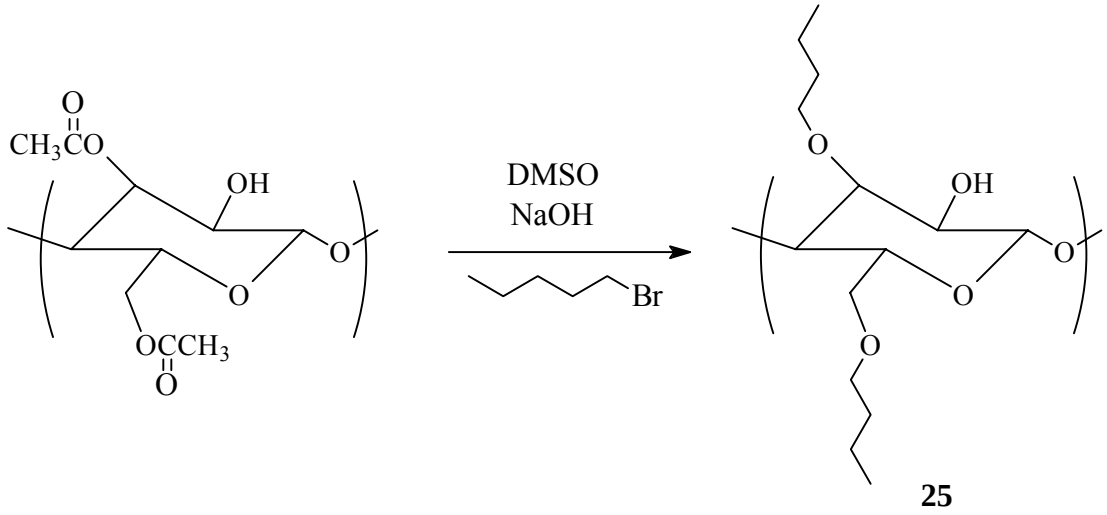

Scheme 33: alkyl functionalization of cellulose acetate

The butyl celluloses obtained (**25**) were randomly substituted on the hydroxylic positions and they showed a degree of substitution between 1.9 and 2.8, where the degree of substitution (DS) is the average number of substituents on a monomeric unit, ranging form 0 (0 %) to 3 (100 %). Such derivatives are suitable precursors for the next functionalization with the chloroethyl-terthiophene **4**, prepared as described in chapter 3.2.1., also performed by a Williamson ether synthesis. We used a butyl cellulose with DS_{butyl} = 1.9 (**25a**) as precursor cellulose derivative for the introduction of the terthiophene side chains by means of the etherification reaction (sch. 34).

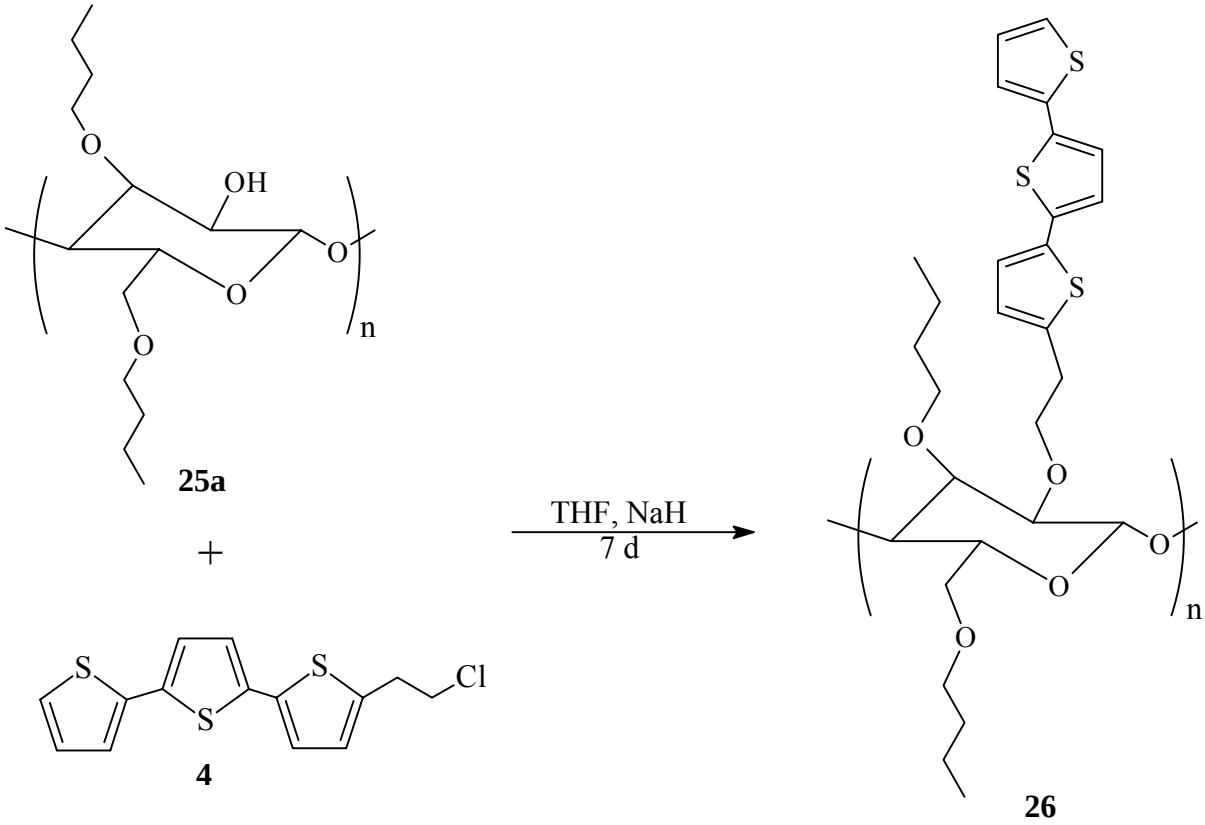

Scheme 34: introduction of the terthienyl moiety on butylcellulose

The resulting polymer **26** was well soluble in organic solvents and showed a DS_{TT} = 0.35. The low substitution degree, with respect to the available free –OH groups, can be rationalized by steric interactions between the oligothiophene and the butyl-substituted cellulose derivative.
The presence of terthiophene on the polymer was confirmed in the ^{1}H-NMR by a broad signal in the region 6.8 - 7.3 ppm, corresponding to the aromatic protons of terthiophene. Beside that, the polymer shows an absorption band at 375 nm in the UV spectrum due to the conjugated chromophore, causing an orange coloration of the material. Elemental analysis was used to calculate the DS of the terthiophene groups.

3.4.2. Synthesis of butylcellulose bearing sexithiophene side chains

As for the synthesis of the terthiophene-carrying cellulose derivative, butylcellulose was chosen as the soluble cellulose precursor for the functionalization with sexithiophene.

The introduction of the sexithiophene moiety on cellulose was possible performing a Williamson ether synthesis between the free –OH groups of butylcellulose and the proper modified sexithiophene PenSTOHTs (**7**), prepared as described in chapter 3.2.2.1.. The hydroxylic residues on cellulose were activated with butyllithium, because this reagent could be added from a solution of known concentration with a better accuracy than adding solid NaH. The use of a stochiometric amount of BuLi was necessary in order to avoid the acid-base side reaction of the excess of BuLi with PenSTOHTs (**7**, sch. 35). Such reaction would generate an alcoholate on the unprotected hydroxyethyl group of PenSTOHTs, that could lead to undesired homopolymerization of the molecule *via* a polycondensation reaction[*].

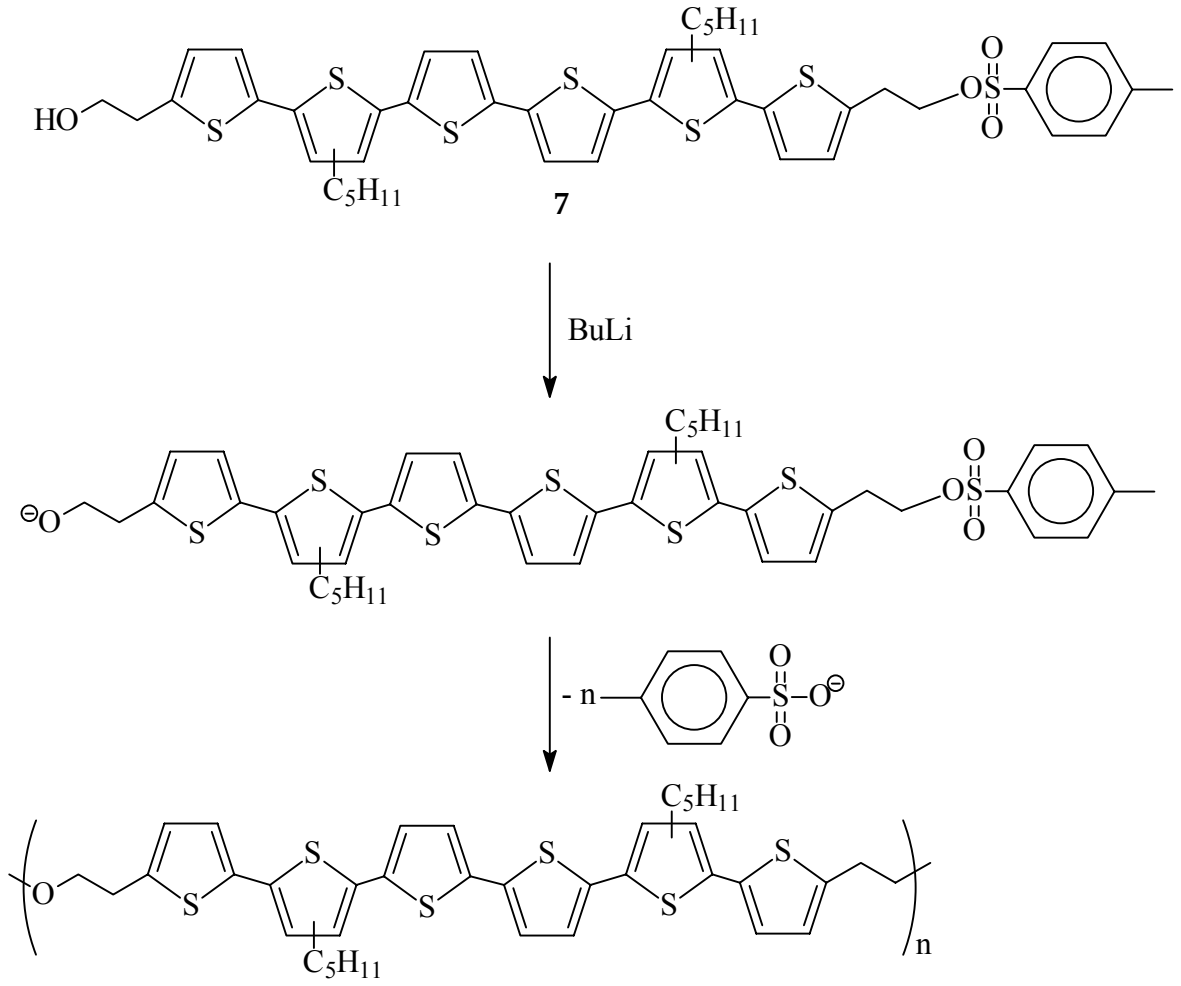

Scheme 35: side reactions between excess of BuLi and PenSTOHTs

[*] The proton exchange between the *in situ* formed cellulose alcoholate and the –OH groups of PenSTOHTs can nevertheless not be excluded but only neglected.

We used a butylcellulose with a DS_{butyl} = 2.6 (**25b**) as cellulose precursor to be functionalized with the sexithiophene moiety **7**, as described in scheme 36.

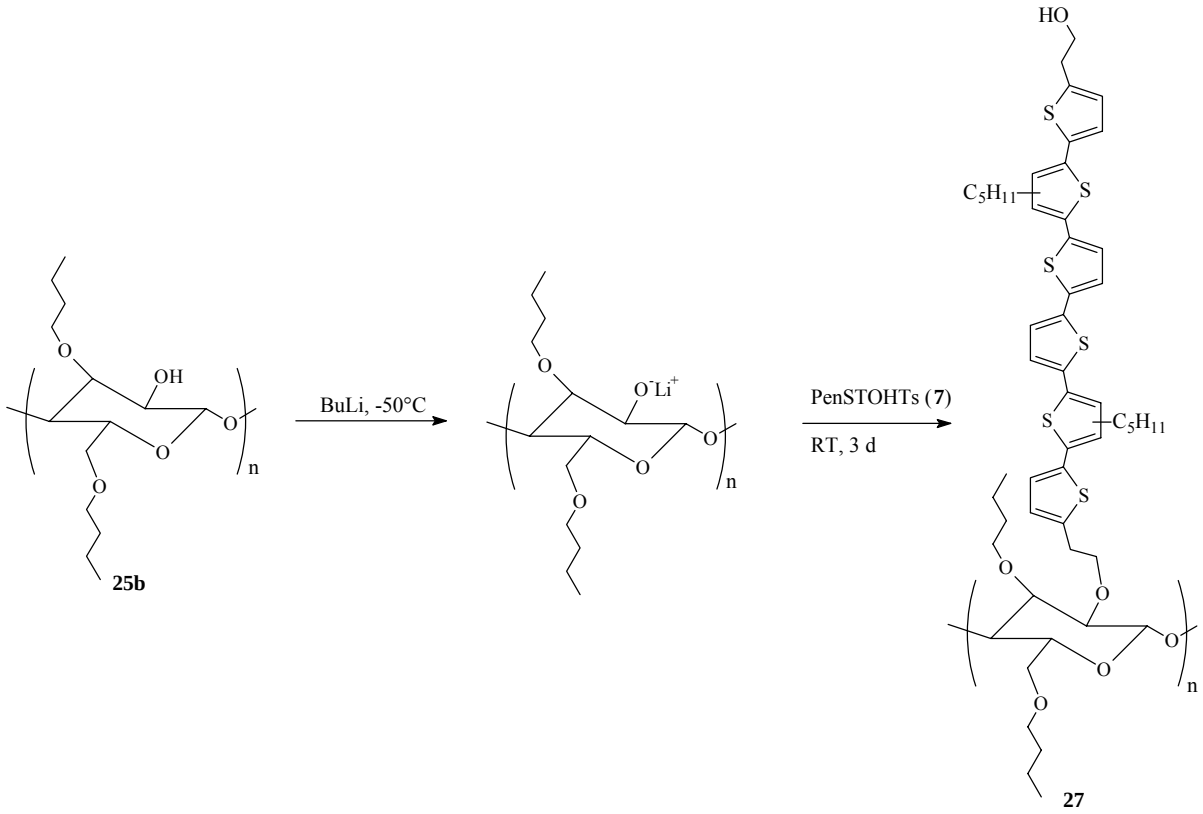

Scheme 36: introduction of the sexithienyl moiety on butylcellulose

The polymer resembled the good solubility of the precursor butylcellulose but showed a very low content of sexithiophene groups. According to the results of the elemental analysis, DS_{ST} = 0.06, that means that a deprotonation of PenSTOHTs by the lithium-cellulose precursor could not be completely avoided. The presence of the chromophore was confirmed by the appearance of an absorption band at 423 nm in the UV-Vis spectrum together with a orange coloration gained by the polymer. However, no signals due to the sexithiophene pendant could be detected in the aromatic region of the ^{1}H-NMR spectrum, probably due to its low content.

As for the synthesis of butylcellulose with terthiophene side groups **26** (see chapter 3.4.1.), also in this case the low percentage of substitution of the conjugated moiety can be explained with the high steric hindrance of such molecule, that causes a limitation in its reactivity toward the alcoholate residues on cellulose, indeed surrounded by the butyl side chains.

3.4.3. Introduction to the LB technique

In this section only a brief introduction is given about the basic features of the LB technique. For a more detailed insight the reader is referred to ref. 83. The LB technique is a unique method to achieve supramolecular organization of molecules of low or high molecular weight into layers. A monolayer is obtained upon spreading the substance at the air-water interface in a LB trough. For low molecular weight molecules the requirement for such an organization is mainly an amphiphilic character of the substance, that allows the hydrophilic part to point into the water phase and the hydrophobic tail to point out to the gas phase. The layers can then be deposited on a solid substrate by dipping and undipping it into the LB trough, forming two layers of anisotropic disposed molecules for each dipping-undipping cycle.

A disadvantage of LB-films of low molecular weight molecules is the lack of stability, because the layers undergo with time a temperature depending reorganization that destroys the LB architecture. Such drawback can be overcome by using macromolecules as LB active substance, where chemical bonds between each monomeric unit provide for a gained stability of the layered architecture.

Beside amphiphilic macromolecules, it has been found that also anisotropic shaped polymers can be successfully spread at the air water interface (ref. 84 and therein), once they are provided with flexible side chains that behave as an internal solvent. Such polymers are commonly referred to as “hairy rods”, representing the stiff main chain the “rod” and the flexible side chains the hairy part.

The LB technique is performed by spreading a dilute solution of the substance on the water layer of the LB trough, where it will form a monolayer. After spreading, the layer is compressed by a moving barrier until the (macro)molecules reach a nematic liquid-crystalline phase, that can be then transferred to the substrate by dipping and undipping cycles (fig. 18).

It is during the transfer that the molecules dispose anisotropically along the dipping direction, due to a shearing force, enabling one to obtain an oriented supramolecular architecture at a macroscopic level on the substrate.

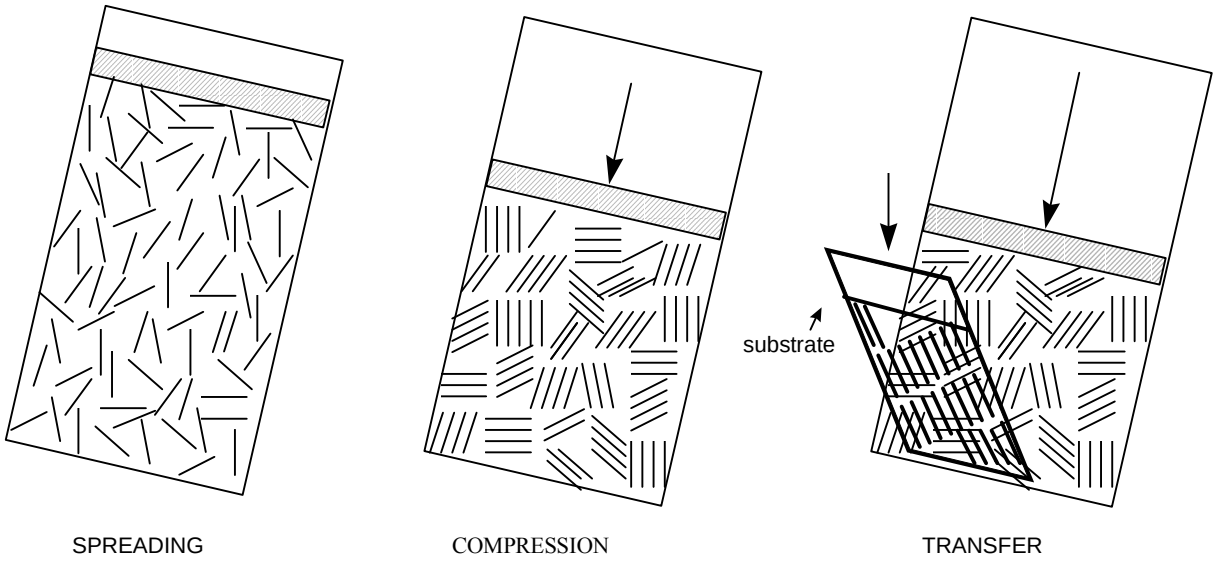

Figure 18: description of the LB technique from substance spreading to transfer to a substrate

Amphiphilic low molecular weight substances with an hydrophilic head and an hydrophobic tail will assemble on the substrate in head-to-head / tail-to-tail layers (fig. 19A). Hairy rods macromolecules will deposit as aligned rods embedded in the liquid-like flexible side chains (fig. 18B).

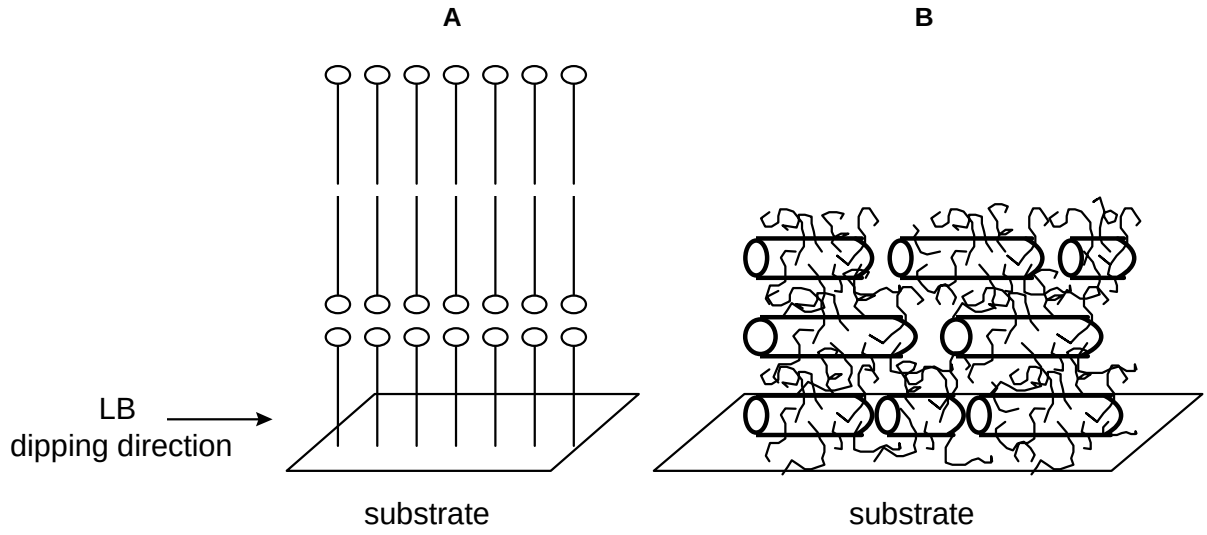

Figure 19: low molecular weight (A) and *hairy-rod* (B) molecules assembled on substrates by the LB technique

In order to perform the LB assembling process, the molecules must form a stable film at the air-water interface. To verify this feature the spread substance is first isothermal compressed

to investigate the monolayer stability. Plotting the surface pressure against the area of the trough available for the molecules, a diagram as showed in figure 20 is usually obtained.

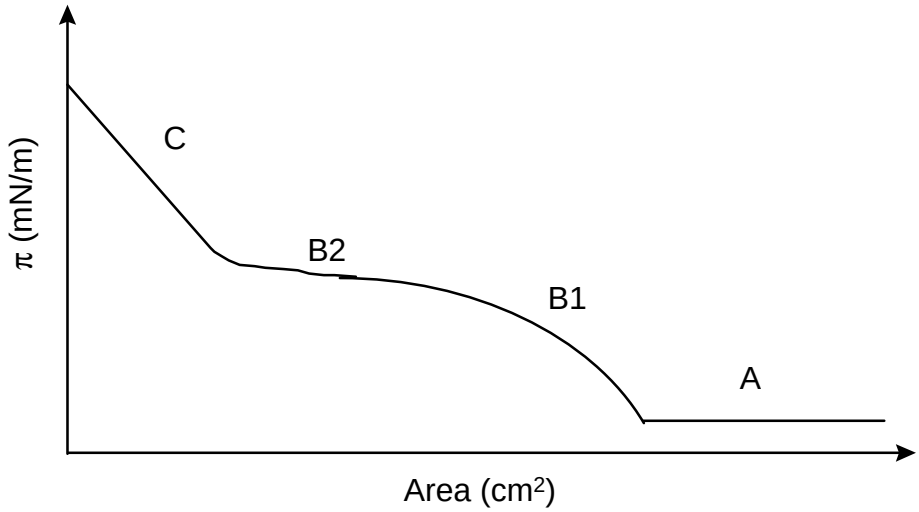

Figure 20: pressure vs. area plot of a substance spread at the air-water interface

After the molecules are spread over the surface, the surface tension does not change upon compression as long as the available area of the trough is much larger than the intrinsic molecular area. This corresponds to the gas-like behavior[85] (zone A). Further compression leads the film to show an almost linear-like dependence of surface pressure on the area (zone B1, fig. 20). Further decreasing the available surface causes the film to assemble into a multilayer so that the pressure does not change within a certain range of surface values (zone B2, fig. 20), since the molecules slide one over the other. Exceeding further the compression will lead to a collapse of the multilayered structure corresponding to high surface pressures (zone C, fig. 20). If the investigated substance shows a reversible behavior in the area values corresponding to the B1 zone and the pressure values are constant with time (fig. 19), that means that the spread film is stable at the air-water interface.

The transfer of the monolayer to the solid substrate is performed at a constant pressure that is chosen from the isothermal plot. The chosen pressure value must not exceed the limiting pressure of the B1 zone (fig. 20), since only in the B1 zone the molecules are disposed as a monolayer. The optimal pressure value for the transfer corresponds to the lowest molecular area at which the molecules are still in a monolayer assembly (end of zone B1, fig. 20). This allows a close-packing of the molecules in each transferred monolayer.

It is possible to follow the transfer process monitoring the decrease of the trough area with time. During the constant pressure-deposition of the substance on the substrate (i.e. loss of molecules by the water surface), the barrier compresses the film on the trough, in order to keep the setted pressure constant by diminishing the available area. The difference between the initial trough area and the area at a time "*t*" is in principle the area transferred to the substrate. Thus, plotting the trough area against time, the progress of the transfer is represented by a line with negative slope. At the end of the run, the transfer ratio can be calculated as the ratio between the value of the transferred area (surface difference before and after the transfer, from the plot) and the total area dipped into the trough (i.e. the substrate area multiplied for the number of dipping-undipping cycles).

In the present work we studied the LB film formation of the butylcellulose derivatives containing terthiophene or sexithiophene side chains. Such polymers are composed of a *hairy rod*-like polymeric chain (butylcellulose) and conjugated side chains.

Our objective was to study whether the structural order that is observed in the LB films of cellulose derivatives could induce supramolecular order in the short *rigid rod*-like terthienyl or sexithienyl side chains during the LB deposition of the oligothiophene-carrying cellulose. In other words, we were looking for effects of orientation of the electrochemically active side groups with regard to the plane of the substrate.

3.4.4. Preparation, characterization and applications of LB films of butylcellulose bearing terthiophene side chains

The investigated cellulose derivative **26**, hereafter referred to as BCTTE, carries butyl and terthiophene side chains with a respective degree of substitution of DS_{butyl} = 1.9 and DS_{TT} = 0.35. Such polymer was spread on the LB trough and the obtained monolayer was submitted to isothermal compressions at different temperatures to investigate its behavior at the air-water interface.

Figure 21 shows the plots obtained at 5°C, 12°C and 20°C, where the molecular area refers approximately to the average area per monomeric unit, calculated by dividing the trough area by the number of repeating units (i.e. the substituted glucopyranose units) contained in the total mass of the polymer spread to the surface. This was possible by knowing the DS of both the butyl and terthienyl side chains, as shown below:

$$PM_{monomer} = PM_{cellulose\ monomer} + DS_{butyl}\cdot(PM_{butyl} - 1) + DS_{TT}\cdot(PM_{terthienyl\ group} - 1)$$

$$DS_{butyl} = 1.9$$

$$DS_{TT} = 0.35$$

$$PM_{monomer} = 162 + 1.9\cdot(57 - 1) + 0.35\cdot(275 - 1) = 364.3$$

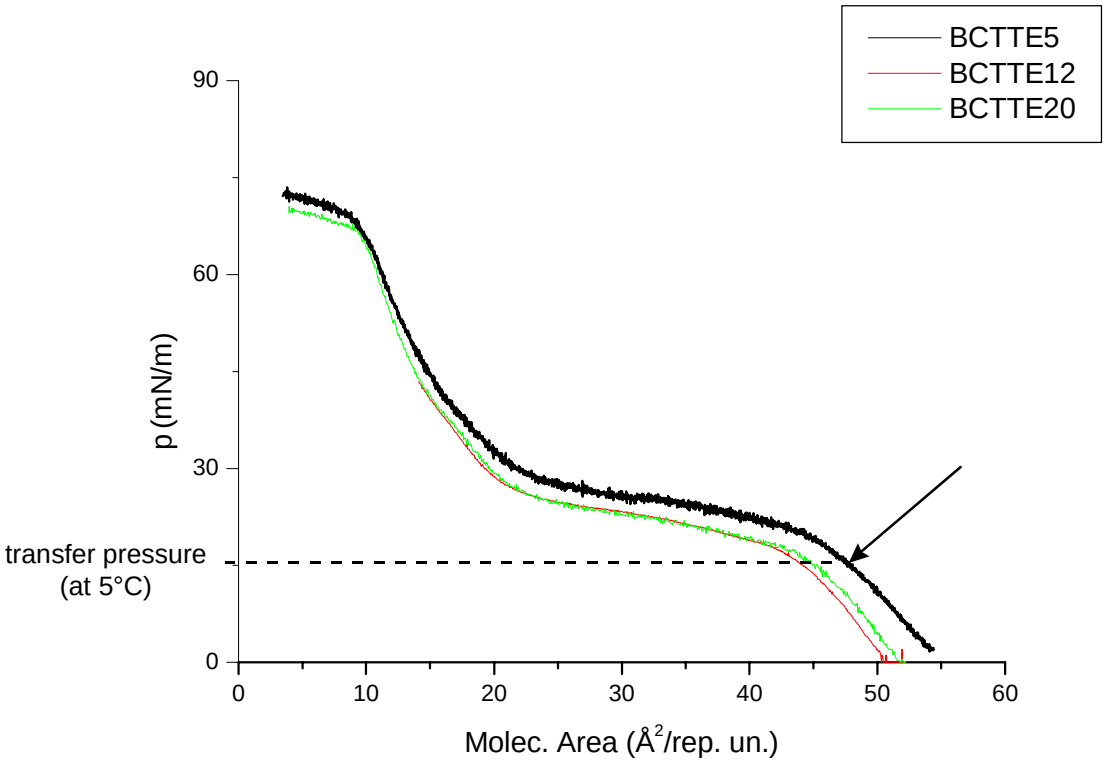

Figure 21: pressure-area isotherms of BCTTE

It can be seen that the polymer forms stable monofilms at all the three investigated temperatures. The pressure-area isotherms show a behavior which is totally in agreement with the literature data about the spreading of cellulose ethers[76,77]. The deposition of the polymer on different substrates was performed choosing the proper pressure (tab. 3), obtained by the plot in figure 21. It was chosen that corresponding to a molecular area (pointed out in fig. 21) at which the polymer chains are close one to another but do not overlap to form a multilayer. Different substrates were used for the depositions, together with different transfer conditions, as shown in table 3. All the substrates were hydrophobized by exposure to 1,1,1,3,3,3-

hexametyldisilazane (HMDS) vapors before LB transfers to assure its wettability by the polymer. The transfer ratio was on average 70 %.

Table 3: substrates, LB transfer conditions and thickness of LB films of BCTTE

Sample	**Substrate**	**T** (°C)	**π** (mN/m)	**nr. layers**	**thickness** (Å)	
					d	d_m
NRSi4	Au-covered Si	12	14.5	50	384	7.7
NRAu32	Au-cov. glass	5	17	40	271	6.8
NRAu33	Au-cov. glass	5	17	40	297	7.4
NRAu36	Au-cov. glass	12	14.5	40	385	9.6
NRAu37	Au-cov. glass	12	14.5	40	353	8.8
NRQu1	quartz	5	16	40	327	8.2
NITO1	ITO	12	14.5	50	516	10.3
NITO3	ITO	12	14.5	120	1014	8.4

The thickness of the obtained films was determined by X-rays reflectometry. The reflectogram showed a set of fringes, which were interpreted as Kiessig-fringes of the layered structure. As example the reflectogram of the substrate NRAu32 is shown in figure 22.
The total thickness *d* of the multilayer assemble was calculated with the following formula:

$$d = \frac{\lambda}{2\sin\theta}$$

with $\lambda = 1.54$ Å the wavelength of the x-ray beam.

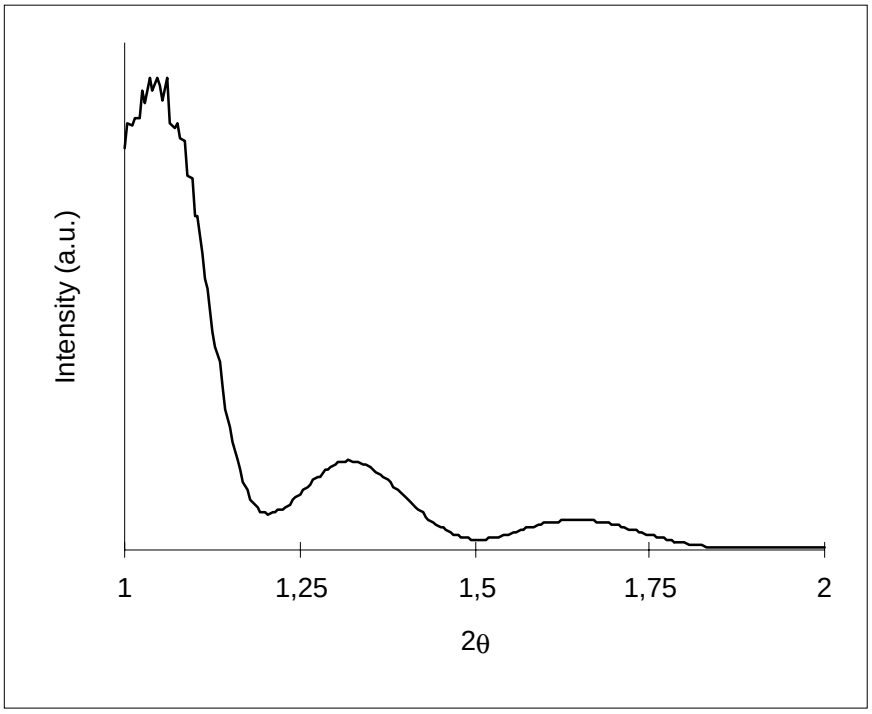

Figure 22: X-ray reflectogram of sample NRAU32

From the reflectogram the difference between two reflection maxima was calculated, 2θ = 0.325, and the thickness of 40 monolayers of this sample could be obtained by the formula below:

$$d = \frac{1.54}{2\sin(0.1625)} = 271 \text{ Å}$$

The thickness per monolayer d_m was found dividing the total thickness by the number of monolayers (40), finding thus $d_m \approx 7$ Å.

Considering all samples (see table 3), the thickness per monolayer was estimated as roughly $d_m \approx 8$ - 9 Å on average. This value is supported by similar data reported in the literature[77] (for isopentylcellulose LB layers: $d_m = 7.9 – 8.8$ Å).

The substrates were investigated by polarized UV-Vis spectroscopy in order to determine a possible orientation of the chromophores in the *x*,*y* plane (substrate plane). This is possible because the transition moment of the optical absorption of the terthiophene residue is strongly polarized along the long axis of the molecule, so that a stronger absorption along a certain direction would mean a preferred orientation of the molecule along that direction.

Naming *y* the dipping direction and *x* the direction perpendicular to *y*, we observed only a slightly stronger absorbance along the LB dipping direction (A_y) with respect to the

perpendicular direction (A_x), as illustrated in figure 23 for the sample NRAU32. The dichroic ratio $R = A_y/A_x$ was on average only 1.05, that is the alignment of the terthiophene chromophores as a consequence of possible shear alignment during the transfer is almost negligible.

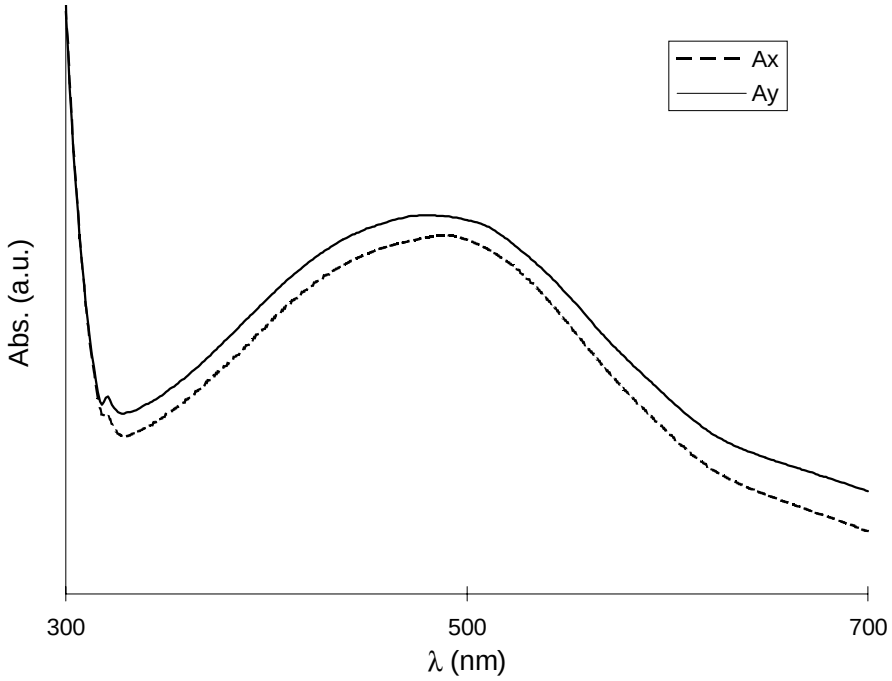

Figure 23: polarized UV-Vis spectra of NRAU32

The terthiophene chromophore is fluorescence active, so we also recorded fluorescence spectra with polarized light of the sample on quartz substrate. The excitation wavelength was $\lambda_{exc} = 390$ nm, and the maximum of the emission occurred at $\lambda_{max} = 495$ nm (fig. 24).

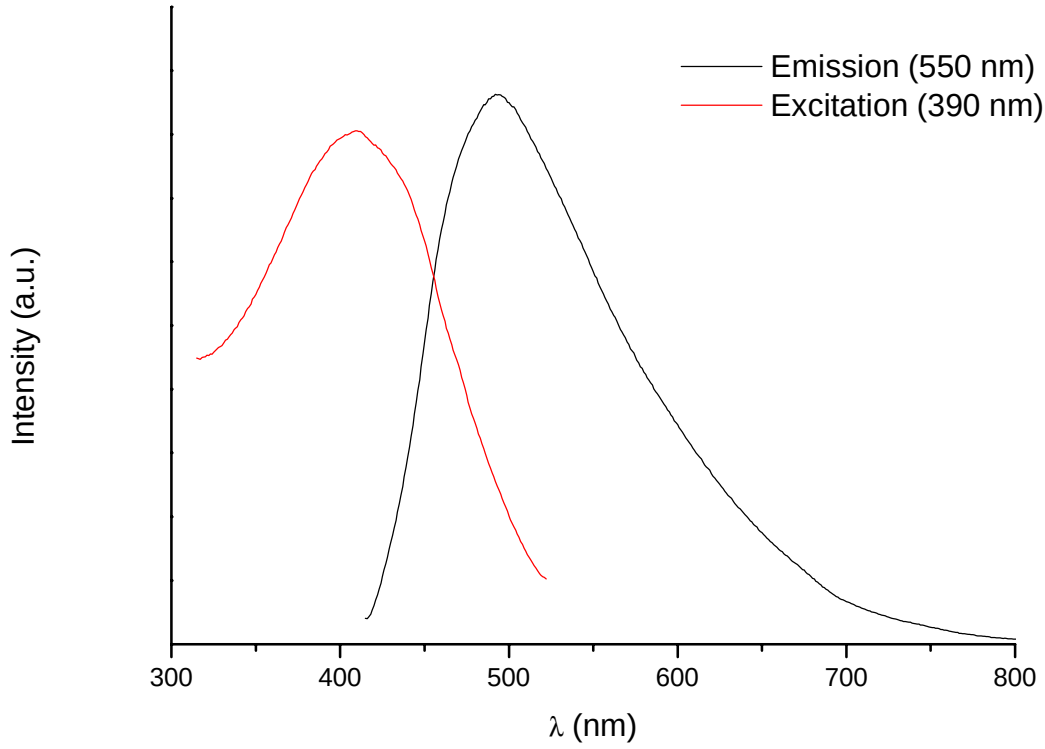

Figure 24: unpolarized excitation and emission spectra of sample NRQu1

Figure 25 describes schematically the orientations of substrate and polarizers during the recording of the polarized fluorescence emission. Figure 26 shows the four spectra recorded in the polarized mode, where *xx*, *xy*, *yx* and *yy* mean the respective orientations of the excitation polarizer and the emission polarizer referred to the *x*,*y* plane of the substrate. The polarization ratio *p* was calculated as follows:

$$p = \frac{I_{//} - I_{\perp}}{I_{//} + I_{\perp}}$$

where $I_{//}$ is the emission intensity when the excitation and emission polarizers are parallel and $I_{\perp}$ is the emission intensity when the two polarizers are perpendicular[86]. We found a value for *p* of about 20 %, confirming the small alignment of the terthienyl side chains observed in the UV spectra (by complete alignment *p* = 100 %).

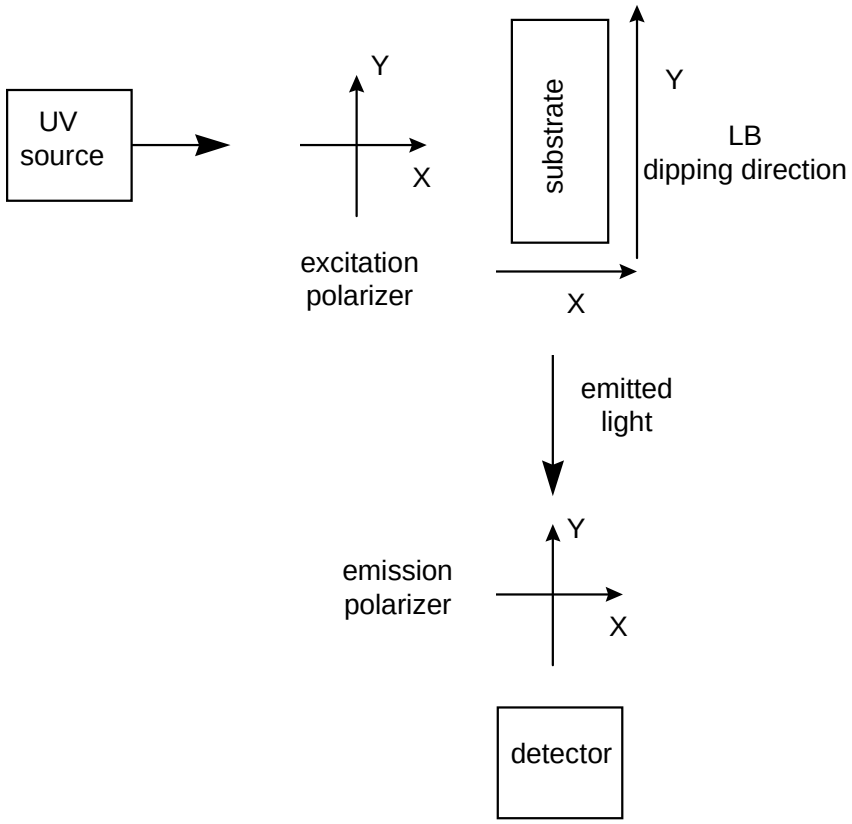

Figure 25: experimental setup for polarized fluorescence measurements on sample NRQu1

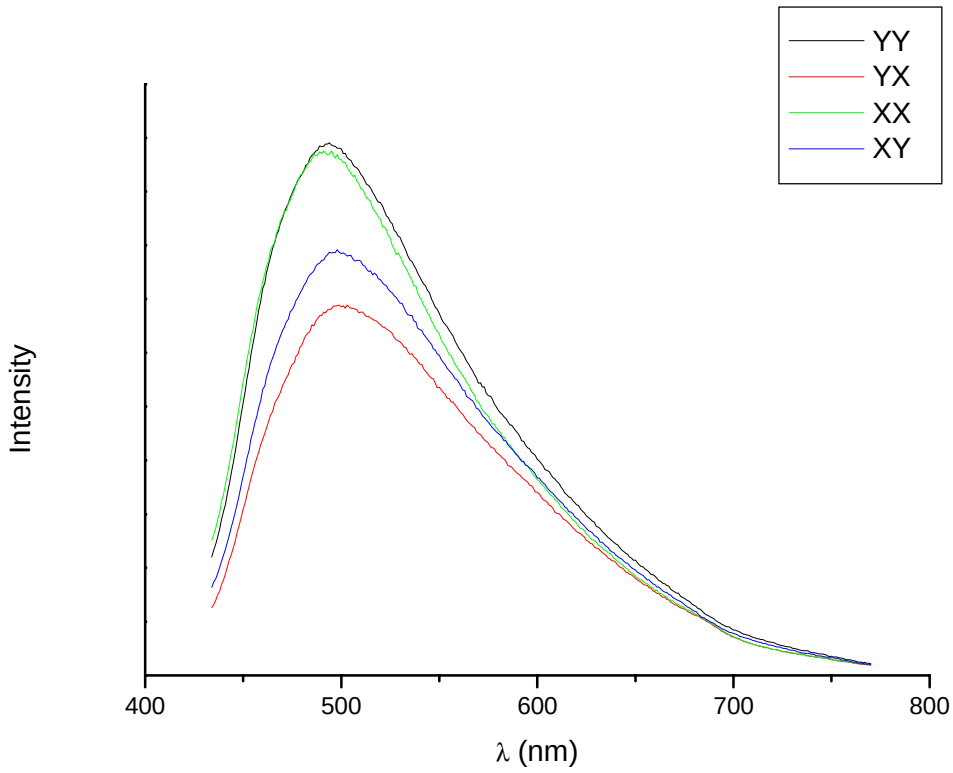

Figure 26: polarized fluorescence spectra of sample NRQu1

The LB films of BCTTE on ITO substrates were investigated by cyclic voltammetry (CV) in order to compare the electrochemical response of the LB architecture with literature data describing the electrochromic properties of polymer bound terthiophene moieties in homogeneous solution[31].

None of the samples prepared showed an electrochemical response: this may be explained by the assumption that the sterically hindered terthiophene moieties do not have sufficient mobility in the layered architecture of the LB-film to get into contact with the electrode surface. As this could depend also on the small amount of the electroactive moieties embedded in the confined geometry of the layered structure, we recorded the cyclic voltammogram of a solution of BCTTE (fig. 27).

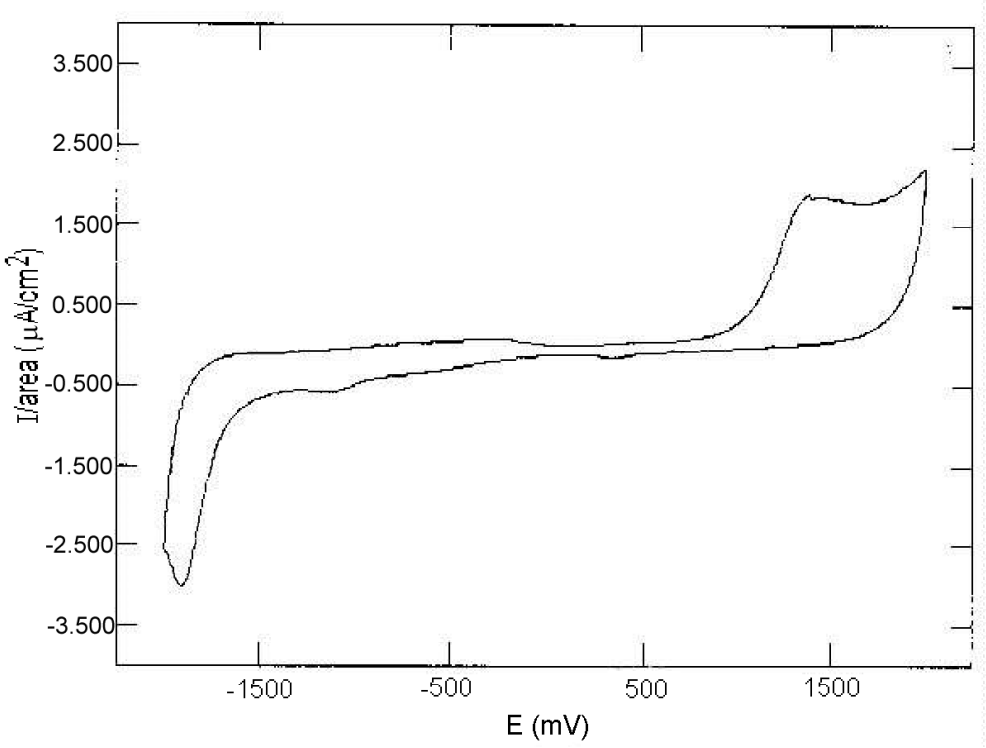

Figure 27: CV of a CH_2Cl_2 solution of BCTTE

In this case of an unconfined geometry it was possible to observe an oxidation wave at about 1.1 V/SCE. However, the oxidation was irreversible as no reduction peaks appeared in the CV. This can be interpreted as the formation of the cation-radical of the terthienyl side groups, which then likely undergoes side reactions at the free α-position, but the nature of the side reaction remains unclear. Indeed, because of the small DS of the terthienyl side groups,

the coupling between two side groups has a very low probability and can be excluded. The coupling would have been otherwise detected by the appearance of another oxidation wave at lower potential in the CV (presence of a sexithiophene moiety). However, in solution, the contact of the terthiophene groups with the electrode to form the radical cation followed by rapid deactivation of the intermediate by side reactions is straightforward. A radical-radical coupling reaction, that is formation of sexithiophene moieties, is prevented by comparatively high dilution of the terthiophene-species. Thus, electrochemical crosslinking in solution was not observed.

3.4.4.1.Grafting thiophene onto terthiophene bearing cellulose

In previous work in the group[87]the electrochemical polymerization of 3-pentylthiophene (3pT, **28**) was carried out on electrodes covered by LB films of butylcellulose. The polythiophene "islands" so formed showed a certain degree of anisotropy, observed by polarized optical microscopy.

Consequently, substrates covered first by gold then by a number of LB layers of BCTTE were used as anodes for the oxidative polymerization of 3pT. The terthienyl moiety can work as the initiator of such oxidative polymerization (sch. 37), as its oxidative potential is lower than that of the alkylthiophene monomer: 1.01 V/SCE[63] for terthiophene vs. 1.84 V/SCE of 3pT[13].

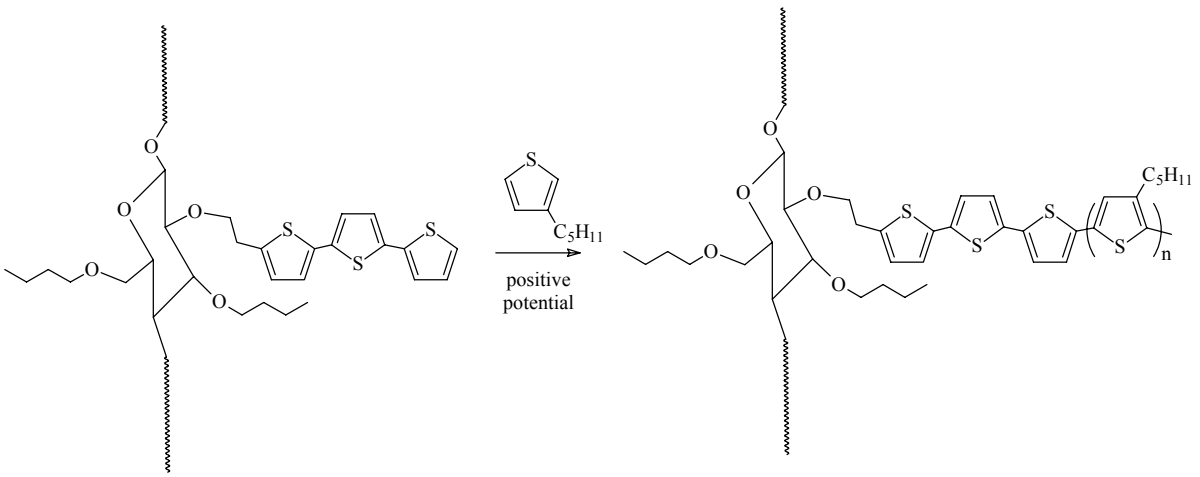

Scheme 37: graft of thiophene on cellulose through the terthienyl moiety

Such feature of terthienyl groups was already observed in our previous work dealing with the grafting of thiophene onto methacrylate copolymers bearing terthienyl side groups in solution[30].

Our aim was to study whether the presence of the partially oriented terthienyl side groups (that initiate the polymerization in the LB matrix) could improve the macroscopic anisotropy of the P3pT phase, that was formed as oriented islands on the substrate[87]. Further, we were interested to see whether the polythiophene chains composing the islands showed any anisotropy at a molecular level. The terthienyl side groups might be able to induce such anisotropy by chain alignment in the polythiophene domains, the growth of which takes place by grafting onto the rigid and partially ordered (albeit of small degree) terthiophene segments of the modified cellulose.

Therefore the electropolymerization of 3pT was performed using substrates covered by LB layers of BCTTE as anodes, as schematically shown in figure 28.

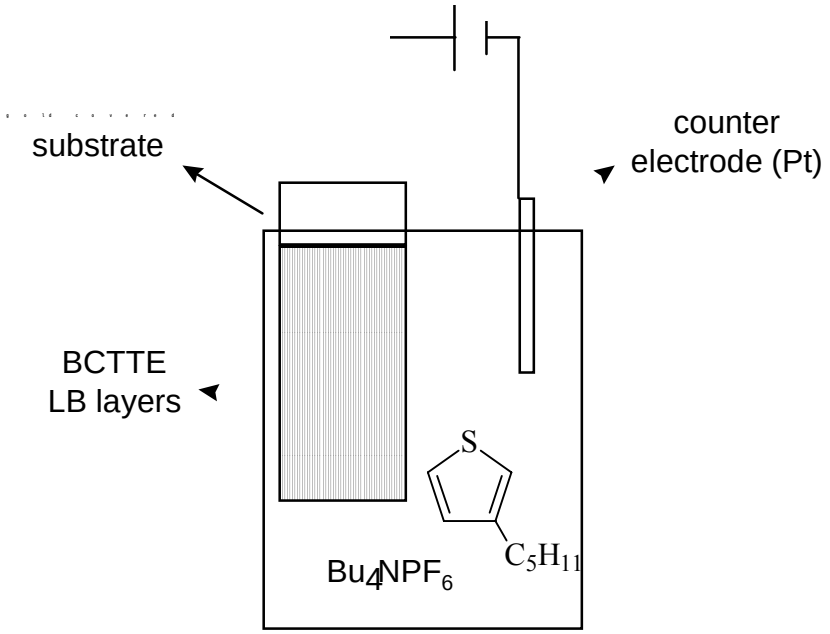

Figure 28: electropolymerization cell for thiophene graft on LB films of BCTTE

The electropolymerization conditions are summarized in table 4.

Table 4: electropolymerization conditions

Solvent	CH_3CN
Concentration of 3pT	0.2 M
Concentration of Bu_4NPF_6	0.1 M
Polymerization time	10 s
Galvanostatic condition	5 mA/cm^2

After polymerization the substrates were washed with CH_3CN and dried in air.
The formation of the expected polymer could be readily observed by UV-Vis spectroscopy as demonstrated in figure 29.

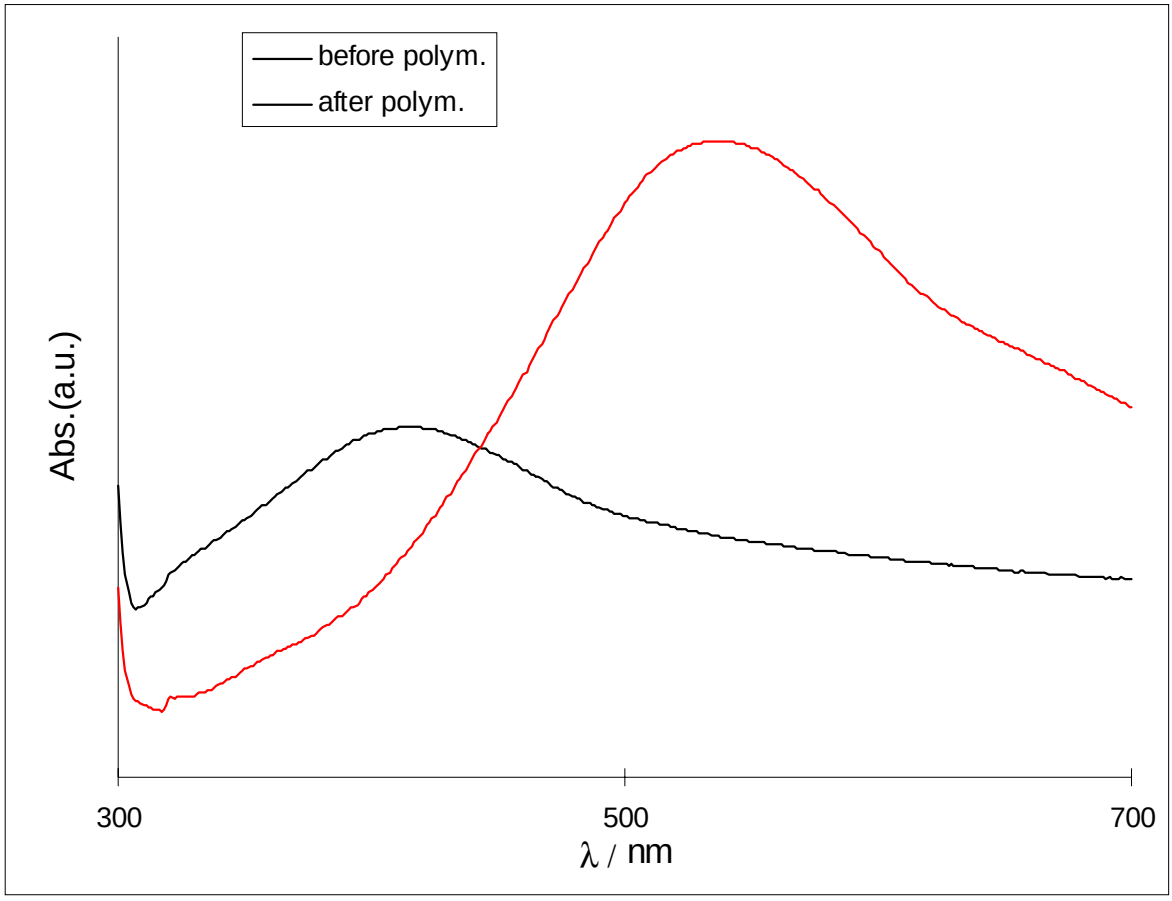

Figure 29: UV-Vis spectra of sample NRAu37 before and after 3pT-polymerization

In the spectra, the band due to the terthienyl moiety with an absorption maximum at 375 nm disappears after the polymerization of 3pT, while another band with an absorption maximum at about 500 nm appears. This can be attributed to the formation of poly(3-pentylthiophene)[2].

That means that the terthienyl moiety has expanded its conjugation length through the graft of more thiophene units, leading to the appearance of the new, red-shifted, absorption band.
When the electropolymerization of 3pT was carried out on samples covered by LB layers of butylcellulose (i.e. without terthiophene side chains) under the same reaction conditions, the obtained P3pT was obtained in a rather oxidized state. In the UV-Vis spectrum of the samples immediately after the polymerization (example of fig. 30), the broad band in the region 500-700 nm is in fact due to the presence of oxidized chains of polythiophene[1].

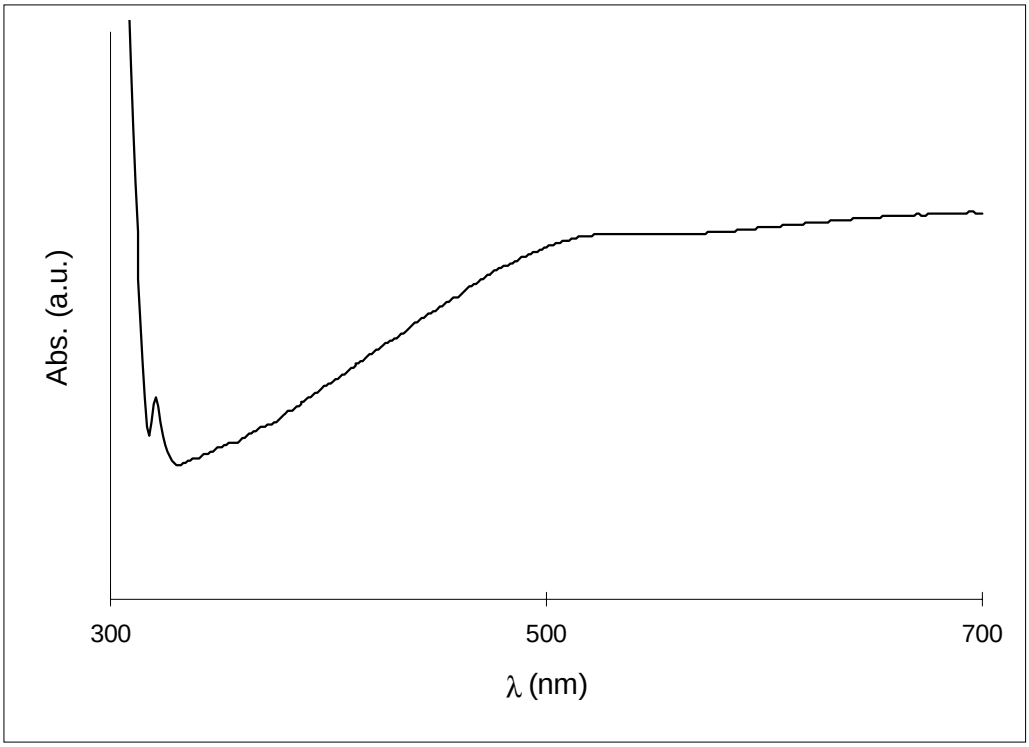

Figure 30: UV-Vis spectrum of a butylcellulose-covered substrate after 3pT polymerization

P3pT was formed on the substrates covered by LB films of BCTTE as islands, which were then observed through an optical microscope (fig. 31). On average, the islands had a diameter of ca. 75 μm. They were circular shaped and randomly oriented, as shown in figure 31, and did not show any anisotropy in the optical microscope. It is worth mentioning that the formation of islands is suppressed and continuous films are rather formed if the electropolymerization is carried out on plane gold electrodes.

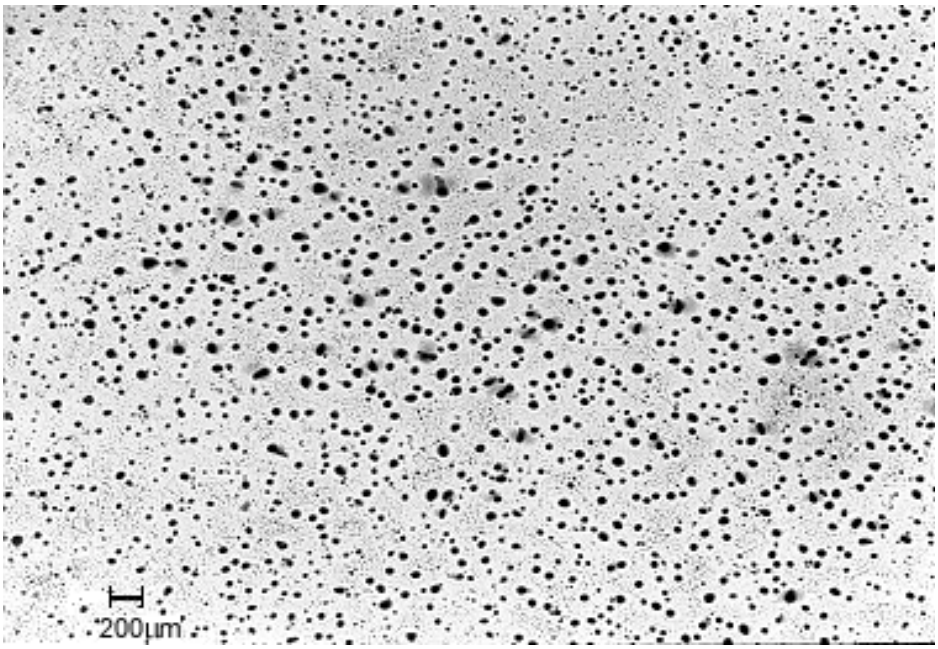

Figure 31: optical microscope picture of sample NRAu37

On the other hand, by analysis with UV polarized light, a stronger absorbance of the P3pT chains along the LB dipping direction (A_y, figure 32) than perpendicular to the dipping direction (A_x) was observed. The degree of anisotropy was estimated by the dicroic ratio *R* to be on average 1.23.

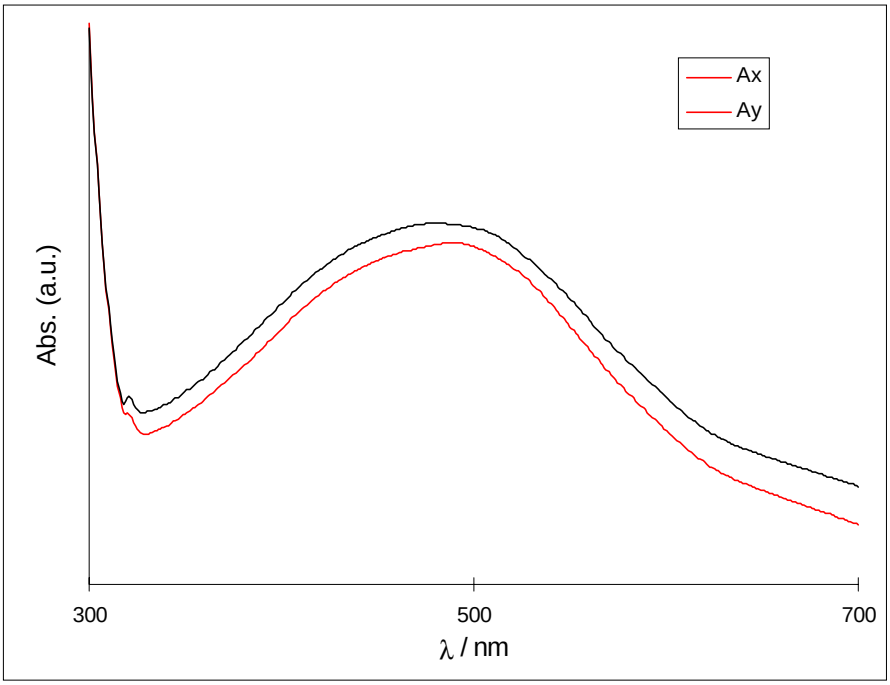

Figure 32: polarized UV-Vis spectra of sample NRAu32 after 3pT-polymerization

This preferential alignment of the poly(3pT) chains can be due either to the terthiophene side chains, even if only partially oriented along the *y* axis, or to the aligning properties of the cellulose backbones, which are highly oriented[88] *.

3.4.5. Characterization and properties of LB films of butylcellulose bearing sexithiophene side chains

The butylcellulose derivative bearing sexithiophene side chains **27**, hereafter referred to as BCST, was spread at the air water interface to test its capability to form stable monolayers at different temperatures. Figure 33 shows the surface pressure (π) vs. area diagrams at 5 °C, 12 °C and 19 °C.

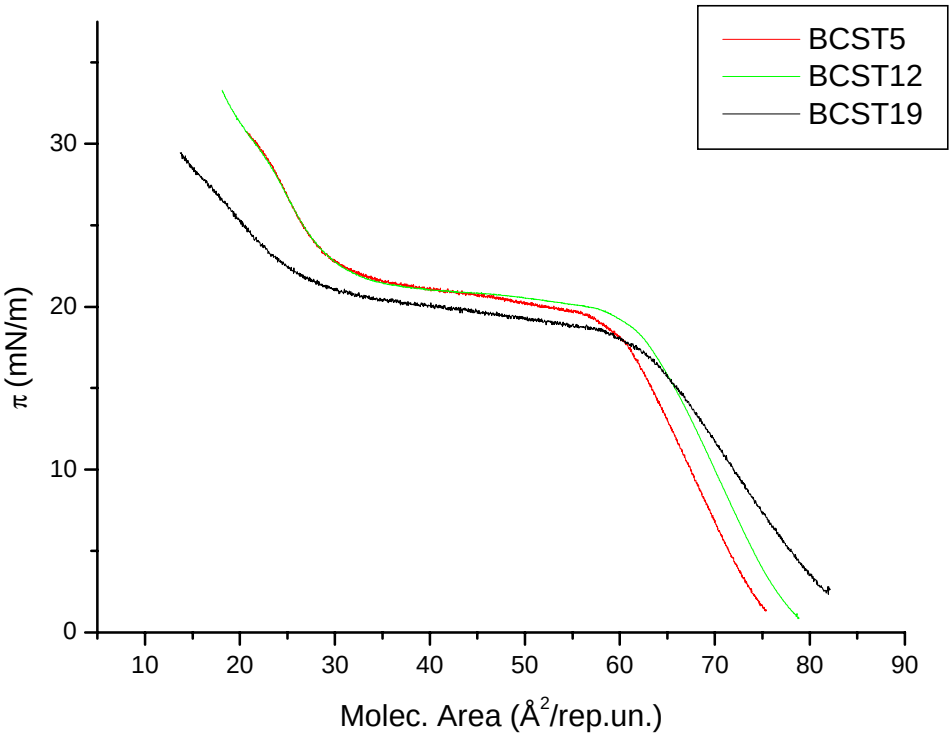

Figure 33: pressure-area isotherms of BCST

* In the literature (ref. 87) no investigation of the anisotropy of the P3pT chains at a molecular level was carried out.

The behavior of the polymer upon compression is very similar to the one of BCTTE, although the two cellulose derivatives are different regarding the degrees of substitution of both the butyl and the oligothiophene side chains, as well as of course the length of the oligothiophenes. The limiting area value at which the monolayers begin to lose the reversible behavior on compression-decompression is higher for BCST (ca. 60 $Å^2$) with respect to BCTTE (ca. 45 $Å^2$), due probably to the higher steric hindrance of the former's side groups.
It was attempted to transfer the BCST monolayers on different solid substrates, such as glass, gold-covered glass and ITO, following the transfer conditions reported in table 5.

Table 5: LB transfer conditions of BCST

Substrate	T (°C)	π (mN/m)	Nr. Layers
ITO	19	10	100
Au-covered glass	19	10	50
Au-covered glass	5	14	50
Glass	5	14	40

None of the trials to transfer the monolayers on the substrates was successful, as only a partial deposition occurred. The transfer plot for the best result obtained is reported in figure 34.

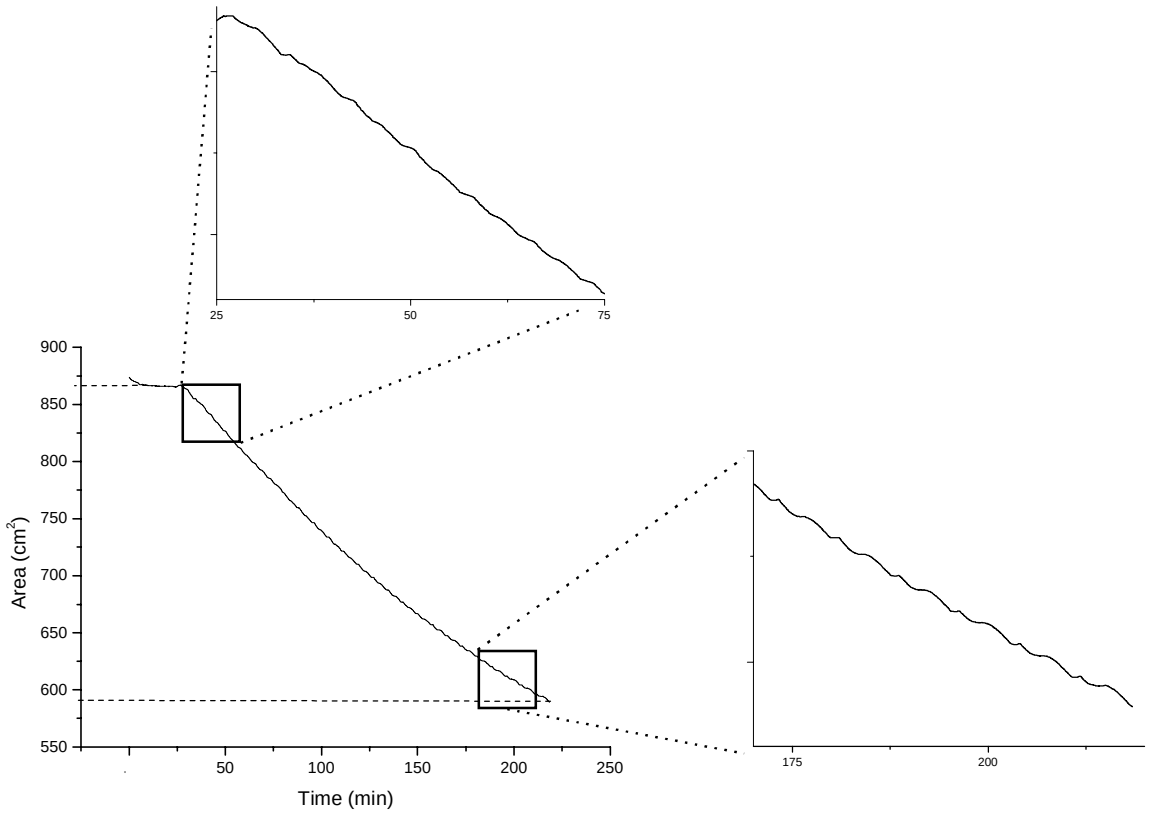

Figure 34: area-time plot during transfer of LB monolayers of BCST

The plot shows the planned transfer of 50 layers on two gold-covered glass substrates of 4 cm^2 area each. A complete transfer (100 % ratio) would give a total transferred area of $50 \cdot 4 \cdot 2$ $cm^2 = 400$ cm^2. But as calculated from the plot of figure 34 only 300 cm^2 were transferred on both substrates, corresponding to a 75 % ratio. Such a ratio was observed on average also in the transfer of BCTTE layers (see chapter 3.4.4.), but there the layered structure showed an ordered geometry by analysis with x-rays, while in this case no reflection peaks were observed in the x-rays reflectogram. Such unordered geometry was expected already by analyzing the area-time plot of the transfer. In fact, the transferred area was not constant at every dipping or undipping step (magnified plot zones of fig. 34), but rather random.

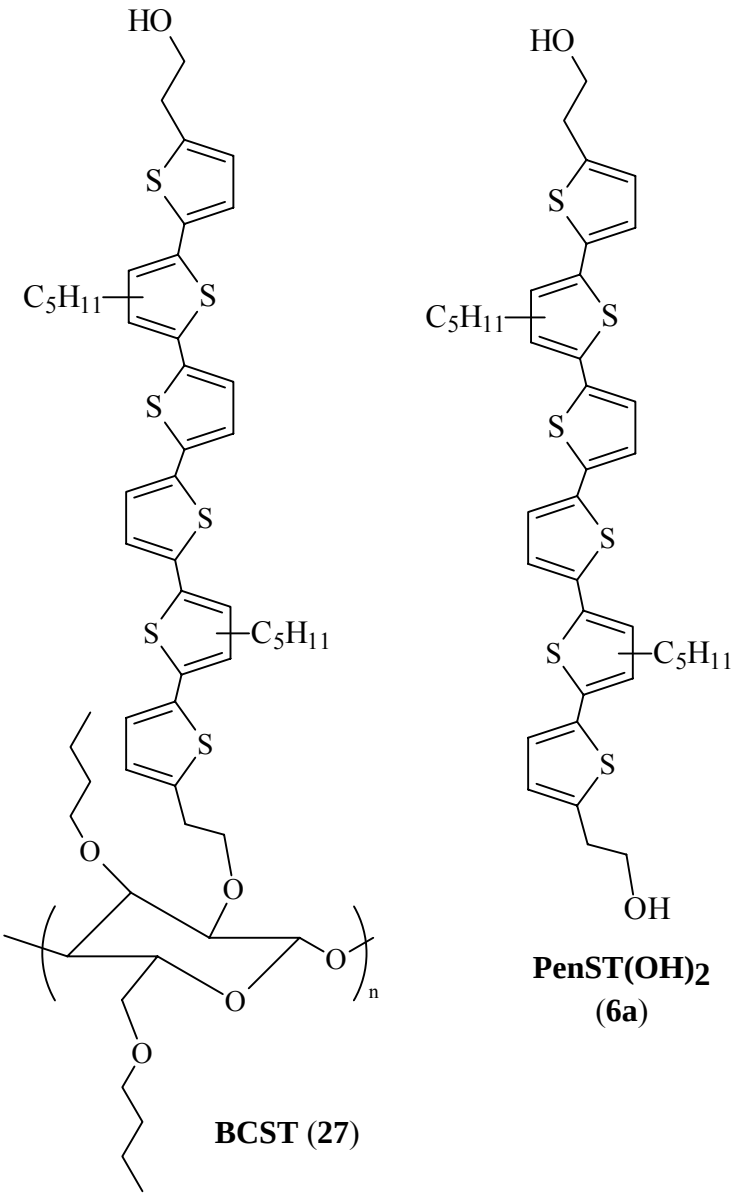

Figure 35: Butylcellulose with sexithiophene side chains covalently linked (left) and side chain model (right)

In order to understand such unexpected behavior of the BCST monolayers upon transfer, we investigated the formation of monolayers at the air-water interface by single molecules of $PenST(OH)_2$, which represent the oligothiophene side chains in the BCST polymer (fig. 35). We measured therefore the π-area isotherms for such low molecular weight moiety at the same temperatures as for the cellulose derivative, i.e. 5 °C, 12 °C and 19 °C (fig. 36).

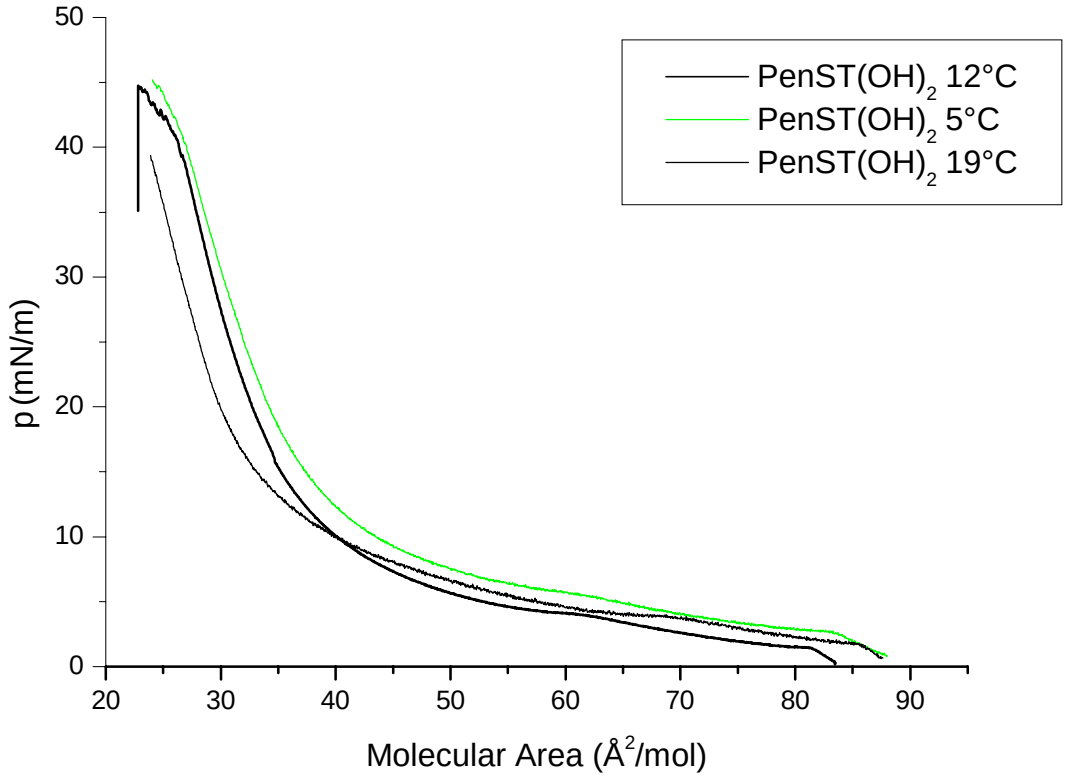

Figure 36: pressure-area isotherms for $PenST(OH)_2$

The behavior at the air-water interface of the molecule can be described as a „solid film" behavior[85] due to the close packing of the system similar to the one of the bulk phase. Such behavior was already observed in a work[89] dealing with LB monolayers of several oligothiophenes, including unsubstituted sexithiophene. In that case, the isotherm shows the same trend as observed in our experiments. Only the values for the molecular area are different, since in our case a disubstituted sexithiophene was used. The authors, Nakayara *et al*., suggest the aggregate formation of the conjugated chains on the water surface, due to the rigid π-electron rich backbone that tends to form π stacks.

In the case of polymer BCST, where the sexithiophene molecules are present as side groups, the possible formation of aggregates could act as physical cross-linking points on the water surface that surface-anchor the monolayers and disturb the transfer process onto the solid substrates. In the literature[90] the formation of aggregates at the air-water interface was observed also for a polyester containing alkyl sexithiophene in the main chain. As consequence, the transferred films of such aggregated monolayers showed defects.

The possibility to transfer monolayers of PenST(OH)$_2$ on quartz solid substrates was also investigated, performing the transfer at the very low surface pressure of π = 3.5 nM/m and at 5 °C.

Again, a low transfer ratio was observed and also in this case the x-rays reflectogram of the samples did not show any reflection peak, due to a disordered geometry of the monolayers on the solid surface.

By polarized UV-Vis analysis of the substrates covered with such monolayers of PenST(OH)$_2$ (fig. 37), a higher absorption along the LB dipping direction (A_y) compared to the perpendicular direction (A_x) was found. The chromophore main axis is therefore preferentially aligned along the LB dipping direction in the random packed LB monolayers.

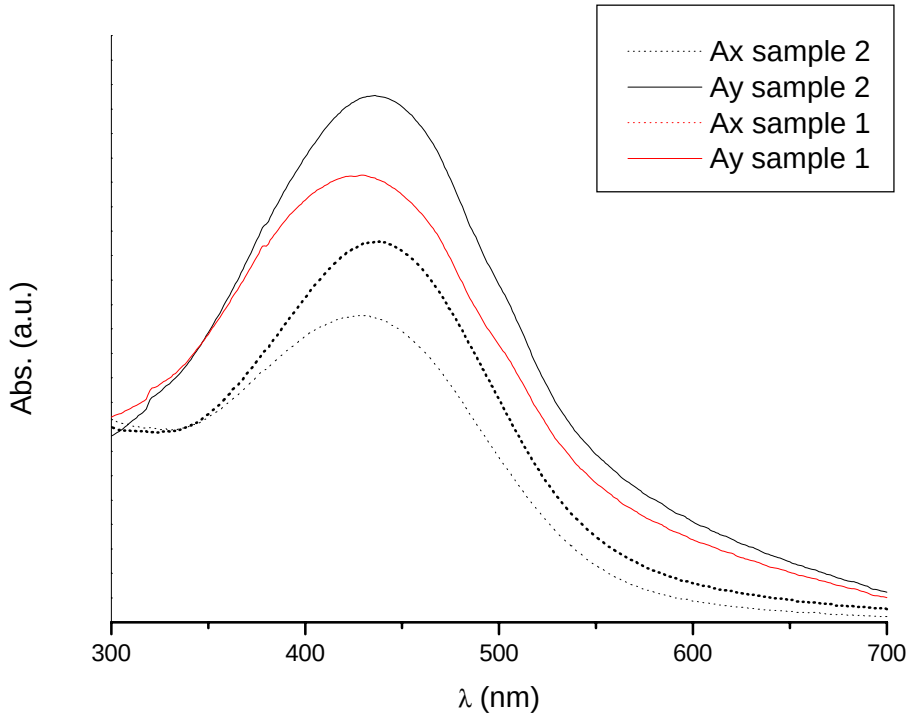

Figure 37: polarized UV-Vis spectra of samples sub#1 and sub#2

The absorption maximum of the substrates is red shifted with respect to the maximum of the chromophore in solution, since that of sample sub#1 is at 430 nm and that of sub#2 at 436 nm, while the absorption in solutions had maximum at 416 nm, 422 nm and 427 nm in hexane, ethanol and toluene, respectively. The bathochromic shift in the UV-Vis spectra in the solid

state can be attributed to the formation of π-stacks of the aromatic chains that cause a diminution of the band gap[75].

3.5. Attempts to polymerize acrylic monomers bearing sexithiophene side chains

Beside the investigation of cellulose derivatives carrying sexithiophene side chains, we were also interested in the study of a homopolymer bearing sexithiophene side groups.
Therefore an acrylic monomer with sexithienyl pendants (**8**, PenSTOHA, see chapter 3.2.2.2.) was synthesized (fig. 38).

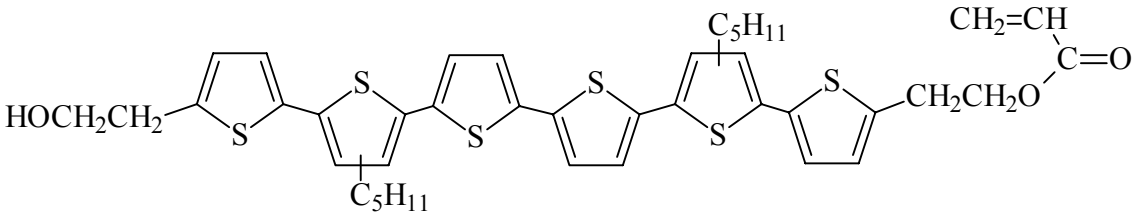

PenSTOHA
(**8**)

Figure 38: acrylic monomer bearing a sexithiophene side chain

This acrylate was attempted to polymerize by two different free radical polymerization reactions, whose conditions are reported in table 6.

Table 6: radical polymerization condition for PenSTOHA

Run	Initiator[a]	Solvent	Temperature	Time
I	AIBN	THF	60 °C	7 d
II	DP	Dioxane	80 °C	5 d

[a]AIBN: 2,2'azo-bis(isobutyrronitrile), DP: dibenzoyl peroxide

Both polymerization attempts were not successful: after pouring the reaction mixtures in methanol, no polymer precipitate was obtained. The absence of the expected polymer was also confirmed by GPC analysis on the methanol solution, where only low molecular weight oligomers were present (fig. 39)

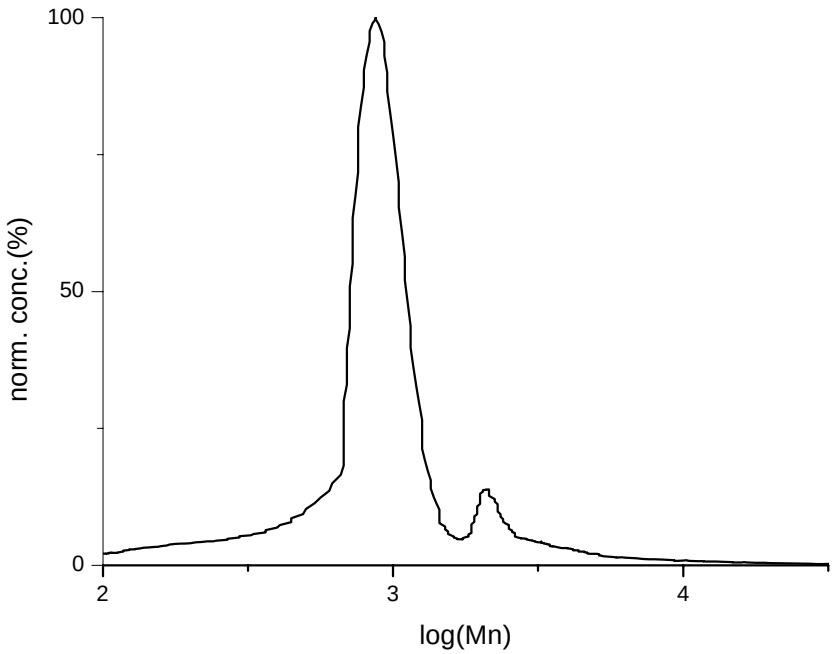

Figure 39: GPC analysis after the radical polymerization run **I**

The fact that the polymerization did not take place in the two reaction runs, where different initiators, solvents, temperatures and reaction times were used, suggested that the sexithiophene moiety must play a primary (negative) role in the polymerization. A low polymerization degree was also found in the free radical polymerization of a vinyl terthiophene described in literature[47], which was carried out under similar conditions and gave a poly(vinylterthiophene) with only 7 monomer units *per* macromolecule on average. Thus, the presence of an electron rich π-system in the acrylate could probably inhibit the propagation of the reaction. In order to verify such possibility, we performed the polymerization of a common methacrylate monomer, i.e. methylmethacrylate (MMA), both in presence and in absence of the disubstituted PenST$(OH)_2$ (**6a**, fig. 35), that represents the side chain group of the acrylate monomer PenSTOHA (**8**, fig. 38). The polymerization conditions are reported in table 7.

Table 7: Conditions of polymerization of MMA with and without $PenST(OH)_2$

Run	Monomer	„Inhibitor“	Initiator	Solvent	Temperature	Time	$\overline{Mn}$ [a]
III	MMA	-	AIBN	THF	60 °C	3 d	4800
IV	MMA	$PenST(OH)_2$ 1 %	AIBN	THF	60 °C	3 d	4700
V	MMA	-	BP	Dioxane	80 °C	3 d	4700
VI	MMA	$PenST(OH)_2$ 1 %	BP	Dioxane	80 °C	3 d	4900

[a]: GPC

The polymerization was stopped pouring the reaction mixtures in methanol and collecting the precipitate. The GPC analysis on each sample showed about the same polymerization degree for the obtained PMMAs, which was found to be on average ca. 50. Thus, on the basis of such experimental results, it seems that the added sexithiophene (runs **IV** and **VI**) does not play any role in the propagation of free radicals. However, it cannot be distinguished between a sterical or intramolecular electronic effect of the oligothiophene side chains.

We chose therefore to perform an anionic polymerization of the acrylate bearing sexithiophene side chains **8**, after having protected its base-sensitive free –OH group as described in scheme 38.

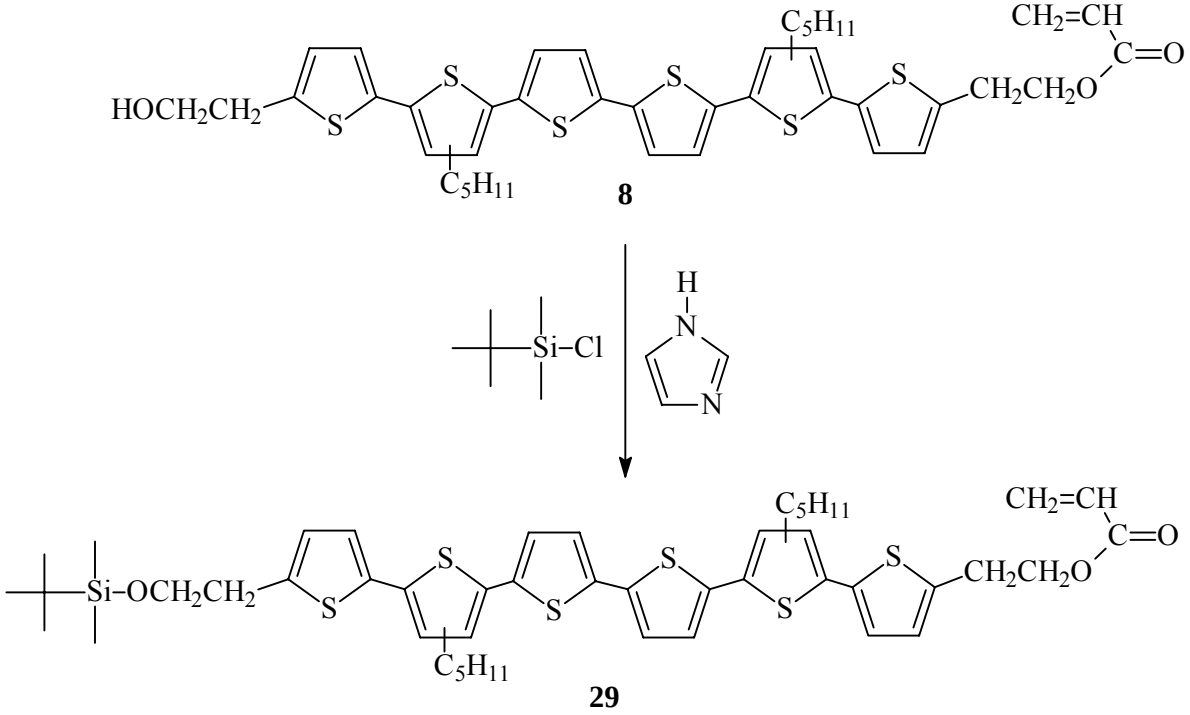

Scheme 38: OH-protection of the acrylate bearing sexithiophene side groups **8**

Such monomer **29**, PenSTASi, is stable to basic conditions and can therefore undergo an anionic polymerization reaction initiated by BuLi.

The polymerization mixture in THF was stored 7 d at room temperature with 1 % *n*-buthyllithium (BuLi) under strictly inert conditions. It was then poured into methanol, but also in this case no precipitate due to polymer formation was observed. GPC analysis on a sample of the methanolic solution (fig. 40) showed an average molecular weight $\overline{Mn}$ = 1300 g/mol, slightly higher than the monomer's molecular weight (PM = 890 g/mol), and the presence of a low molecular weight oligomer (≈ 3200 g/mol) corresponding to about 3 linked monomer units. A similar low molecular weight oligomer was also observed after the attempted radical polymerization (see fig. 39).

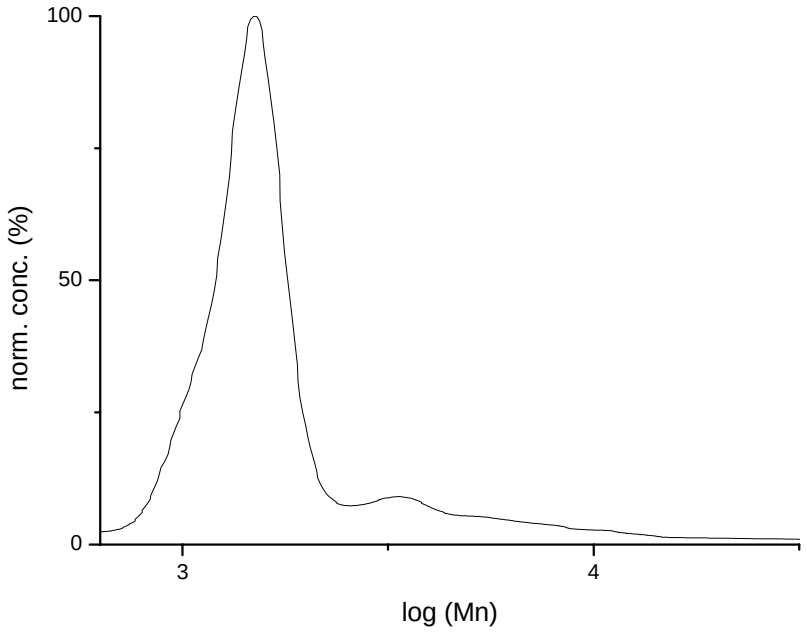

Figure 40: GPC analysis after anionic polymerization

Regardless to the different polymerization techniques and conditions carried out, all attempts to polymerize the acrylate monomer with sexithiophene pendants were not successful.

A reasonable explanation can be found considering the high steric hindrance represented by the sexithiophene side groups of the monomer, that is separated from the acrylic double bond by only two methylene units. In a recent review[91] about the polymerization of

macromonomers toward to the synthesis of dendrimers, it is stated that monomers in which the dendron (i.e. the steric hindered side group) is bound too tightly to the polymerizable functionality do not give high molecular weight polymers and that oligomeric products are often found instead of polymers. In particular, in a work[92] describing the polymerization of methacrylic macromonomers, only a low polymerization degree $\overline{P} = 6$ was found after the radical polymerization of the macro-methacrylate **30** (fig. 41). This result supports the hypothesis that in our case the steric hindrance of the sexithiophene side groups played an important role in preventing the formation of the expected polymer.

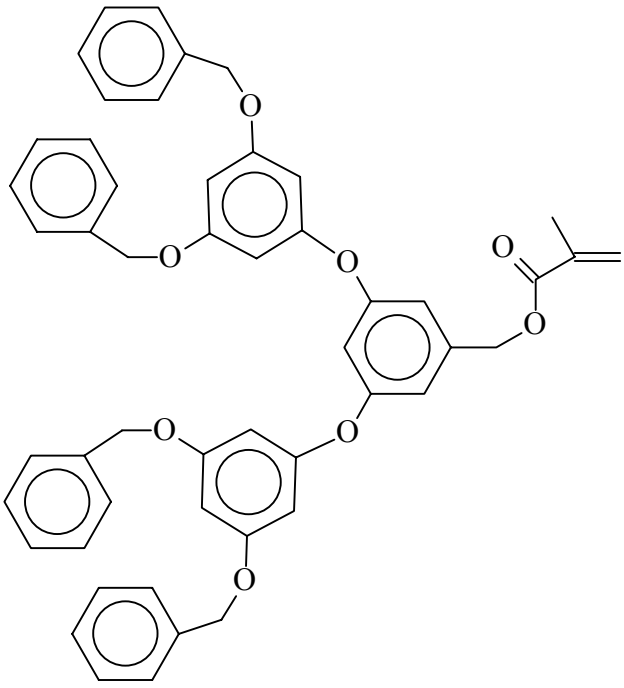

Figure 41: methacrylic macromonomer described in ref. 92

An alternative explanation can be found in the tendency of the sexithiophene moieties to form aggregates. Such tendency could lead, during the polymerization process, to a situation in which π-stacks between the side groups are formed, causing a cyclic conformation where back-biting occurs and no further monomers can be attached (fig. 42).
However, also in the case of the anionic polymerization, side reactions due to a small amount of impurities as well as moisture cannot be strictly ruled out due to the restricted monomer availability.

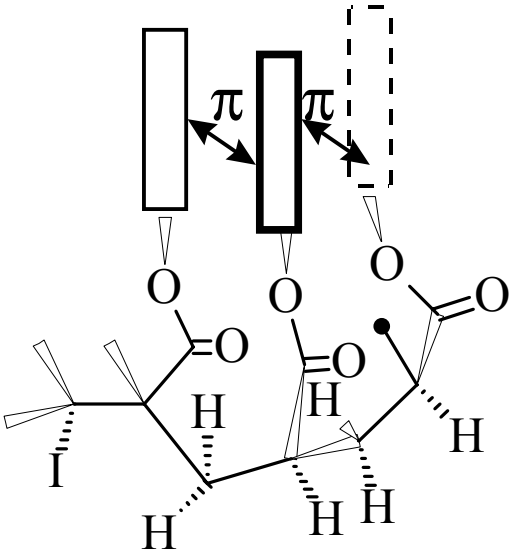

Figure 42: possible conformation of the growing acrylic chain

3.6. Synthesis and properties of poly(p-phenylene-ethynylene) bearing sexithiophene side chains

The aim of the work was the synthesis of a homopolymer with sexithiophene pendants, in order to obtain a geometry in which a rigid polymer main chain is surrounded by the electroactive sexithienyl groups (see chapter 2).

On the basis of the unsuccessful radical polymerizations of the acrylic monomers PenSTOHA and PenSTASi (**8**, **29**, respectively), we decided to perform another polymerization reaction that showed already satisfactory results with steric hindered macromonomers. We chose therefore to perform a *Hagihara-Sonogashira* coupling to polymerize 1,4-diethynylbenzenes with 1,4-diiodobenzenes, since such polymerization was successful also with high molecular weight monomers[91].

For that purpose we prepared (see chapter 3.2.2.3.) the two monomers **15** and **18** shown in figure 43.

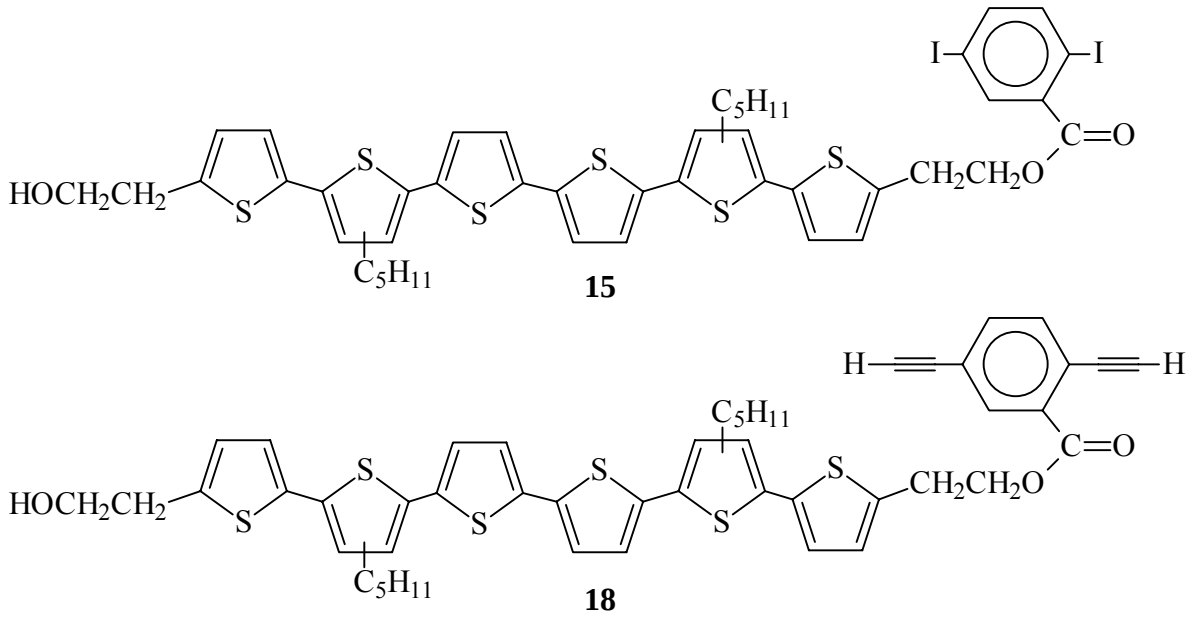

Figure 43: disubstituted benzenes carrying sexithiophene side chains

The palladium catalyzed polymerization occurs according to scheme 39, using copper iodide as co-catalyst and triethylamine as base.

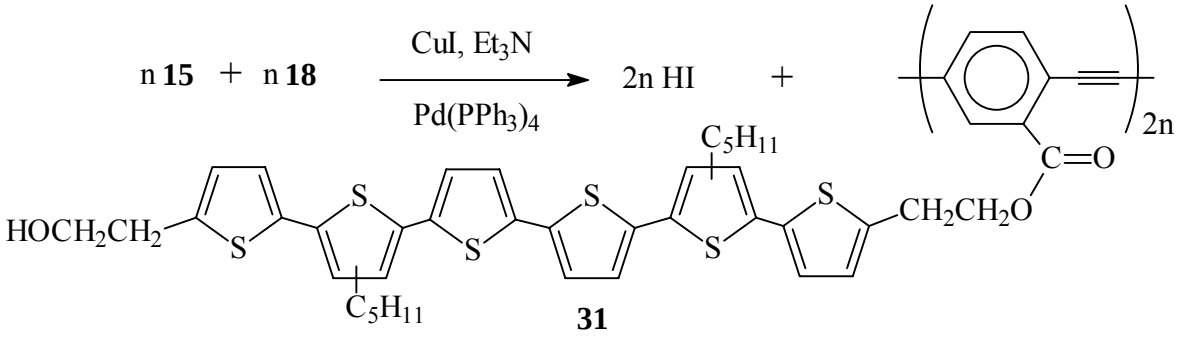

Scheme 39: *Hagihara-Sonogashira* polymerization of disubstituted benzenes bearing sexithiophene side chains

The reaction was stopped after 6 d at 60 °C by precipitating the mixture in diethyl ether, as in the usual precipitation solvent methanol also the monomers are insoluble. The redissolution of such precipitate was not complete, and the successive reprecipitation of the soluble fraction gave as well a not redissolvable precipitate. We collected therefore the insoluble material which was further washed stirring overnight the suspension in diethyl ether.

In order to characterize the obtained product, we run GPC analysis (fig. 44) of a THF-soluble fraction, present in negligible amount but sufficient for detection in the GPC experiment due

to the high extinction coefficient of the sexithienyl chromophore. Such fraction was found to have an average molecular weight $\overline{Mn}$ = 5600 g/mol, corresponding to a polymerization degree $\overline{P}$ = 7 ($PM_{repeating\text{-}unit}$ = 848 g/mol). That demonstrates that the polycondensation reaction occurred and allows to expect a higher molecular weight of the insoluble fraction.

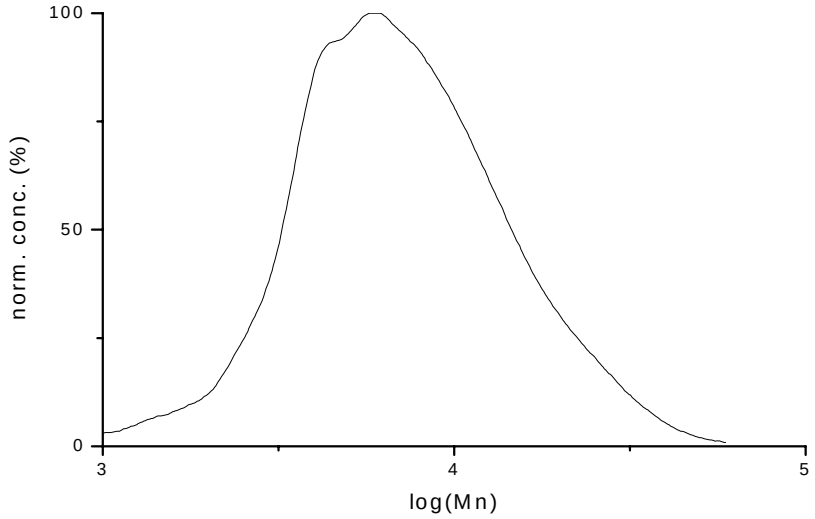

Figure 44: GPC analysis on THF-fraction of **31**

Attempts to measure the average molecular weight by means of the MALDI-TOF spectroscopy was not successful . In figure 45 the infrared spectra of the polymer **31** (hereafter referred to as BzAcST) and of the monomer **18** are shown.

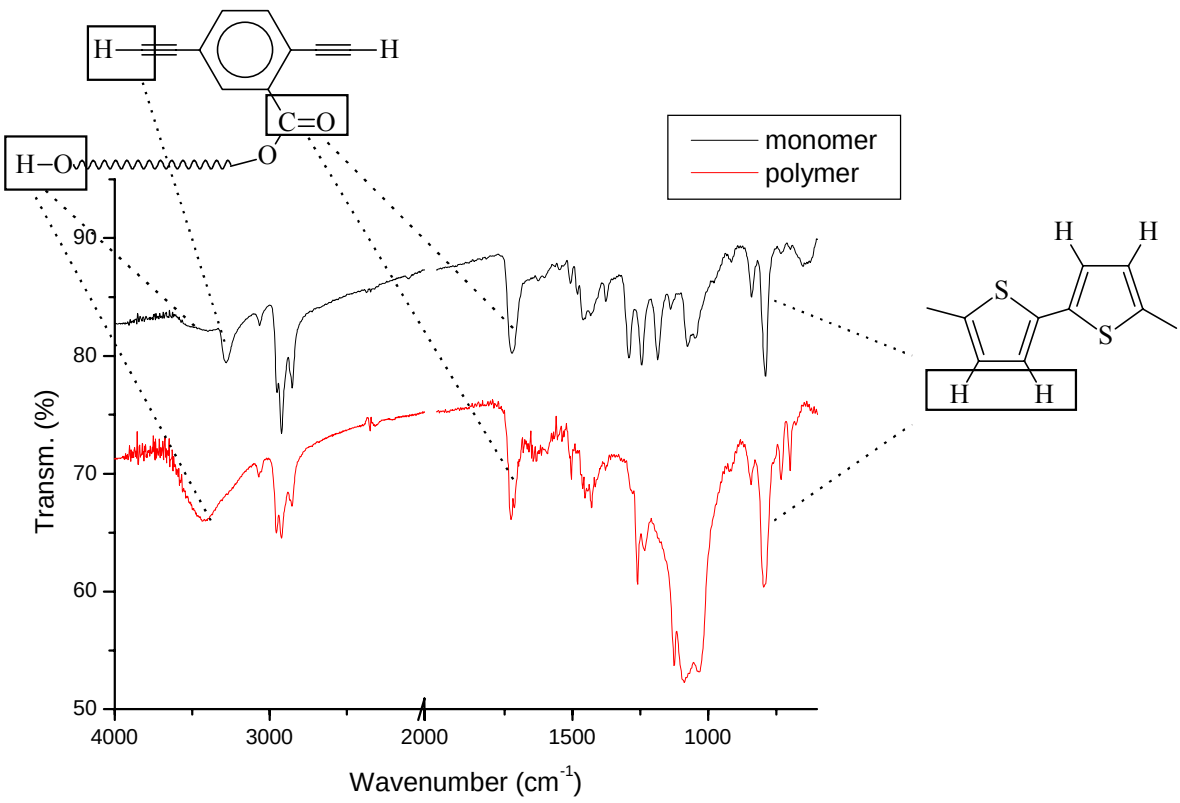

Figure 45: IR spectra of **18** and the polymer BzAcST

The features that arise from the spectra demonstrate the occurred polymerization of the monomers. In fact, the band present in the monomer's spectrum at about 3300 cm^{-1}, corresponding to the stretching mode of the acetylenic C-H bond, disappears in the spectrum of the polymer, indicating the formation of the bond between the acetylenic and the benzenic carbons. The symmetric disubstituted triple bond in the polymer does not have instead any IR-active vibration modes. The bands due to the functional groups that did not partecipate in the polymerization, are present in both spectra: at 1725 cm^{-1} the stretching band of the carbonyl group ($\nu_{C=O}$), at 788 cm^{-1} the absorption of the conjugated thiophenes (ρ_{C-H}) and the broad band centered at ca. 3430 cm^{-1} due to the free –OH (ν_{O-H}). These data confirm the expected structure of the polymer **31** reported in scheme 39.

The insolubility of the polymer is probably due to the effects of (i) the rigid main chain, whose free rotation is further hindered by the bulky side groups, and of (ii) the –OH pendants, through which hydrogen bonds perform a physical cross-linking.

Such insolubility should be overcome by the copolymerization of monomers with alkyl side chains of different length[93], in order both to improve interactions with solvent and to decrease those between the backbones, that favor the solid state.

The *differential scanning calorimetry* (DSC) analysis confirms the presence of a rigid backbone, since no glass transition was detected. In the scanned temperature range (0-200 °C) the material does not show either a first order transition, which could eventually occur at higher temperatures due to contribution on the melting temperature (*Tm*) of both the hydrogen bonds (increasing the melting enthalphy, ΔHm) and the rigidity of the backbone (decreasing the melting enthropy, ΔSm), as stated by the formula:

$$Tm = \frac{\Delta Hm}{\Delta Sm}$$

Beside that, the material might also not have any *Tm*. In fact, the sexithienyl side groups are present as three isomers (see chapter 3.2.2.1.) that are randomly distributed along the polymer main chain. This might prevent the regular packing of the polymer chains and therefore their crystallization.

3.6.1. Investigation of the electrical conductivity

Conjugated oligo- and polythiophenes show electrical conductivity upon doping, i.e. the chemical or electrochemical oxidation of the molecule generates positive free charge carriers along the conjugated main chain (see *Introduction*).

Thus, in order to investigate this property, the insoluble poly(p-phenylene-ethynylene) carrying sexithiophene pendants BzAcST must first undergo a doping reaction. Due to its unprocessability, the doping can be performed only by a chemical oxidation of a polymer suspension. Therefore we suspended the polymer in a suitable solvent (see *Experimental Part* for reaction conditions) and added three equivalents of $FeCl_3$, since this procedure was already successfully adopted in a previous work[30], describing the $FeCl_3$-doping of insoluble methacrylates bearing polythiophene pendants.

After work-up, the doped BzAcST was compressed into a pellet, onto which gold was evaporated to ensure electrical contacts. The conductivity was measured in the alternate current (AC) mode as a function of frequency and temperature (fig. 46).

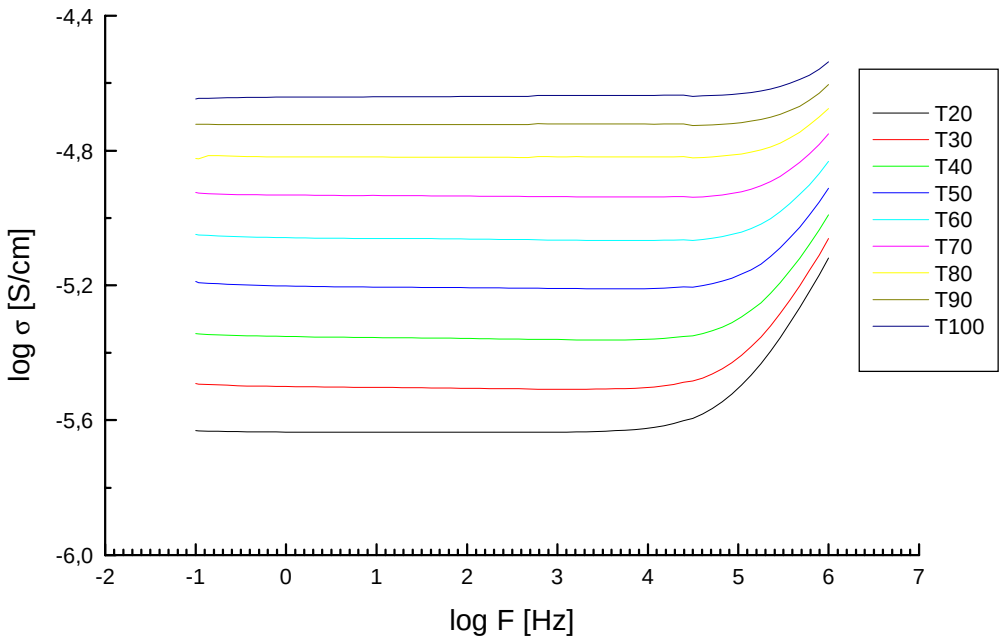

Figure 46: AC conductivity measurement of a gold covered BzAcST pellet

The plateau intercept gives the value of the conductivity at the corresponding temperature, which at 20 °C was found to be $\sigma_{20} = 2.5 \cdot 10^{-6}$ S/cm. Such value, typical for semiconductors, is lower than the one measured on a poly(vinylsexithiophene) in a previous work[40], which was ca. $\sigma = 10^{-4}$ S/cm after electrochemical doping. Such difference arise mostly from the different structures of the two polymers (fig. 47). In our case the electroactive sexithiophene is more diluted by the non conductive main chain. The poly(p-phenyleneethynylene) main chain is not oxidized by $FeCl_3$ and therefore does not contribute to the conducting process (ref. 94 and therehin). Also the insolubility of the polymer could have prevented a complete oxidation by the dopant ($FeCl_3$).

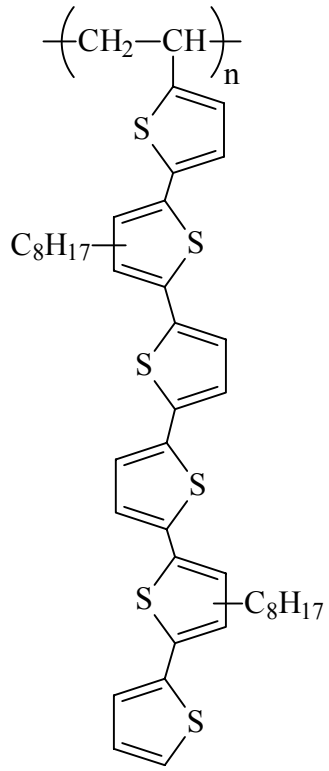

poly(vinylsexithiophene)

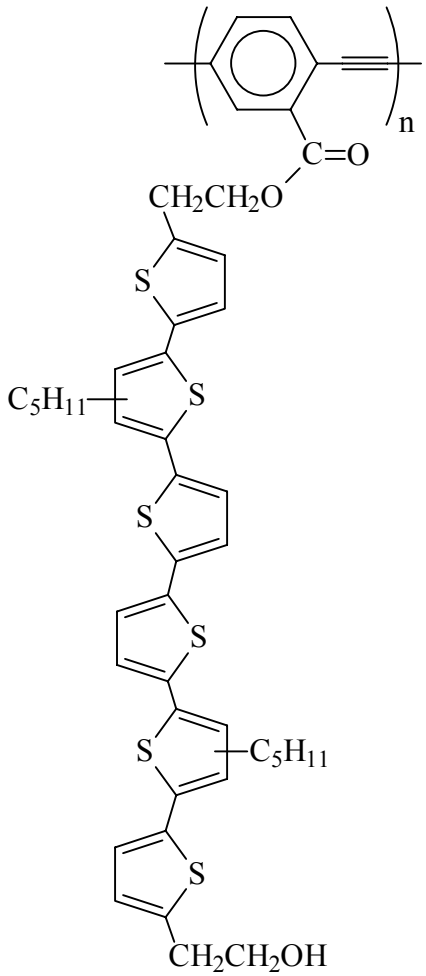

BzAcST

Figure 47: comparison between the structures of two monomers bearing a sexithiophene moiety

The conductivity process for conjugated poly- and oligomers can be qualitatively summarized as a generation of positive charges along the conjugated chain that can move through the material by hopping from chain to chain[1]. This interchain transport requires an activation energy that is the average of the energy gaps between the chain-couples involved in the charge hopping[95]. E_{att} is correlated to the conductivity by the Arrhenius equation, that can be written as:

$$\sigma = Ae^{-\frac{Eatt}{RT}}$$

Taking the logarithm of both members of the above equation, one obtains:

$$\log \sigma = -\frac{Eatt}{RT} + const$$

By plotting the logarithm of the electrical conductivity as a function of the inverse temperature, the slope $-\frac{Eatt}{R}$ of the interpolated line gives the activation energy E_{att}, according to Hill's method[96]. From the plot in figure 48 such energy for BzAcST was calculated.

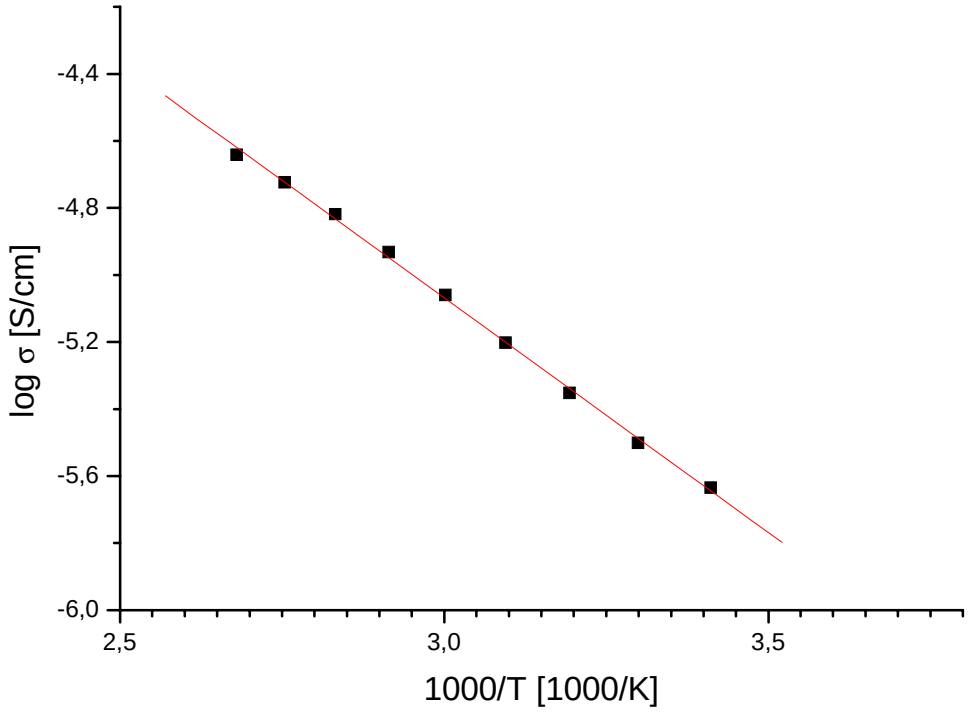

Figure 48: activation plot of conductivity vs. inverse temperature

The value for E_{att} is 4.4 eV, one order magnitude higher than the value found in the literature[40] (E_{att} = 0.3 eV) indicating a more difficult charge transport in our polymer. This might be both due to a less degree of doping or to the hindered movement of the charge carriers across the rigid polymer.

$FeCl_3$-doped BzAcST was investigated by IR analysis. In figure 49 is shown the expanded region in which the typical bands of the oxidized oligothiophene appear. Such bands are the intense absorptions between 1050-1150 cm^{-1} and 1300-1400 cm^{-1}, and the less intense absorption around 790 cm^{-1}. This absorptions are related to ring stretching modes and C-H

bendings of doped oligothiophene, in good agreement with the values of the IR-spectrum of oxidized sexithiophene[62].

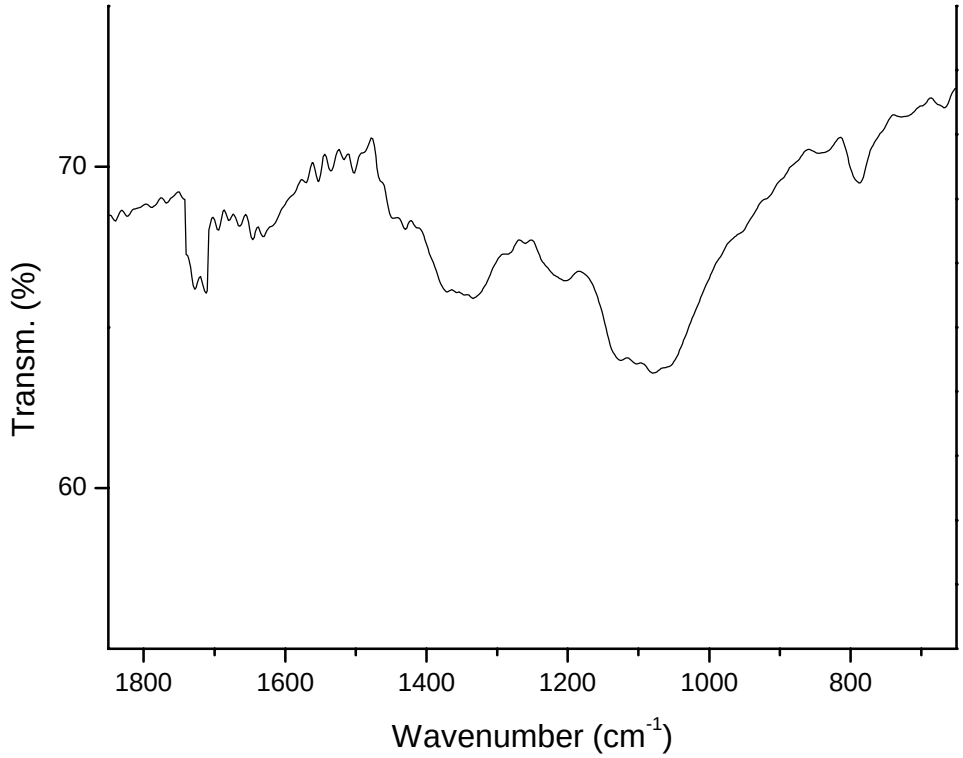

Figure 49: IR spectrum of $FeCl_3$-doped BzAcST pellet

4. SUMMARY

In the present work a series of thiophene oligomers of three and six thiophene units were synthesized, starting from thiophene, and characterized. Polymers containing these electroative side groups were then prepared by two strategies. The oligomers were attached to existing polymer systems and were connected to a polymerizable unit leading to monomer containing the oligothiophenes as side groups. Subsequently the properties of the monomers and the polymers were investigated.

A butylcellulose derivative carrying terthienyl side chains (BCTTE, **26**) was synthesized starting from cellulose acetate and 5-(2-chloroethyl)-2,2':5',2"-terthiophene (**4**). The polymer had a degree of substitution (DS) of the butyl and terthienyl side chains of DS_{butyl} = 1.9 and DS_{terth} = 0.35, respectively. It was successfully spread on a Langmuir-Blodgett (LB) trough and then transferred to several solid substrates. X-rays reflectometry showed an ordered architecture of the cellulose backbones. However, the terthiophene side groups were found as isotropically aligned by polarized UV-Vis spectroscopy. When used as anode material in the electropolymerization of 3-pentylthiophene (**28**), polythiophene was grafted onto the cellulose backbone through the terthienyl side groups. The polythiophene chains showed an average anisotropic alignment of 20 % along the LB dipping direction, calculated by means of polarized UV-Vis spectroscopy.

A second butylcellulose derivative carrying sexithienyl side chains (BCST) was synthesized and investigated, starting from butylcellulose and 2-[β',β""-dipentyl-5"""'-(2-hydroxyethyl)-2,2':5',2":5",2"':5"',2"":5"",2"""'-sexithiophen-5-yl]-ethyl p-toluensulfonate (**7**). The polymer showed formation of stable LB monolayers at the air-water interface, but its transfer onto solid substrates was not successful.

A poly(p-phenylene-ethynylene) bearing sexithienyl side chains (BzAcST, **31**) was prepared by reaction of the two monomers 2-[β',β""-dipentyl-5"""'-(2-hydroxyethyl)-2,2':5',2":5",2"':5"',2"":5"",2"""'-sexithiophen-5-yl]-ethyl 2,5-diiodobenzoate (**15**) and 2-[β',β""-dipentyl-5"""'-(2-hydroxyethyl)-2,2':5',2":5",2"':5"',2"":5"",2"""'-sexithiophen-5-yl]-ethyl 2,5-diethynylbenzoate (**18**). The polymer was obtained as insoluble product. Upon oxidation with $FeCl_3$ (doping) of the polymer suspension, BzAcST showed an electrical conductivity of $\sigma = 2.5 \cdot 10^{-6}$ S/cm, a typical value for semiconductors. The IR spectrum of the doped polymer presented the diagnostic bands of oxidized sexithiophene in good agreement with literature results.

Along with the monomer and polymer synthesis, an α,α'-disubstituted sexithiophene, β',β''''-dipentyl-5,5''''-bis-(2-hydroxyethyl)-2,2':5',2'':5'',2''':5''',2'''':5'''',2''''':sexithiophene (**6a**), was synthesized and characterized. The UV-Vis absorption of the chromophore was investigated as a function of temperature and different solvents, showing a blue-shift of the absorption maximum with increasing temperature and a red-shift changing the solvent from hexane to ethanol to toluene. Monitoring the change of the UV-Vis spectrum upon electrochemical oxidation, the oxidized chromophore showed a new broad absorption band, red shifted with respect to the π-π* transition of the neutral state. Upon reduction, the new band disappeared and the UV-Vis spectrum of the chromophore was restored. Such oxidation-reduction cycles were totally reversible. This feature, together with the absorption maximum falling in the visible region, makes this chromophore a suitable compound for the development of an electrochemical sensor.

Attempts to polymerize acrylic monomers carrying sexythienyl side chains both *via* radical polymerization, as in the case of 2-[β',β''''-dipentyl-5''''-(2-hydroxyethyl)-2,2':5',2'':5'',2''':5''',2'''':5'''',2''''':sexithiophen-5-yl]-ethyl acrylate (**8**), and anionic polymerization, as in the case of 2-{β',β''''-dipentyl-5''''-[2-(tertbutyldimethylsiloxy)ethyl]-2,2':5',2'':5'',2''':5''',2'''': 5'''',2''''' -sexithiophen-5-yl}-ethylacrylate (**29**), were not successful, probably due to the steric hindrance of the oligothiophene side group. However, due to the time consuming and therefore restricted availability of the monomers, a screening of the polymerization conditions towards the formation of polymeric material was not possible.

5. OUTLOOK

Butylcellulose derivatives carrying oligothiophene side chains need further efforts in the investigation of their properties at the air-water interface, with the outlook of possible applications of their LB films in designing electronic devices.

In the case where the side chains are terthiophene groups, a higher degree of substitution of the side moieties is required in order to observe an electrochemical response of the chromophore when submitted to proper potentials.

Since in the case of the cellulose derivative carrying sexithiophene side chains the transfer of the LB monolayers on solid substrates was disturbed by aggregates formation even at low degree of substitution (DS_{sexith} = 0.06), a change of the chemical structure of the sexithiophene moiety appears necessary in order to avoid aggregate formation. Probably shielding the rigid conjugated chain by a higher number of proper substituents could avoid aggregate formation and therefore lead to an ordered deposition of the monolayers onto solid substrates.

Alternatively, aiming at the synthesis of a homopolymer carrying sexithiophene side chains, the polymerization by the *Hagihara-Sonogashira* method was proved to be a successful strategy. In order to obtain a processable polymer, this should have a rather "soft" segment in the main chain that provides for chain mobility of the system and counterbalances thus the negative effect of the stiff side chains (i.e. the sexithiophene groups). Therefore, an alternative strategy could be represented by the synthesis of a benzene-based monomer, with e.g. an alkyl or oligoethylenoxy sequence in the main chain, where the iodo and the acetylenic functionality (i.e. the polymerizable functionalities) are present at two different benzene rings connected by the flexible chain (fig. 50). The possibility to deal with a processable polymer bearing the electroactive moiety as side groups allows one to study in detail all the electrochemical properties shown by the sexithiophene (e.g. electrochromism and electrical conductivity) and to optimize the structure-property relationships needed to address the material to the suitable applications.

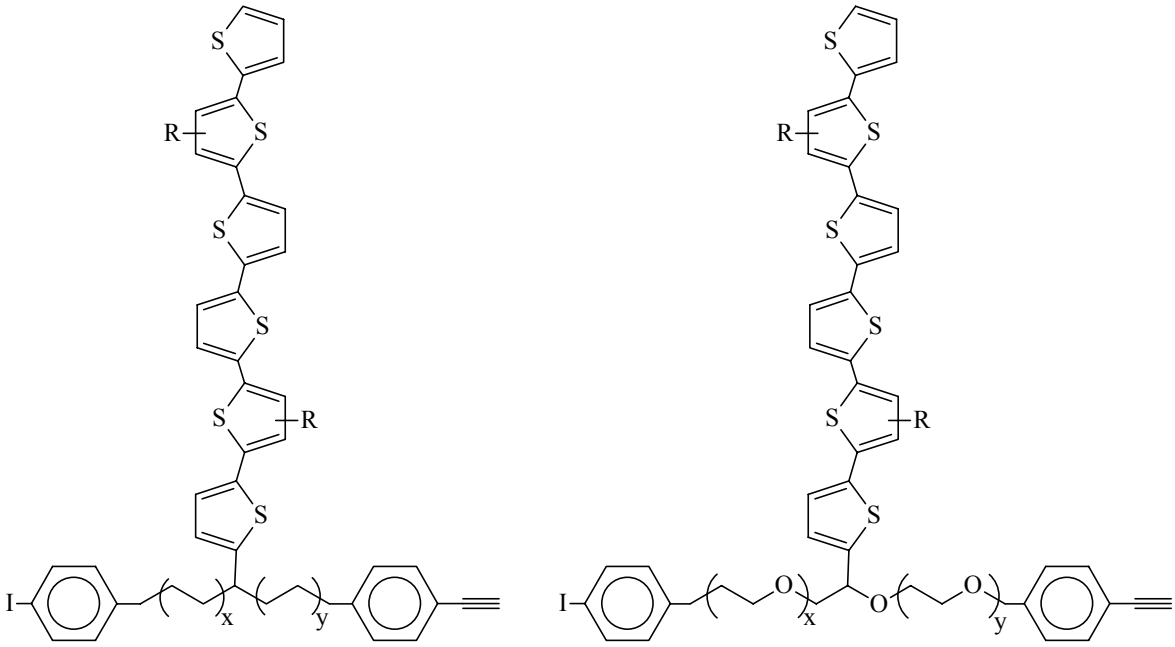

figure 50: suggested structures of monomers leading to processable polymers

6. EXPERIMENTAL PART

Devices and Methods

NMR spectroscopy- **^{1}H-NMR** spectra were recorded on a BRUKER AMX 250 (250 MHz for the proton and 62.90 MHz for the carbon) or AMX 500 (500 MHz for the proton and 75.48 MHz for the carbon), at room temperature unless stated otherwise. The specific solvent signal is used as standard: dimethyl-d_6 sulphoxide [DMSO], 2.49 ppm; chloroform-*d* [$CDCl_3$], 7.24 ppm; tetrachloroethane [TCE], 5.91 ppm. The follow abbreviations are used for the spin coupling multiplicity: **s** = singlet, **d** = doublet, **dd** = doublet of doublet, **t** = triplet, **tt** = triplet of triplet, **q** = quartet, **m** = multiplet.

Mass Spectrometry: The spectrometric measurement using the the field-desorption (FD) mode was performed on a ZAB 2-SE-FPD.

FT-IR Spectroscopy: FT-IR spectra were measured as KBr pellets on a Perkin Elmer Paragon 1000 spectrometer.

UV-Vis Spectroscopy: The UV-Vis absorption spectra were recorded on a Perkin Elmer Lambda 9 UV/VIS/NIR spectrophotometer.

Fluorescence Spectroscopy: The measurements for fluorescence excitation and emission spectra were executed on a SPEX Fluorolog 22 with an Xe-arc lamp Osram XBO 450 W as source of excitation.

Chromatography: The preparative column chromatography was performed using silica gel 60 (grain size 230 - 400 mesh, Merck) as stationary phase. The columns were filled with the stationary phase suspended in the respective solvent.

Elementary Analyses: Elementary analyses (EA) were executed in the analysis laboratory of the Institute for Organic Chemistry of the Johannes Gutenberg University in Mainz.

Gel Permeation Chromatography: For the analytic gel permeation chromatography (GPC) a Waters system was used. A combination of three Styragel columns of the company PSS was used, with SDV gel particles of the size of 10 μm and had in each case a dimension of 0.8 x 30 cm. Porosity amounted to 10^3, 10^4 and 10^6 Å. The flow was 1 ml/min. The measurements were executed at ambient temperature, and THF was used as eluent. Detection was performed spectroscopically (UV) or by means of the refractive index. The molecular weight was obtained from polystyrene calibrated SEC columns.

Differential Scanning Calorimetry: The DSC investigations were performed on a Perkin Elmer DSC 7 calorimeter.

Melting Points: The melting points were determined with a melting point microscope with heating desk Thermovar of the company Renriches.

Light Microscopy: For the investigation of morphology of electrochemically obtained polythiophene the light microscope Axiophot of the company Zeiss was used.

Cyclic Voltammetry: The measurements were performed on a EG&G Princetown Applied Research Potentiostat/Galvanostat Model 173. The samples were both in solution or on solid substrates, and in each case CH_2Cl_2 was used as liquid phase and Bu_4NPF_6 or $KClO_4$ as inert electrolyte. The reference electrode was a solid AgCl-covered silver wire and the counter electrode a platinum folium. The scanning rate was 100 mV/s.

Electrical Conductivity: The AC-conductivity was measured on a Schlumberger Impedance/Gain-Phase Analyser SI 1260 with a pressed pellet of the sample.

Langmuir-Blodgett Trough: The LB monolayers were studied on a Lauda FW2 trough. Substances were spread from $CHCl_3$ solutions (5 mg in 10 ml).

Chemicals

If not differently indicated, commercially available chemicals from different supplying companies (Aldrich, Deutero, Fluka, Merck, Riedel-de Haën and Sigma) were used as received. All solvents were at least "p.a." quality. The water-free solvents were distilled according to the literature procedures and handled under argon. Argon of the quality 4.8 was used directly from the gas cylinder.

Tetrahydrofurane (THF) was distilled from sodium before use.

Diethyl ether (Et_2O) was distilled from sodium/potassium alloy before use.

Dimethylsulfoxide (DMSO) was dried over molecular sieves.

Triethylamine (Et_3N) were distilled over calcium hydride and stored under argon.

Iron (III) trichloride ($FeCl_3$) was dried under vacuum.

Acryloyl chloride was distilled before use.

2,2'-Azo-bis(isobutyrronitrile) (AIBN) was recrystallized from ethanol before use.

Dibenzoyl peroxide (DPB) was recrystallized from ethanol before use.

3-Octylthiophene was distilled and kept under argon before use (106 °C, 3 mm Hg)

3-Bromothiophene (46 °C, 10^{-2} mbar), 2-bromothiophene (45 °C, 20 mm Hg) and 2,5-dibromothiophene **1a** (90 °C, 10^{-2} mbar) were distilled and kept under argon before use.

Synthesis of monomers

2,5-Dibromo-3-pentylthiophene (**1b**) *and 2,5-dibromo-3-octylthiophene* (**1c**)

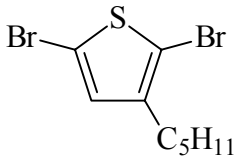

1b

Both compounds were prepared according to the following procedure. As example the synthesis of **1b** is described.

4.0 ml (24.49 mmol) of 3-pentylthiophene (**28**) were dissolved in 20 ml of $CHCl_3$. A solution of 2.5 ml of bromine in 20 ml of $CHCl_3$ was added dropwise within one hour under exclusion of light at room temperature. The reaction mixture was stirred for 3 hours. Then 30 ml 1N KOH was added and after 1 h the organic phase was separated and washed 3 times with water. After drying over $MgSO_4$ the solvent was evaporated and the crude product was purified by chromatography column using hexane as eluent. 6.93 g (22.2 mmol, yield 91 %) of pure **1b** were obtained as colorless liquid.

^{1}H-NMR ($CDCl_3$): 0.90 ppm (t, 3 H, -CH_3), 1.30 ppm (m, 4 H, -CH_2-), 1.55 ppm (m, 2 H), 2.50 ppm (t, 2 H, -CH_2-), 6.85 ppm (s, 1 H, thiophene-H)

2,2':5'2"-terthiophene (**2a**), *3'-pentyl-2,2':5'2"-terthiophene* (**2b**) *and 3'-octyl-2,2':5'2"-terthiophene* (**2c**)

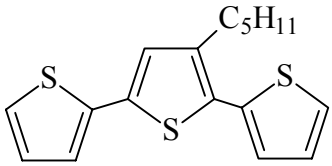

2b

The three compounds were prepared according to the following procedure. As an example the synthesis of **2b** is described.

A solution under argon of 2 ml (20.98 mmol) of 2-bromothiophene in 15 ml dry Et_2O was slowly added to 506 mg (20.82 mmol) of pure Mg under argon. The mixture was stirred until

complete dissolution of the Mg, then slowly portionwise added to a dry solution of 3.157 g (10.12 mmol) of **1b** and 151 mg (0.185 mmol) of Palladium (II) 1,1'-bis(diphenylphosphino)ferrocene chloride / CH_2Cl_2 (1:1 complex) in Et_2O (25 ml), at 0 °C under argon. After complete addition the mixture was stirred overnight, then refluxed for 1 hr and finally hydrolyzed with saturated aq. NH_4Cl solution. The two phases were separated and the organic phase was washed 3 times with water and dried over Mg_2SO_4. 2.82 g (8.86 mmol, yield 88 %) pure **2b** were isolated as yellow crystals after purification by column chromatography, using hexane as eluent.

^{1}H-NMR ($CDCl_3$): 0.90 ppm (t, 3 H, -CH_3), 1.30 ppm (m, 4 H, -CH_2-), 1.65 ppm (m, 2 H, -CH_2-), 2.70 ppm (t, 2 H, -CH_2-), 7.00 – 7.35 ppm (m, 6 H, terth.)

FD-Mass (M/z): exact mass = 318.1; found mass = 318.3, 636.6 ($2M^+$)

UV-Vis (THF): λ_{max} = 354 nm, ε_{max} = 23500

5-(2-Hydroxyethyl)-2,2':5',2"-terthiophene (**3**)

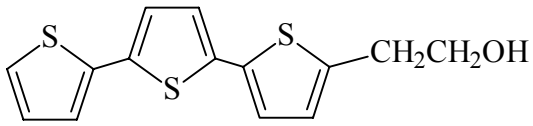

3

Terthiophene (57 mg, 0.230 mmol) was added under argon to a solution of *n*-butyllithium (BuLi) in hexane (0.07 ml x 1.6M, 0.112 mmol) and diisopropylamine (0.016 ml, 0.113 mmol) in 5 ml THF at -78 °C. After stirring for 2 h, a solution of ethylene oxide in THF (1 ml, 0.116 mmol) was slowly dropped in the reaction medium, and stirred for additional 16 h. The mixture was hydrolyzed with saturated aq. NH_4Cl solution. $CHCl_3$ was added and the two phases were separated. The organic phase was washed 3 times with water and then dried over anhydrous Na_2SO_4. The crude product was purified by column chromatography, using ethylacetate / hexane (3:1) as eluent. 50 mg (0.171 mmol, 74 % yield) of **3** were collected as yellow-green crystals.

^{1}H-NMR ($CDCl_3$): 1.65 ppm (s, 1 H), 3.15 ppm (m, 2H, -C<u>H</u>$_2$-CH_2O), 3.80 ppm (m, 2 H, -CH_2-C<u>H</u>$_2$O), 7.00-7.20 ppm (m, 7 H, terth.).

UV-Vis (THF): λ_{max} = 357 nm, ε_{max} = 24400

5-(2-chloroethyl)-2,2':5',2''-terthiophene (**4**)

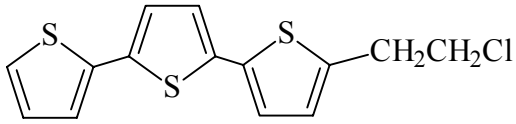

4

A solution of 50 mg of **3** (0.171 mmol) in 2 ml THF was added to an excess of $SOCl_2$ (3 ml, 41.57 mmol) and Et_3N (0.1 ml, 0.72 mmol) at 0° C. After stirring 20 h at r.t., the mixture was refluxed for 1 h and then the solvent and the excess of $SOCl_2$ were removed under vacuum. Water and $CHCl_3$ were added to the crude product, and the organic phase was washed 3 times with water and then dried over anhydrous Na_2SO_4. After filtration and evaporation of the solvent 45 mg (0.15 mmol, yield 88 %) of **4** were collected as yellow-green crystals.

^{1}H-NMR ($CDCl_3$): 3.35 ppm (m, 2 H, -C<u>H</u>$_2$-CH_2Cl), 3.45 ppm (m, 2 H, -CH_2-C<u>H</u>$_2$Cl), 6.80-7.50 ppm (m, 7 H, terth.).

UV-Vis (THF): λ_{max} = 401 nm, ε_{max} = 25500

β',β''''-dipentyl-2,2':5',2'':5'',2''':5''',2'''':5'''',2''''':sexithiophene (**5a**) *and β',β''''-dioctyl-2,2':5',2'':5'',2''':5''',2'''':5'''',2''''':sexithiophene* (**5b)**

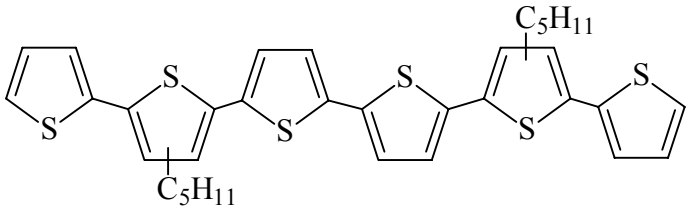

5a-b

Both compounds were prepared according to the following procedure. As an example the synthesis of **5a** is described.

6.448 g (20.28 mmol) of **2b** were dissolved in 75 ml dry THF under argon and the solution was cooled down to –70 °C. Then, 4.9 ml of a 1.6M solution of BuLi in hexane (7.84 mmol) were added and the mixture was stirred for 30 min. 2.108 g (15.73 mmol) of $CuCl_2$ were rapidly poured into the mixture at –50 °C, which was then kept stirring overnight up to r.t.. After hydrolysis with saturated aqueous NH_4Cl solution, the organic solvents were

evaporated, $CHCl_3$ was added and the organic phase was washed with saturated aqueous NH_4Cl and 2 times with water. The organic layer was dried over $MgSO_4$, the solvent evaporated and the crude product was repeatedly purified by silica gel column chromatography, using a hexane / ethylacetate 10:1 mixture as eluent.

1.350 g (2.13 mmol, yield 21 %) of **5a** (three isomers) were isolated as red powder.

^{1}H-NMR ($CDCl_3$): 0.90 ppm (t, 3H, -CH_3), 1.40 ppm (m, 4H, -CH_2-), 1.70 ppm (m, 2H, -CH_2-), 2.75 ppm (t, 2H, -CH_2-), 7.10 – 7.40 ppm (m, 6H, sexith.)

FD-Mass (M/z): exact mass = 634.1 ; found mass = 634.0

UV-Vis (THF) : λ_{max} = 422 nm, ε_{max} = 37000.

Melting Point (heating rate 6°/min): T_m = 94 – 97 °C

β',β''''-dipentyl-5,5''''-bis-(2-hydroxyethyl)-2,2':5',2'':5'',2''':5''',2'''':5'''',2''''-sexithiophene (**6a**):

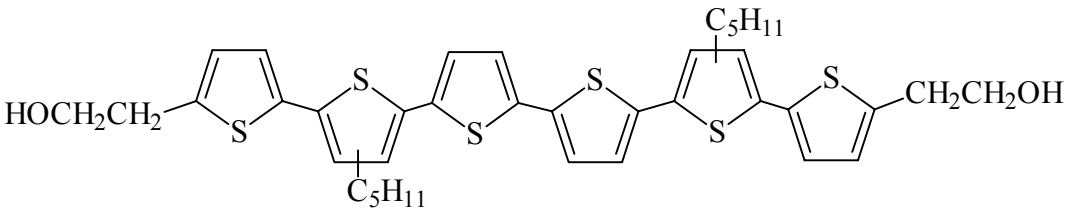

6a

1.350 g (2.13 mmol) of **5a** were dissolved in 20 ml of dry THF under argon. The solution was cooled down to –70 °C and then 2.9 ml of a 1.6M hexane solution of BuLi (4.64 mmol) were added. After stirring for 30 min, 0.25 ml (5.11 mmol) ethylene oxide (pre-cooled at –30 °C) were dropped into the solution, and stirred overnight. After hydrolysis with 3 % aq. HCl, the organic solvents were evaporated, $CHCl_3$ was added and the organic phase was washed 3 times with water and dried over $MgSO_4$. 535 mg (0.741 mmol, yield 35 %) of **6a** were isolated as orange powder after repeated purification by means of silica gel column chromatography (eluent: hexane / acetone 5:2).

^{1}H-NMR ($CDCl_3$): 0.90 ppm (t, 3 H, -CH_3), 1.35 ppm (m, 4 H, -CH_2-), 1.55 ppm (m, 2 H, -CH_2-), 2.70 ppm (m, 2 H, -CH_2-), 3.05 ppm (m, 2 H, -C$\underline{H_2}$-CH_2OH), 3.85 ppm (m, 2 H, -C$\underline{H_2}$-OH), 6.75 ppm (dd, 1 H, sexith.), 6.85 (dd, 1 H, sexith.), 6.95 - 7.10 ppm (m, 3 H, sexith.)

FD-Mass (M/z): exact mass = 722.2; found mass = 722.6

FT-IR (cm^{-1}): 3432 (b), 2924, 2856, 1634, 1456, 1260, 1046, 796.

UV-Vis (EtOH) : λ_{max} = 422 nm, ε_{max} = 48800.

Melting Point (heating rate 6°/min): T_m = 84 – 86 °C

β',β''''-dioctyl-5,5''''-bis-(2-hydroxyethyl)-2,2':5',2'':5'',2''':5''',2'''':5'''',2''''-sexithiophene (**6b**)

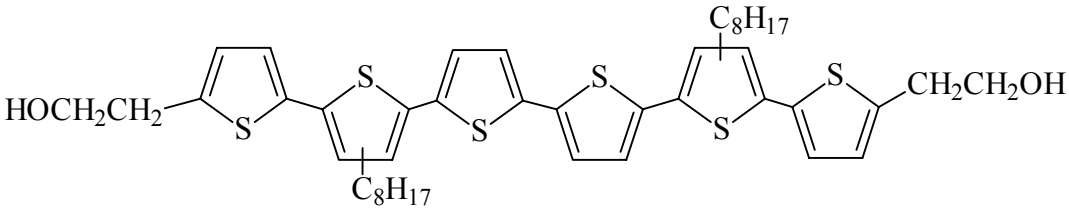

6b

The product was obtained according to the following procedure as for **6a**, excepted that the amount of ethylene oxide was calculated as weight difference and added as 0.25 ml of a solution of 840 mg ethylene oxide in 20 ml dry THF (0.24 mmol) to a solution of 55 mg (0.08 mmol) OctST in 3 ml THF under argon.

15 mg (0.018 mmol, yield 23 %) pure **6b** were obtained.

^{1}H-NMR ($CDCl_3$): 0.85 ppm (t, 3 H, -CH_3), 1.35 ppm (m, 10 H, -CH_2-), 1.60 ppm (m, 2 H, -CH_2-), 2.70 ppm (m, 2 H, -CH_2-), 3.10 ppm (m, 2 H, -C$\underline{H_2}$-CH_2OH), 3.80 ppm (m, 2 H, -C$\underline{H_2}$-OH), 6.75 ppm (dd, 1 H, sexith.), 6.85 (dd, 1 H, sexith.), 6.95 - 7.10 ppm (m, 3 H, sexith.)

FD-Mass (M/z): exact mass = 821.3; found mass = 822.0

2-[β',β''''-dipentyl-5''''-(2-hydroxyethyl)-2,2':5',2'':5'',2''':5''',2'''':5'''',2''''-sexithiophen-5-yl]-ethyl p-toluensulfonate (**7**)

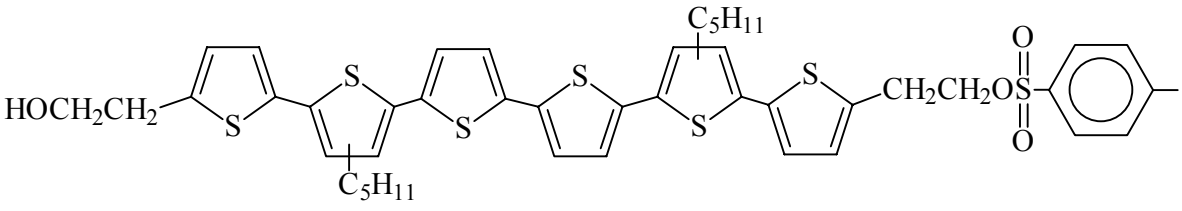

7

50 mg (0.069 mmol) of **6a** were dissolved in 3 ml THF and 2 ml H_2O. 1 ml of a solution of 100 mg NaOH in 20 ml H_2O (0.125 mmol) was added. The solution was cooled down to –5 °C and 13 mg (0.079 mmol) of p-toluensulfonyl chloride in 1 ml THF were added. The reaction mixture was stirred overnight, the organic solvent was evaporated, $CHCl_3$ was added and the organic phase was washed 3 times with water and dried over $MgSO_4$. The product was purified by column chromatography (eluent: hexane / ethylacetate 2:1). 15 mg (0,016 mmol, yield 23 %) of pure **7** were isolated as orange powder.

^{1}H-NMR ($CDCl_3$): 0.90 ppm (t, 6 H, -CH_3), 1.25 ppm (m, 8 H, -CH_2-), 1.60 ppm (m, 4 H, -CH_2-), 2.30 (s, 3 H, Ts-CH_3). 2.70 ppm (m, 4 H, -CH_2-), 3.00 ppm (m, 4 H, -C$\underline{H}_2$-CH_2O), 3.80 ppm (t, 2 H, -CH_2-C$\underline{H}_2$OH), 4.40 ppm (m, 2 H, -CH_2-OTs), 6.70 - 7.05 ppm (m, 10 H, sexith.), 7.20 ppm (d, 2 H), 7.65 ppm (dd, 2 H).

FD-Mass (M/z): exact mass = 876.1; found mass = 875.6.

2-[β',β''-dipentyl-5'''-(2-hydroxyethyl)-2,2':5',2'':5'',2''':5''',2'''':5'''',2'''''-sexithiophen-5-yl]-ethylacrylate (**8**)

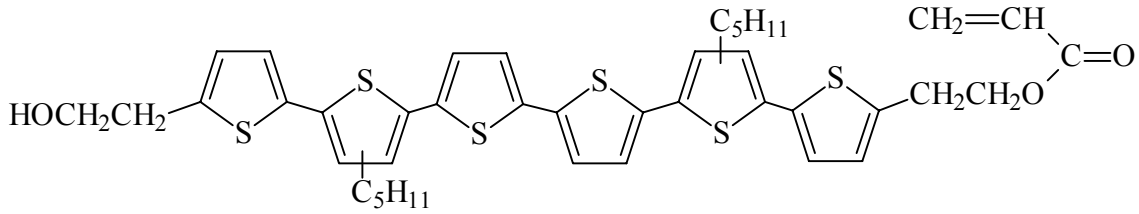

8

535 mg (0.741 mmol) **6a** and 0.15 ml (1.08 mmol) Et_3N were dissolved in 15 ml dry THF under argon. 1 ml of a solution of 0.75 ml of acryloyl chloride in 10 ml dry THF (0.431 mmol) were added dropwise into the solution at 0 °C. After stirring overnight, the crude mixture was hydrolyzed with 1 % aq. HCl for 30 min, the organic solvent was evaporated, $CHCl_3$ was added and the organic phase was washed with water 3 times. The organic phase was dried over $MgSO_4$ and the solvent evaporated. The product was purified by column chromatography (eluent: hexane / acetone 5:2).

200 mg (0.258 mmol, yield 35 %) of pure **8** were isolated as red powder.

70 mg (0.08 mmol, yield 11 %) of pure **8b** were isolated as red powder.

^{1}H-NMR ($CDCl_3$): 0.90 ppm (t, 6 H, -CH_3), 1.40 ppm (m, 8 H, -CH_2-), 1.60 ppm (m, 4 H, -CH_2-), 2.70 ppm (m, 4 H, -CH_2-), 3.05 ppm (m, 2 H, -C$\underline{H}_2$-CH_2OH), 3.15 ppm (m, 2 H, -C$\underline{H}_2$-

OH), 3.85 ppm (m, 2 H, -C<u>H</u>$_2$-CH$_2$OC-), 4.40 ppm (m, 1 H, -CH$_2$-OC(=O)-), 5.80 ppm (d, 1 H, H_{trans}), 6.10 ppm (dd, 1 H, CH$_2$=C<u>H</u>-), 6.40 ppm (d, 1 H, H_{cis}), 6.70 ppm (dd, 2 H, sexith.), 6.85 (dd, 2 H, sexith.), 6.95 - 7.10 ppm (m, 6 H, sexith.)

^{13}C-NMR (CDCl$_3$): 14.02, 22.51, 29.35, 29.49, 29.70, 30.16, 30.24, 31.75, 33.63, 63.35, 64.51, 123.50, 123.94, 124.19, 126.02, 126.37, 128.36, 130.99, 130.57, 134.00, 134.22, 134.59, 134.81, 135.05, 135.25, 135.86, 136.11, 136.37, 136.60, 139.70, 139.87, 140.49, 142.08, 165.01

FD-Mass (M/z): exact mass = 776.2; found mass = 776.8, 338.5 (M^{2+})

Saponification of 2,2'-[β',β''''-dipentyl-2,2':5',2'':5'',2''':5''',2'''':5'''',2''''']-sexithiophen-5-yl]-bis(ethylacrylate) (**8b**)

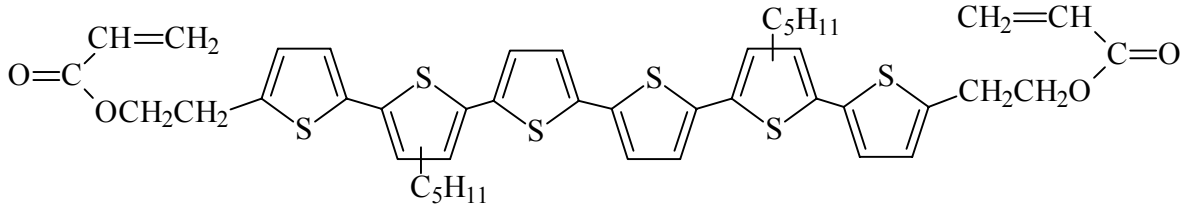

8b

70 mg (0.08 mmol) of **8b** were hydrolyzed *via* reaction with 17 mg of NaOH (0.42 mmol) in 5 ml THF/H$_2$O (4:1) for 16 h at r.t.. THF was then evaporated, CHCl$_3$ was added and the organic phase was separated and washed with diluted aq. NaOH, diluted aq. HCl and water. The phase was dried over anhydrous MgSO$_4$, the solvent evaporated and 50 mg (0.07 mmol, yield 86 %) of the product **6a** was recycled for another acrylating reaction after purification by column chromatography (hexane / acetone 5:2).

FD-Mass (M/z): exact mass = 830.2; found mass = 831.0 (M^+), 415.5 (M^{2+})

2,5-diiodobenzoic acid (**10**)

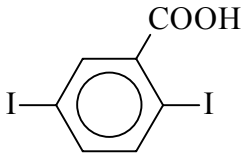

10

10.06 g (38 mmol) of 2-amino-5-iodobenzoic acid (**9**) and 5.92 g (43 mmol) K_2CO_3 were stirred in 50 ml H_2O. After dissolution of the acid, 18 ml (162 mmol) of H_2SO_4 (9M) were added and the solution was cooled down to 0 °C. Then 2.55 g (37 mmol) $NaNO_2$ in 10 ml H_2O were added dropwise within one h and the resulting solution was stirred at 0 °C for 2 h. Then a solution of 18.20 g KI (110 mmol) in 10 ml H_2O was cooled to 0 °C and added portionwise to the diazonium salt mixture. After 1 h stirring at 0 °C, it was heated for 30 min at 60 °C. After cooling to r.t. $CHCl_3$ was added, the organic phase washed 3 times with water and dried over $MgSO_4$.

The crude product was dissolved in aq. KOH (1M) and precipitated in 37 % aq. HCl for 2 times. 9.01 g (24.1 mmol, yield 63 %) pure **10** were obtained as white crystals.

^{1}H-NMR ($CDCl_3$): 7.50 ppm (d, 1H), 7.70 ppm (d, 1H), 8.15 ppm (d, 1H)

2,5-diiodobenzoyl chloride (**11**)

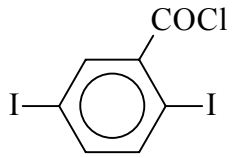

11

5 ml (69.28 mmoli) $SOCl_2$ were added to 1.1 g (2.94 mmol) of **10** at 0 °C. After addition, the mixture was refluxed for 2 h, then excess $SOCl_2$ was removed by evaporation at reduced pressure. The crude product was recrystallized 2 times from CCl_4. 205 mg (0.52 mmol, yield 18 %) pure **11** were isolated as white powder.

^{1}H-NMR ($CDCl_3$): 7.50 ppm (d, 1H), 7.70 ppm (d, 1H), 8.15 ppm (d, 1H)

β',β''''-dipentyl-5(2-hydroxyethyl)-5''''-[2(tert-butyldimethylsiloxy)ethyl]-2,2':5',2'':5'',2''':5''',2'''':5'''',2'''''-sexithiophene (**12**)

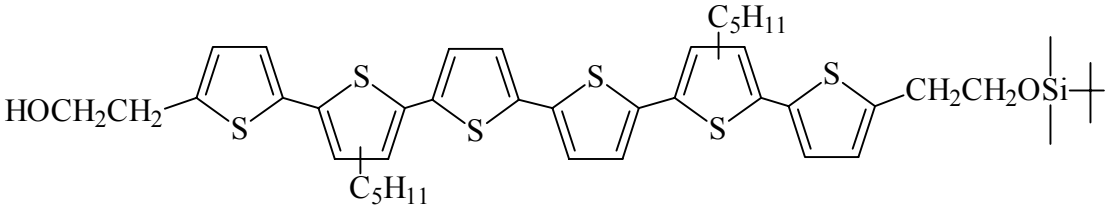

12

604 mg (0.84 mmol) **6a** and 155 mg (2.28 mmol) imidazole were dissolved in 5 ml DMF (waterfree grade). 119 mg (0.79 mmol) solid tert-butyldimethylchlorosilane was added portionwise under argon at room temperature. After stirring overnight, the crude mixture was precipitated in water, filtrated and then dissolved in $CHCl_3$. The organic phase was washed 3 times with water and dried over $MgSO_4$. The crude product was purified by column chromatography using a hexane / acetone (3:1) as eluent. 300 mg (0.36 mmol, yield 43 %) pure **12** were isolated as orange-red powder.

^{1}H-NMR ($CDCl_3$): 0.00 ppm (s, 9 H, t-butyl), 0.90 ppm (t, 6 H, -CH_3), 1.30 - 1.40 ppm (m, 14 H, -CH_2-, Si-CH_3), 1.60 ppm (m, 4 H, -CH_2-), 2.75 ppm (m, 4 H, -CH_2-), 3.05 ppm (m, 4 H, -C$\underline{H_2}$-CH_2O-), 3.90 ppm (m, 4 H, -C$\underline{H_2}$-O-), 6.75 ppm (d, 2 H, sexith.), 6.80 ppm (d, 2 H, sexith.), 6.85 ppm (d, 2 H, sexith.), 7.00 - 7.15 ppm (m, 6 H, sexith.)

FD-Mass (M/z): exact mass = 836.3 ; found mass = 836.5

Deprotection of β',β''''-dipentyl-5,5''''-bis[2(tert-butyldimethylsiloxy)ethyl]-2,2':5',2'':5'', 2'''':5'''',2''''':5''''',2''''''-sexithiophene (**13**)

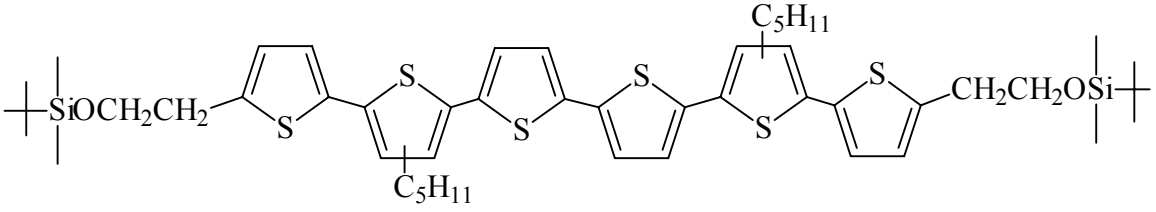

13

200 mg (0.21 mmol) of the product obtained by the bis-addiction of tert-butyldimethylchlorosilane on both–OH groups of **6a** (above reaction) were dissolved in 10 ml THF and 1.5 ml (1.5 mmol) of a 1M THF solution of tetra(*n*-butyl)ammonium fluoride were added. After stirring overnight, water was added, the organic solvent was evaporated and

$CHCl_3$ was added. The organic phase was washed 3 times with water and dried over $MgSO_4$. The crude product was purified by column chromatography using hexane as eluent. 141 mg (0.19 mmol, 93 %) of pure **6a** were obtained as red powder.

^{1}H-NMR ($CDCl_3$): 0.00 ppm (s, 9H), 0.90 ppm (t, 3H, -CH_3), 1.30 ppm (m, 4H, -CH_2-), 1.40 ppm (s, 6H, Si-CH_3), 1.60 ppm (m, 2H, -CH_2-), 2.75 ppm (m, 2H, -CH_2-), 3.05 ppm (m, 2H, -C$\underline{H}_2$-CH_2OSi), 3.85 ppm (m, 2H, -C$\underline{H}_2$-OSi), 6.75 ppm (d, 1H, sexith.), 6.85 (d, 1H, sexith.), 6.95 - 7.15 ppm (m, 3H, sexith.)

FD-Mass (M/z): exact mass = 950.3 ; found mass = 950.7, 475.3 (M^{2+})

2-{β',β''-dipentyl-5'''-[2-(tert-butyldimethylsiloxy)-ethyl]-2,2':5',2'':5'',2''':5''',2'''':5'''',2'''''-sexithiophen-5-yl}-ethyl 2,5-diodobenzoate (**14**)

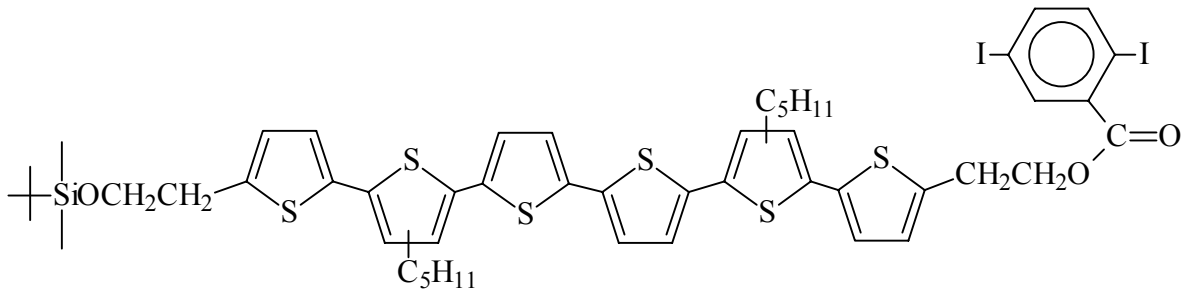

14

The reaction was performed following two different synthetic strategies with different acylating agents, one using **11** and the other using **10** and diisopropylcarbodiimide (DiPCI) as activator.

1) Reaction between of **11** *with* **12**

110 mg (0.132 mmol) of **12** in 3 ml dry THF were added to a solution of 144 mg (0.367 mmol) of **11** and 0.1 ml (0.719 mmol) Et_3N in 4 ml dry THF at 0 °C under argon. The reaction mixture was stirred overnight, water was added and the organic solvent was

evaporated. After addiction of $CHCl_3$, the organic phase was separated and washed 3 times with water, and dried over $MgSO_4$. Column chromatography using hexane / acetone (5:1) as eluent gave 63 mg (0.053 mmol, yield 40 %) of pure **14** and 30 mg (0.028 mmol, yield 21 %) of pure *2-(β',β''''-dipentyl-5''''--(2-hydroxyethyl)-2,2':5',2'':5'',2''': 5''',2'''':5'''',2''''-sexithiophen-5-yl)ethyl 2,5- diiodobenzoate* (**15)**, both as red powders.

2) Reaction of **10** *with* **12** *in the presence of DiPCI as activator*

90 mg (0.714 mmol) of DiPCI were added to a solution of 207 mg **12** (0.248 mmol), 124 mg (0.331 mmol) **10** and 171 mg (0.585 mmol) of 4-(dimethylamino)pyridinium p-toluensulfonate (DPTS) in 15 ml CH_2Cl_2 (waterfree grade), at r.t. under argon. The solution was stirred overnight, the solvent was evaporated and the crude product was repeatedly purified by column chromatography using hexane / acetone (5:1) as eluent. 210 mg (0.176 mmol, yield 71 %) of pure **14** were isolated as red powder.

^{1}H-NMR ($CDCl_3$): 0.00 ppm (s, 9 H, t-butyl), 0.90 ppm (m, 6 H, $-CH_3$), 1.30 - 1.40 ppm (m, 14 H, $-CH_2-$, Si-CH_3), 1.60 ppm (m, 4 H), 2.75 ppm (m, 4 H, $-CH_2-$), 3.10 ppm (m, 2 H, -C<u>H</u>$_2$-CH_2OH), 3.30 ppm (m, 2 H, -C<u>H</u>$_2$-OH), 3.85 ppm (m, 2 H, -C<u>H</u>$_2$-CH_2OC-), 4.50 ppm (m, 1 H, $-CH_2$-OC(=O)-), 6.70 - 7.15 ppm (m, 10 H, sexith.), 7.45 ppm (d, 1 H), 7.70 ppm (d, 1 H), 8.10 ppm (d, 1 H)

FD-Mass (M/z): exact mass = 1192.1 ; found mass = 1192.7

2-[β',β''''-dipentyl-5''''-(2-hydroxyethyl)-2,2':5',2'':5'',2''':5''',2'''':5'''',2''''-sexithiophen-5-yl]-ethyl 2,5- diiodobenzoate (**15**).

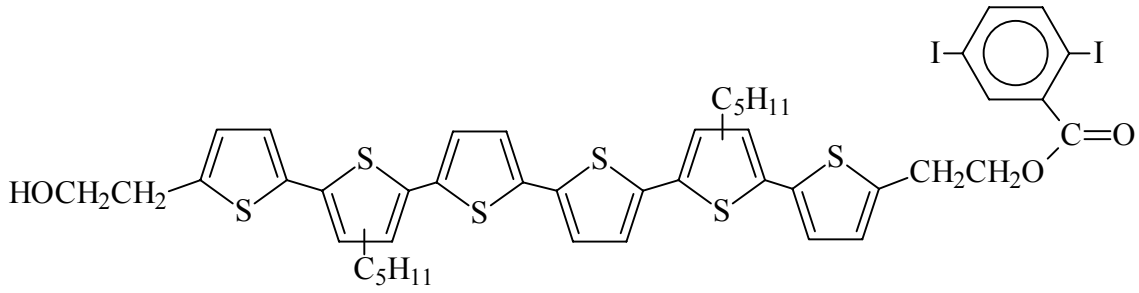

15

The product **15** was obtained both as by-product from the reaction between **11** and **12**, and by the below described deprotection of **14**.

85 mg (0.071 mmol) of **14** were dissolved in 3 ml THF and 1 ml of a 1M THF solution of tetra(*n*-butyl)ammonium fluoride (1.00 mmol) was added. The solution was stirred overnight, water was added and after 1 h the organic solvent was evaporated. $CHCl_3$ was added, the organic phase was separated and washed 3 times with water. After drying over $MgSO_4$, the crude product was purified by column chromatography using hexane / acetone (2:1) as eluent. 57 mg (0.053 mmol, yield 75 %) of pure **15** were obtained as red powder.

^{1}H-NMR ($CDCl_3$): 0.90 ppm (m, 6 H, -CH_3), 1.35 ppm (m, 8 H, -CH_2-), 1.60 ppm (m, 4 H -CH_2-), 2.70 ppm (m, 4 H, -CH_2-), 3.05 ppm (m, 2 H, -C$\underline{H_2}$-CH_2OH), 3.25 ppm (m, 2 H, -C$\underline{H_2}$-OH), 3.85 ppm (m, 2 H, -C$\underline{H_2}$-CH_2OC-), 4.50 ppm (m, 1 H, -CH_2-OC(=O)-), 6.80 - 7.15 ppm (m, 10 H, sexith.), 7.45 ppm (dd, 1 H), 7.70 ppm (d, 1 H), 8.10 ppm (d, 1 H)

^{13}C-NMR ($CDCl_3$): 14.02, 22.51, 25.93, 29.35, 29.49, 29.70, 30.16, 30.21, 31.79, 33.84, 65.90, 65.81, 93.03, 93.38, 123.30, 129.15, 130.55, 134.01, 134.23, 134.57, 134.81, 135.10, 135.35, 135.84, 136.13, 136.36, 136.59, 138.90, 139.67, 139.87, 140.25, 140.50, 141.15, 142.10, 165.00

FD-Mass (M/z): exact mass = 1079.0, found mass = 1078.9

2-{β',β''-dipentyl-5'''-[2-(tert-butyldimethylsiloxy)-ethyl]-2,2':5',2'':5'',2''':5''',2'''':5'''',2'''''-sexithiophen-5-yl}-ethyl 2,5-bis(trimethylsilylethynyl) benzoate (**17**)

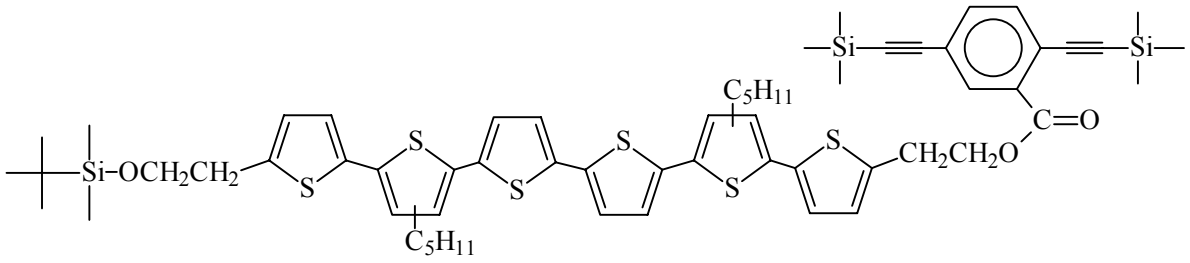

17

210 mg (0.176 mmol) of **14** and 7 mg (0.010 mmol) of Palladium (II) bis(triphenylphosphine) chloride were dissolved in 10 ml THF under argon atmosphere. 5 mg (0.026 mmol) CuI and 0.5 ml (3.797 mmol) Et_3N and then 0.5 ml (3.54 mmol) trimethylsilylacetylene were added to the solution. The temperature was raised up to 40 °C and the solution was stirred overnight. Then the solvent was evaporated and the crude product

was dissolved in $CHCl_3$ and washed 3 times with water. After drying over $MgSO_4$, the crude product was purified by repeated column chromatography using hexane / acetone (4:1) as eluent. 84 mg (0.074 mmol, yield 42 %) of pure **17** were isolated as red powder.

^{1}H-NMR ($CDCl_3$): 0.00 ppm (s, 9 H, t-butyl), 0.85 ppm (m, 6 H, -CH_3), 1.25 - 1.40 ppm (m, 18 H, -CH_2-, Si-CH_3), 1.60 ppm (m, 4 H), 2.70 ppm (m, 4 H, -CH_2-), 3.00 ppm (m, 2 H, -C$\underline{H}_2$-CH_2OH), 3.20 ppm (m, 2 H, -C$\underline{H}_2$-OH), 3.80 ppm (m, 2 H, -C$\underline{H}_2$-CH_2OC-), 4.50 ppm (m, 1 H, -CH_2-OC(=O)-), 6.70 - 7.10 ppm (m, 10 H, sexith.), 7.45 ppm (dd, 2 H), 7.90 ppm (d, 1 H)

^{13}C-NMR ($CDCl_3$): 14.02, 18.31, 22.51, 25.93, 29.35, 29.48, 29.68, 30.13, 30.20, 31.74, 33.84, 65.93, 65.86, 93.03, 93.37, 123.30, 129.19, 130.57, 134.00, 134.22, 134.59, 134.81, 135.04, 135.27, 135.84, 136.13, 136.36, 136.59, 138.88, 139.70, 139.87, 140.22, 140.48, 141.14, 142.10, 164.80

FD-Mass (M/z): exact mass = 1132.3 ; found mass = 1132.2

2-[β',β''-dipentyl-5'''-(2-hydroxyethyl)-2,2':5',2'':5'',2''':5''',2'''':5'''',2'''''-sexithiophen-5-yl]-ethyl 2,5-diethynylbenzoate (**18)**

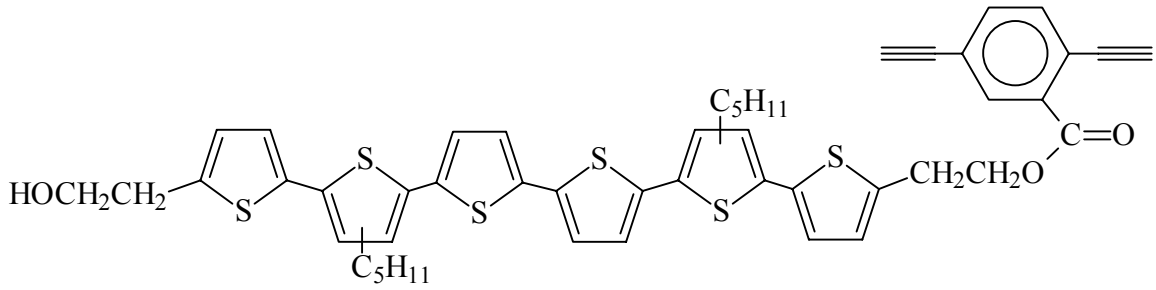

18

84 mg (0.074 mmol) of **17** were dissolved in 3 ml THF and 1 ml of a 1M THF solution of tetra(*n*-butyl)ammonium fluoride (1.00 mmol) was added. The solution was stirred overnight, water was added and after 1 h the organic solvent was evaporated, $CHCl_3$ was added, the organic phase was separated and washed 3 times with water. After drying over $MgSO_4$, the crude product was purified by column chromatography using hexane / acetone (2:1) as eluent. 45 mg (0.051 mmol, yield 70 %) of pure **18** were obtained as red powder.

^{1}H-NMR ($CDCl_3$): 0.90 ppm (m, 6 H, -CH_3), 1.35 ppm (m, 8 H, -CH_2-), 1.60 ppm (m, 4 H, -CH_2-), 2.75 ppm (m, 4 H, -CH_2-), 3.10 ppm (m, 2 H, -C<u>H</u>$_2$-CH_2OH), 3.25 ppm (s, 1 H, ≡CH), 3.35 ppm (m, 2 H, -C<u>H</u>$_2$-CH_2OC), 3.50 ppm (s, 1 H, ≡CH), 3.90 ppm (m, 2 H, -CH_2-C<u>H</u>$_2$OH), 4.50 (m, 2 H, -CH_2-C<u>H</u>$_2$-OC), 6.80 - 7.10 ppm (m, 10 H, sexith.), 7.60 ppm (dd, 2 H), 8.10 ppm (d, 1 H)

^{13}C-NMR ($CDCl_3$): 14.02, 22.50, 26,04, 29.35, 29.50, 29.68, 30.16, 31.22, 31.79, 33.84, 65.90, 69.98, 78.00, 84.30, 122,02, 123.21, 123.30, 129.15, 130.55, 134.02, 134.19, 134.57, 135.00, 135.10, 135.24, 136.13, 136.33, 136.59, 166.00,

FD-Mass (M/z): exact mass = 874.2; found mass = 874.5

FT-IR (cm^{-1}): 3400 (b), 3064, 2924, 2856, 2104, 1722, 1456, 1292, 1246, 1186, 1074, 1030, 840, 792, 648.

UV-Vis (EtOH): λ_{max} = 425 nm; ε_{max} = 42250

Melting Point (heating rate 6°/min): T_m = 55 – 57 °C

β',β''''-dioctyl-5-bromo-2,2':5',2'':5'',2''':5''',2'''':5'''',2''''':sexithiophene (**19**)

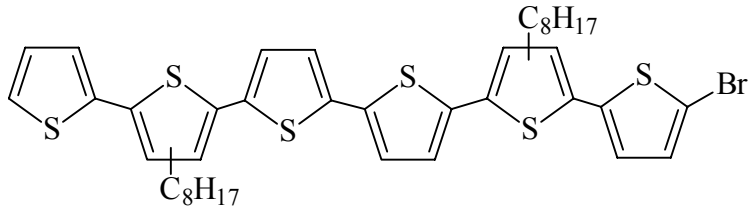

19

425 mg (0.592 mmol) of **5b** were dissolved in 15 ml DMF under argon. A solution of 100 mg (0.562 mmol) of N-bromosuccinimide in 5 ml DMF was slowly added dropwise at r.t.. After stirring for 3 h, the reaction mixture was poured in ice, $CHCl_3$ was added and the organic phase was washed 3 times with water and dried over $MgSO_4$. The crude product was purified by column chromatography, using different eluent mixtures (hexane / ethylacetate 10:1 seemed to be the best), but it was not possible to isolate the monobromo-adduct (**19**) neither from the dibromo-adduct (**19b**) nor from unreacted **5b**.

FD-Mass (M/z): exact mass (**5b**) = 718.2; exact mass (**19**) = 796.1; exact mass (**19b**) = 874.0; found mass = 718.2, 796.1, 874.0

β',β''''-dioctyl-5-methyl-2,2':5',2'':5'',2''':5''',2'''':5'''',2''''':sexithiophene (**22**)

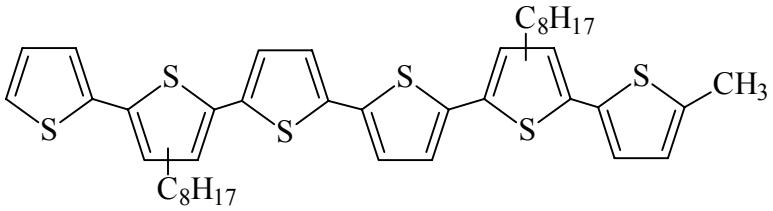

22

A solution of 220 mg (0.306 mmol) of **5b** in 5 ml dry THF was cooled down to –60 °C under argon and 0.19 ml of a 1.6M hexane solution of BuLi (0.304 mmol) were added. After 30 min, 0.4 ml (0.422 mmol) of dimethyl sulfate were dropped into the solution at -50 °C and the solution was stirred overnight. Water and a few drops of pyridine were slowly added, the organic solvents were evaporated, $CHCl_3$ was added and the organic phase was washed with diluted aq. HCl and 3 times water, and dried over $MgSO_4$. The crude product was purified by column chromatography, using different eluent mixtures (hexane / ethylacetate 10:1 seemed to be the best), but it was only possible to obtain the product in a mixture of **5b** and **22** (170 mg).

FD-Mass (M/z): exact mass (**5b**) = 718.2; exact mass (**22**) = 732.2; found mass = 718.6, 732.6

β',β''''-dioctyl-5-(2-hydroxyethyl)-5''''''-methyl-2,2':5',2'':5'',2''':5''',2'''':5'''',2''''':sexithiophene (**23**)

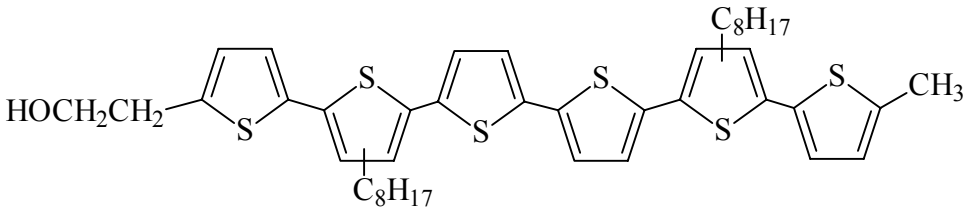

23

A mixture of **5b** and **22** (170 mg) was dissolved in 3 ml dry THF under argon, then the solution was cooled down to –60 °C and 0.16 ml of a 1.6M hexane solution of BuLi (0.256 mmol) were added. After 30 min, 0.95 ml (1.12 mmol) of a THF solution of ethylene oxide

(1.72 g in 33 ml) was added at –45 °C, and stirred overnight. After hydrolysis with 3 % aq. HCl, the organic solvents were evaporated, $CHCl_3$ was added and the organic phase was washed 3 times with water and dried over $MgSO_4$. The crude product was purified by column chromatography, using different eluent mixtures (hexane / acetone 3:1 seemed to be the best), but it was only possible to obtain a mixture of **23** and the α-hydroxyethylsexithiophene **24**.

FD-Mass (M/z): exact mass (**23**) = 762.2; exact mass (**24**) = 776.2; found mass = 762.7, 776.7

3-pentylthiophene (**28**)

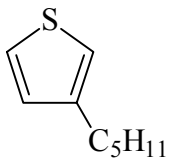

28

A solution of 50.20 g (0.20 mol) of *n*-pentylbromide in 300 ml dry Et_2O was slowly dropped to 4.80 g (0.196 mol) of pure Mg. After the addition the mixture was stirred under gentle reflux until complete dissolution of the Mg, and then added portionwise to a solution of 18 ml (0.192 mol) of 3-bromothiophene and 635 mg (1.17 mmol) of Nickel (II) 1,3-bis(diphenylphoshino)propane chloride in 200 ml dry Et_2O at 0 °C. The crude mixture was stirred overnight, then cautiously hydrolyzed with 20 ml 1 % aq. HCl and washed 3 times with water. After drying the organic layer over anhydrous Na_2SO_4 and evaporation of the solvent, 28.03 g (0.182 mol, 91 % yield) pure **28** were collected after distillation (44 °C, 0.5 mbar) as colorless liquid.

^{1}H-NMR ($CDCl_3$): 0.90 ppm (t, 3 H, -CH_3), 1.30 ppm (m, 4 H, -CH_2-), 1.65 ppm (m, 2 H, -CH_2-), 2.60 ppm (t, 2 H, -CH_2-), 7.00 ppm (d, 1 H), 7.20 – 7.40 ppm (dd, 2 H)

2-{β',β''-dipentyl-5'''-[2(tertbutyldimethylsiloxy)ethyl]-2,2':5',2'':5'',2''':5''',2'''':5'''',2'''''-sexithiophen-5-yl}-ethylacrylate (**29**)

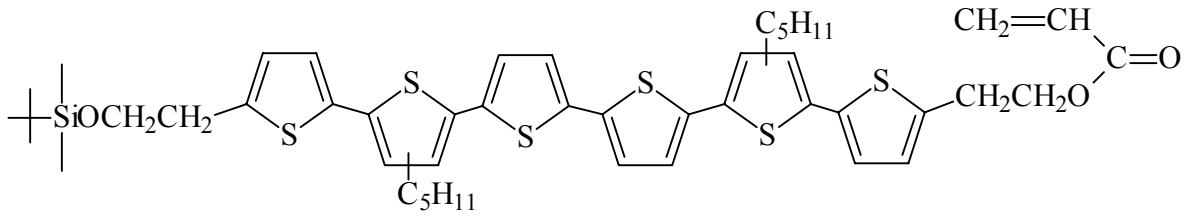

29

To a solution of 155 mg (0.200 mmol) **8** and 42 mg (0.620 mmol) imidazole in 2.5 ml DMF (waterfree grade), 94 mg (0.62 mmol) solid tert-butyldimethylchlorosilane was added portionwise under argon at room temperature. After stirring overnight, the crude mixture was precipitated in water, filtrated and then dissolved in $CHCl_3$. After washing 3 times with water, the organic phase was dried over $MgSO_4$. The crude product was purified by means of a small chromatography column using methanol as eluent. 165 mg (0.185 mmol, yield 93 %) pure **29** could be isolated as red powder.

^{1}H-NMR ($CDCl_3$): 0.00 ppm (s, 9H, t-butyl), 0.90 ppm (t, 6H, $-CH_3$), 1.35 ppm (m, 8H, $-CH_2-$), 1.40 ppm (s, 6H, CH_3-Si-), 1.60 ppm (m, 4H, $-CH_2-$), 2.70 ppm (m, 4H, $-CH_2-$), 3.00 ppm (m, 2H, -C<u>H</u>$_2$-CH_2OSi), 3.15 ppm (m, 2H, -C<u>H</u>$_2$-OSi), 3.80 ppm (m, 2H, -C<u>H</u>$_2$-CH_2OC-), 4.40 ppm (m, 1H, $-CH_2$-OC(=O)-), 5.80 ppm (d, 1H, H_{trans}), 6.10 ppm (dd, 1H, CH_2=C<u>H</u>-), 6.40 ppm (d, 1H, H_{cis}), 6.70 - 7.10 ppm (m, 10H, sexith.)

FD-Mass (M/z): exact mass = 890.3; found mass = 890.4, 445.6 ($2M^{+/2}$)

Synthesis of polymers

Butylcellulose (**25**)

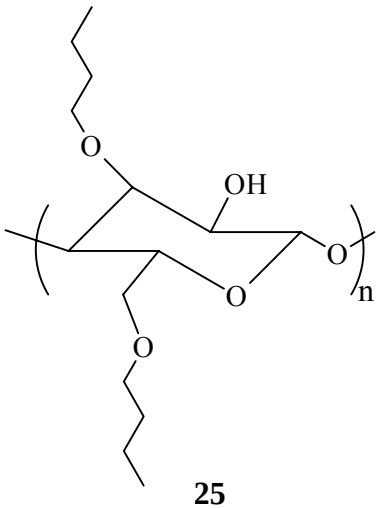

25

Several butylcellulose polymers were synthesized with different degree of substitution (DS) of the free –OH groups. Here the synthesis of one of these polymers is reported as an example.

2.00 g of acetylcellulose with a 40 % degree of substitution (17 mmol free –OH) was dissolved in 100 ml dry DMSO under argon atmosphere. At complete dissolution, 13.67 g (342 mmol) of powdered NaOH and 36.5 ml (340 mmol) of *n*-butylbromide were added and the mixture was stirred at r.t. overnight. The mixture was poured in an excess of water, and the floating polymer was collected and redissolved in CH_2Cl_2. The phase was washed 2 times with water. The organic phase was separated and a small amount of water was added, in order to remove parts of the by-products by azeotropic distillation during the solvent evaporation. The polymer was then dissolved in THF and precipitated two times in an excess of methanol.

2.60 g (yield 86 %) of butylcellulose with DS_{OH} = 2.81 (elemental analysis) were collected as white powder.

^{1}H-NMR ($C_2D_2Cl_4$, 100 °C): 0.85 ppm (-CH_3), 1.30 – 1.40 ppm (-CH_2-), 2.05 ppm (-OH), 2.85 – 4.00 ppm (C$\underline{H}_2$-CH_2O-, H_{cell}), 4.35 ppm (-CH_2-O)

Elemental Analysis: found: C: 64.6 %, H: 10.3 %

(2,2':5',2''-terthiophen-5-yl)-ethyl-butylcellulose (**26**)

25a with DS_{OH} = 1.9 (44 mg, 0.18 mmol -*OH*) and THF-purified NaH (7 mg, 0.29 mmol) were suspended in 6 ml THF and stirred for 2 h under an argon atmosphere. A solution of **4** (45 mg, 0.15 mmol) in 2 ml THF was then added dropwise and the suspension was stirred at r.t. for 6 d. The mixture was then poured into ice, filtered and dissolved with $CHCl_3$. After 3 precipitation steps in MeOH, 25 mg (yield 42 %) of the polymer **26** with $DS_{terthienyl}$ = 0.35 (elemental analysis) were collected as orange powder.

^{1}H-NMR ($CDCl_3$): 0.80-0.95 ppm (-CH_3), 1.15-1.65 ppm (-CH_2-), 2.80-4.00 ppm (-C$\underline{H}_2$-CH_2O-, H_{cell}), 4.20 ppm (-C$\underline{H}_2$-O), 6.80-7.45 ppm (terth.).

Elemental Analysis: found = C: 60.9 %, H: 7.9 %, S: 8.8 %

UV-Vis (film): λ_{max} = 360 nm.

2-[β',β''-dipentyl-5'''-(2-hydroxyethyl)-2,2':5',2'':5'',2''':5''',2'''':5'''',2'''''-sexithiophen-5-yl]-ethyl butylcellulose (**27**)

164 mg (0.210 mmol free –OH) of **25b** with DS_{OH} = 2.605 were dissolved in 10 ml of dry THF under an argon atmosphere and the solution was cooled down to –35 °C. 0.085 ml (0.136 mmol) of a 1.6M solution of BuLi in hexane were added. The solution formed slowly a gel. After 1 h, the temperature was raised to 20 °C and 1 ml of the solution was added, under an argon atmosphere, to a solution of 11 mg (0.012 mmol) of **7** in 3 ml THF at room temperature. After stirring for 3 d, the solution was precipitated in an excess of methanol. The precipitated polymer was collected by centrifugation and the purification was repeated until the methanol phase stayed colorless. 7 mg (yield 37 %) of **27** were collected as light orange powder. $DS_{sexithiophene}$ = 0.062 (elemental analysis).

^{1}H-NMR ($C_2D_2Cl_4$, 100 °C): 0.85 ppm (-CH_3), 1.30 – 1.40 ppm (-CH_2-), 2.05 ppm (-OH), 2.85 – 4.00 ppm (C$\underline{H}_2$-CH_2O-, H_{cell}), 4.35 ppm (-CH_2-O)

Elemental Analysis: found = C: 64.1 %, H: 9.6 %, S: 3.43 %

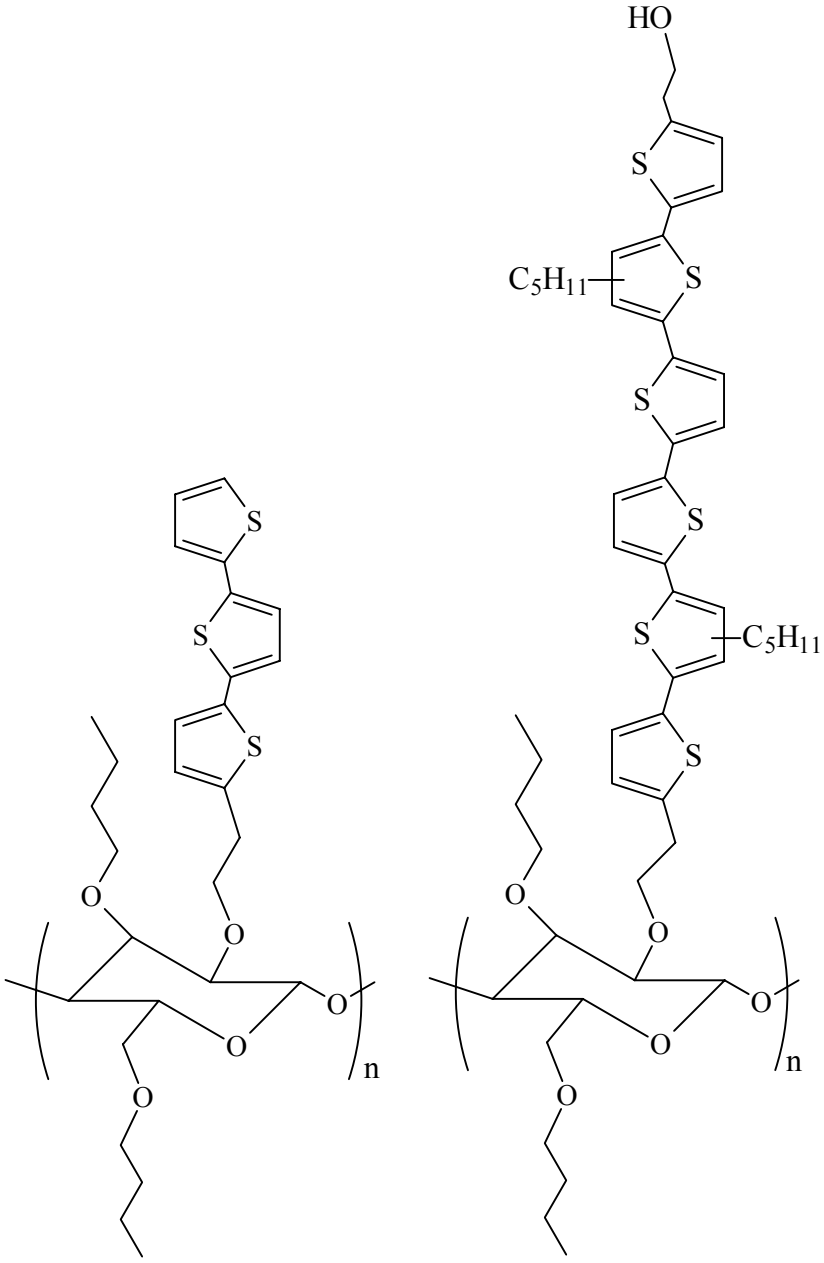

26 **27**

Poly{2-[β',β''''-dipentyl-5''''''--(2-hydroxyethyl)-2,2':5',2'':5'',2''':5''',2'''':5'''',2''''':5''''',2''''''-sexithiophen-5-yl]-ethyl 2,5-bis(ethyn-2-yl)benzoate} (**31**)

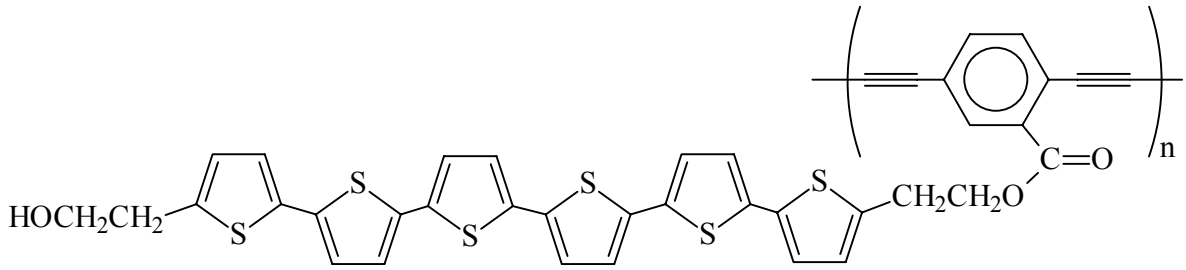

31

47.9 mg (0.044 mmol) of **15** and 38.9 mg (0.044 mmol) of **18** were dissolved under an argon atmosphere in 3 ml dry THF. 1 ml of a suspension of 13.1 mg CuI in 50 ml dry THF (0.0014 mmol), 1 ml of a solution of 15.3 mg of tetrakis(triphenylphosphine) palladium (0.0013 mmol) in 28 ml THF and 0.9 ml of Et_3N (6.47 mmol) were added. The solution was stirred at 60 °C for 6 d, concentrated and the polymer was precipitated in an excess of Et_2O. After the precipitation, most of the polymer was insoluble in organic solvents, so it was repeatedly washed with Et_2O until the ether phase was colorless. 50 mg (yield 65 %) of insoluble polymer **31** were obtained as dark orange powder.

FT-IR (cm^{-1}): 3420 (b), 3066, 2954, 2924, 2858, 1722, 1432, 1258, 1188, 1036, 842, 794, 732, 730.

DSC (scan rate 10°/min): T_g = 61 °C.

Attempts to polymerize the acrylates **8** *and* **29**

-*Via radical initiation*

1) A solution of 290 mg (0.374 mmol) of **8** and 0.6 ml of a solution of 11.8 mg of AIBN in 10 ml dry THF ($4.3x10^{-3}$ mmol) was repeatedly degassed and then kept under an argon atmosphere at 60 °C. After stirring for 7 d at 60 °C, the crude mixture was poured in an excess of methanol, but not precipitate was obtained. GPC analysis of the methanol fraction confirmed the absence of a polymer.

2) A solution of 160 mg (0.206 mmol) of **8** and 0.2 ml of a solution of 25 mg of dibenzoyl peroxide in 10 ml dioxane ($2.1x10^{-3}$ mmol) was repeatedly degassed and then kept under an argon atmosphere at 80 °C. After stirring for 5 d at 80 °C, the crude mixture was poured in an

excess of methanol, but not precipitate was obtained. GPC analysis of the methanol fraction confirmed the absence of a polymer.

-*Via anionic initiation*

To a solution of 165 mg (0.185 mmol) of **29** in 5 ml dry THF, 0.1 ml of a 0.16M solution of BuLi in dry THF were added under an argon atmosphere at room temperature. After stirring for 7 d the crude mixture was poured in an excess of methanol, but not precipitate was obtained. GPC analysis of the methanol fraction confirmed the absence of a polymer.

Chemical doping of **26**

40 mg (0.046 mmol) of the polymer **26** were suspended under an argon atmosphere in dry nitromethane. A solution of 40 mg (0.247 mmol) of $FeCl_3$ in dry nitromethane was dropped into the suspension, which was then stirred at r. t. for 3 h. The polymer was filtered off and washed under argon with nitromethane until the nitromethane phase stayed colorless.

7. REFERENCES

1) "*Handbook of Conducting Polymers*"- vol.II, G .A. Skotheim Ed., Dekker, Basel (1986)
2) J. Roncali, *Chem. Rev*. **92**, 711 (1992)
3) S. Hotta, M. Soga, N. Sonoda, *Synth. Met*. **24**, 267 (1988)
4) G. Kossmehl, G. Chatzitheodorou, *Makromol. Chem. Rapid Commun*. **2**, 551 (1981)
5) G. Kobmehl, *Makr. Chem. Macrom. Symposia* **4**, 45 (1986)
6) M.B. Inoue, E.F. Velazquez, M. Inoue, *Synth. Met*. **24**, 223 (1988)
7) A.F. Diaz, *Chem. Scripta* **17**, 145 (1981)
8) W. ten Hoeve, H. Wyinberg, *J. Am. Chem. Soc*. **113**, 5887 (1991)
9) R.D. McCollough, R.D. Lowe, M. Jayaraman, D.L. Anderson, *J. Org. Chem*. **58**, 904 (1993)
10) K. Tamao, S. Kodama, I Nakajima, M. Kumada, *Tetrahedron* **38**, 3347 (1982)
11) M.D. Curtis, M.D. McClain, *Chem. Mater.* **8**, 936 (1996)
12) T-A. Chen, R.D. Rieke, *J. Am. Chem. Soc*. **114**, 10087 (1992)
13) J. Roncali, R. Garreau, A Yassar, P. Marque, F. Garnier, M. Lemaire, *J. Phys. Chem*. **91**, 6706 (1987)
14) A. Bolognesi, W. Porzio, G. Zannoni, L. Fannig, *Acta Polym*. **50**, 150 (1999)
15) W. ten Hoeve, H. Wyinberg, *Macromolecules* **24**, 455 (1991)
16) M.R. Bryce, A.D. Chissel, N.R.M. Smith, D. Parker, *Synth. Met*. **26**, 153 (1988)
17) R.K. Khanna, N. Bhingare, *Chem. Mater*. **5**, 899 (1993)
18) C. Kitamura, S.Tanaka, Y.Yamashita, *Chem. Mater*. **8**, 570 (1996)
19) P.F. van Hutten, R.E. Gill, J.K. Herrema, G. Hadziioannou, *J. Phys. Chem*. **99**, 3218 (1995)
20) F. Martinez, R. Voelkel, D. Naegele, H. Naarmann, *Mol. Cryst. Liq. Cryst*. **167**, 227 (1989)
21) M-G. Baek, R.C. Stevens, D.H. Charych, *Bioconjug. Chem*. **11**, 777 (2000)
22) S. Lee, Y. Kang, C. Lee, *Synth. Met*. **117**, 257 (2001)
23) D. Gebeyehu, C.J. Brabec, F. Padinger, T. Fromherz, J.C. Hummelen, D. Badt, H. Schindler, N.S. Sariciftci, *Synth. Met*. **118**, 1 (2001)
24) G. Daoust, M. Leclerc, *Macromolecules* **24**, 455 (1991)
25) K. Kaneto, T. Asano, W. Takashima, K. Sasano, *Polym. Int*. **27**, 249 (1992)
26) F. Andreani, C. Carlini, C. Della Casa, *Chim. & Ind.* **75**, 811 (1993)
27) M.L. Hallensleben, F. Hollwedel, D. Stanke, *Macromol. Chem. Phys*. **196**, 3535 (1995)

28) R.J. Waltman, J. Bargon, A.F. Diaz, *J. Phys. Chem* **87**, 1459 (1983)

29) A.F. Diaz, J. Crowley, J. Bargon, G.P. Gardini, J. B. Torrance, *J. Electroanal. Chem*. **121**, 355 (1981)

30) N. Ranieri, G. Ruggeri, F. Ciardelli, *Polym. Int*. **48**, 1091 (1999)

31) G. Zotti, G. Schiavon, A. Berlin, G. Pagani, *Chem. Mater*. **5**, 430 (1993)

32) P. Bauerle, *Adv*. *Mater*. **4**, 102 (1992)

33) "Electronic Materials: The Oligomeric Approach", K. Müllen, G. Wegner; Wiley-VCH Editor, Weinheim (1998)

34) A. Carpita, R. Rossi, C.A. Veracini, *Tetrahedron* **41**, 1919 (1985)

35) J.K. Herrema, H. Wildeman, F. van Bolhuis, G. Hadziioannou, *Synth. Met*. **60**, 239 (1993)

36) P. Bauerle, T. Fisher, B. Bidlingmeier, A. Stabel, J.P. Rabe, *Angew. Chem. Int. Ed. Engl*. **34**, 303 (1995)

37) G. Zotti, M.C. Gullazzi, G. Zerbi, S.V. Meille, *Synth. Met*. **73**, 217 (1995)

38) J. Kagan, S.K. Arora, *J. Org. Chem*. **48**, 4317 (1983)

39) Y. Ohsedo, I. Imae, Y. Shirota, *Electroch. Acta*, **45**, 1543 (2000)

40) K. Nawa, I. Imae, N. Noma, Y. Shirota, Y. Ohsedo, *Macromolecules* **30**, 380 (1997)

41) N. Di Cesare, M. Belletete, A. Donat-Bouillud, M. Leclerc, G. Durocher, *Macromolecules* **31**, 6289 (1998)

42) M.-A. Sato, M.-A. Sakamoto, M. Miwa, M. Hiroi, *Polymer* **41**, 5681 (2000)

43) H.S. Nalwa, *Polymer*, **32**, 745 (1991)

44) Y. Hong, L.L. Miller, *Chem. Mater.* **7**, 1999 (1995)

45) S. Destri, I.A. Khotina, W. Porzio, C. Botta, *Opt. Mater*. **9**, 411 (1998)

46) Y. Ohsedo, I. Imae, Y. Shirota, *Electroch. Acta* **45**, 1543 (2000)

47) K. Nawa, K. Miyawaki, I. Imae, N. Noma, Y. Shirota, *J. Mater. Chem*. **3**, 113 (1993)

48) H. Nakanishi, Y. Aso, T. Otsubo, *Synth. Met*. **101**, 604 (1999)

49) J.J. Apperloo, R.A. Janssen, P.R.L. Malenfant, J.M.J. Frechet, *Macromolecules* **33**, 7038 (2000)

50) D. Fichou, *J. Mater. Chem*. **10**, 571 (2000)

51) K. Nawa, I. Imae, N. Noma, Y. Shirota, *Macromolecules* **28**, 723 (1995)

52) Y. Wei, Y. Yang, J-Meh, *Chem. Mater*. **8**, 2659 (1996)

53) U. Schöler, K.H. Tews, H. Kuhn, *J. Chem. Phys*. **61**(12), 5009 (1974)

54) B. Liedberg, Z. Yang, I. Engquist, M. Wirde, U. Gelius, G. Götz, P. Baüerle, R.-M. Rummel, C. Ziegler, W. Göpel, *J. Phys. Chem. B* **101**, 5951 (1997)

55) F. Garnier, A. Yassar, R. Hajlaoui, G. Horowitz, F. Deloffre, B. Servet, S. Ries, P. Alnot, *J. Am. Chem. Soc*. **115**, 8716 (1993)

56) W.J. Feast, J. Tsibouklis, K.L. Pouwer, L. Groenendaal, E.W. Meijer, *Polymer* **37**, 5017 (1996)

57) Wei, R. Hariharan, R. Bakthavatchalam, *J. Chem. Soc. Chem. Comm*. 1160 (1993)

58) G. Wegner, *Ber. Bunsenges. Phys. Chem*. **11**, 95 (1991)

59) K. Faid, M. Leclerc, *J. Chem. Soc.Chem. Commun*. 962 (1993)

60) F. Effenberger, F. Wurthner, F. Steybe, *J. Org. Chem*. **60**, 2082 (1995)

61) M.G. Hill, J-F. Penneau, B. Zinger, K.R. Mann, L.L. Miller, *Chem. Mater*. **4**, 1106 (1992)

62) D. Fichou, G. Horowitz, B. Xu, F. Garnier, *Synth. Met*. **39**, 243 (1990)

63) J. P. Ferraris, G. D. Skiles, *Polymer*, **28**, 179 (1987)

64) D. Delabouglise, M. Hmyene, G. Horowitz, A. Yassar, F. Garnier, *Adv. Mater*. **4**, 107 (1992)

65) F. Garnier, G. Horowitz, X.Z. Peng, D. Fichou, *Synth. Met*. **45**, 163 (1991)

66) K.J. Jen, G.G. Miller, R. Elsenbaumer, *J. Chem. Soc. Chem.Comm*. 1346 (1986)

67) J.S. Moore, S.I. Stupp, *Macromolecules* **23**, 65 (1990)

68) M. Stoldt, P. Bäuerle, H. Schweizer, E. Umbach, *Mol. Cryst. Liq. Cryst. Sci. + Technol*. **240**, 127 (1994)

69) P. Bauerle, F. Wurthner, G. Gotz, F. Effenberger, *Synthesis*, 1099 (1993)

70) R. Eckert, H. Huhn, *Z. Elektrochem*. **64**, 356 (1960)

71) I. Levesque, M. Leclerc, *Chem. Mater*. **8**, 2843 (1996)

72) A. Yassar, D. Delabouglise, M. Hmyene, B. Nessak, G. Horowitz, F. Garnier, *Adv. M*ater. **4**, 490 (1992)

73) D. Fichou, B. Xu, G. Horowitz, F. Garnier, *Synth. Met*. **41-43**, 463 (1991)

74) P. Garcia, J.M. Pernaut, P. Hapiot, V. Wintgens, P. Valat, F. Garnier, D. Delabouglise, *J. Phys. Chem*. **97**, 513 (1993)

75) J.K. Herrema, P.F. van Hutten, R.E. Gill, J. Wildeman, R.H. Wieringa, G. Hadziioannou, *Macromolecules* **28**, 8102 (1995)

76) T. Kawaguchi, H. Nakahara, *Thin Solid Films* **113**, 29 (1985)

77) M. Schaub, C. Fakirov, A. Schmidt, G. Lieser, G. Wenz, G. Wegner, P.-A. Albony, H. Wu, M.D. Foster, C. Majrkzak, S. Satija, *Macromolecules* **28**, 1221 (1995)

78) G. Wiegand, T. Jaworek, G. Wegner, E. Sackmann, *Langmuir*, **13**, 3563 (1997)

79) G. Wegner, *Ber. Bunsenges. Phys. Chem*. **95**, 919 (1993)

80) G. Wegner, *Mol. Cryst. Liq. Crist*. **216**, 7 (1992)

81) V. Buchholz, P. Adler, M. Bäcker, W. Hölle, A. Simon, G. Wegner, *Langmuir* **13**, 3206 (1997)
82) H. Tebbe, *Ph.D. Thesis*, Johannes-Gutenberg Universität, Mainz (1996)
83) A. Ulman "Ultrathin Organin Films", Academic Press, Inc. S. Diego (1991)
84) G. Wegner, *Ber. Bunsenges. Phys. Chem*. **95**, 1326 (1991)
85) "Physical Chemistry of Surfaces", A. W. Adamson, John Wiley & Sons Ed. (1990)
86) J.R. Lakowicz, *Principles of Fluorescence Spectroscopy*, Plenum Press, New York,1983
87) C.D. Henry, H. Tebbe, G. Wegner, F. Armand, A. Ruaudel-Teixier, *Adv. Mater*. **9**, 805 (1997)
88) M. Schaub, G. Wenz, G. Wegner, A. Steim, D. Klemm, *Adv. Mater*. **5**, 919 (1993)
89) H. Nakayara, J. Nakayama, M. Hoshino, K. Fukuda, *Thin Solid Film*, **160**, 87 (1988)
90) L.M. Goldenberg, A. Donat- Bouillud, M. Leclerc, M.C. Petty, J. Electroan. Chem. **443**, 266 (1998)
91) A.D. Schlüter, J.P. Rabe, *Angew. Chem. Int. Ed*. **39**, 864 (2000)
92) Y-M. Chen, C-F. Chen, W-H. Liu, Y-F. Li, F. Xi, *Macromol. Rapid Commun*. **17**, 401 (1996)
93) T.M. Swager, C.J. Gill, M.S. Wrighton, *J. Chem. Phys*. **99**, 4886 (1995)
94) D. Ofer, T.M. Swager, M.S. Wrighton, *Chem. Mater*. **7**, 418 (1995)
95) N. Costantini, S. Capaccioli, M. Geppi, G. Ruggeri, *Polym. Adv. Technol*. **11**, 27 (2000)
96) R.M. Hill, *Phys. Stat. Sol. (a)* **35**, k29 (1976)

ACKNOWLEDGEMENTS

First of all I wish to express my gratitude to Prof. Dr. Gerhard Wegner for providing me the best opportunities and for his supervision throughout my thesis.

Prof. Dr. Sigurd Höger I thank for his excellent help concerning the synthetic work of this project.

Dr. Michiel Oosterling I wish to thank for his hints regarding the application of the Langmuir-Blodgett technique.

Christophe Sieber I thank for his support during the electrochemical experiments.

For their help I thank Dr. Adeleide Godt, Gabi Hermann and Dr. Beate Schiewe.

Particular thanks go to the collegues and friends of the *MPI für Polymerforschung* for the great time after work!

Very special thanks I wish to express to my family for their unlimited support during my education, and to Francesca Rosselli who represented "the happy island when the sea was storming".